NEURAL MECHANISMS OF POSITION PERCEPTION

by

JESSICA WRIGHT

A Dissertation submitted to the

Graduate School-Newark

Rutgers, The State University of New Jersey

in partial fulfillment of the requirements

for the degree of

Doctor of Philosophy

Graduate Program in Behavioral and Neural Sciences

written under the direction of

Bart Krekelberg

and approved by

_____

_____

_____

_____

_____

Newark, New Jersey

October 2014

ABSTRACT OF THE DISSERTATION

Neural Mechanisms of Position Perception

By JESSICA WRIGHT

Dissertation Director:
Bart Krekelberg

Visual perception is a reconstruction of the physical visual aspects of the world and subject to various biases, assumptions and noise. One aspect of visual perception is visuospatial localization. Although visual localization is typically accurate, there are various situations where healthy human subjects mislocalize objects, as well as neurological disorders that alter visual localization behavior. These situations result in differences between the perceived and actual position of an object. These perceptual errors are useful to explore the limitations of visuospatial object localization and provide information on the underlying neural mechanisms of position perception. In particular, the following studies investigated how the brain integrates visual information across a spatially extended stimulus and ultimately results in a final percept of position. This project utilized behavioral and fMRI studies combined with transcranial direct current stimulation (tDCS) in healthy human subjects. These methods allowed us to quantify behavioral errors in localization and examine changes in the BOLD signal (as an indirect measure of changes in neural activity) in potential neural correlates of position perception. In Aim 1 we show that factors such as retinal

eccentricity and attentional cues bias localization behavior via alterations of the contribution of specific object components in the integration process. Aim 2 shows that tDCS over posterior parietal cortex (PPC) yields mislocalizations that are consistent with predictions from the interhemispheric competition theory (ICT) of attention. This supports the causal role of PPC in visual spatial localization. Aim 3 extends the results from Aim 2 to show that the BOLD signal changes in PPC predict localization behavior. In addition to novel insights related to position perception, these experiments provide insight into the effects of tDCS on behavior and the interaction of tDCS with the BOLD signal. This work begins to answer how different factors influence position perception and the role of different cortical regions in position perception. This research also has implications for rehabilitation programs for patients with various visual neurological disorders that alter spatial perception.

Acknowledgements

"Have no fear of moving into the unknown. Simply step out fearlessly knowing that I am with you, therefore no harm can befall you; all is very, very well. Do this in complete faith and confidence." Pope John Paul II

My doctoral journey began when I stepped into a world unknown to me; the world of scientific research. I will forever be grateful to the faculty of the Behavioral and Neural Sciences program and the faculty who worked at UMDNJ at the time who saw my potential and invited me to embark on this crazy and exciting journey.

This journey has had its ups and its downs. Luckily, I have not had to walk this path alone. The completion of this thesis would not have been possible without the guidance, encouragement and support of many people. I would like to acknowledge a few key people who have my deepest gratitude.

Primarily, I would like to thank my advisor Bart Krekelberg. Bart, thank you for all you have taught me over the years. You train your graduate students to be researchers by giving them experience and ownership of all parts of the experimental process. From the beginning you empower us to be independent researchers, however, we know your door is open for questions or discussions. There were moments I was not thrilled to be debugging Neurostim or Matlab issues, but you were always there to usually point out my errors and send me back to work. I thank you for believing in my value as a researcher even in the moments when I forgot. I thank you for letting me talk, sometimes at extensive

length, through a research or even personal issue with you. I thank you for sharing in the joys (yes, even sometimes with squeals) and encouraging me in the lows. You have become more than just an advisor. Over these years, you have become a friend and I will always value and fondly remember my time as a member of the KLab.

Adam Morris, thank you for being an anchor and support during the first few years of my thesis work. Now I can appreciate the ways you pushed me to look at the bigger picture, even though, in the moment I sometimes just hoped for a quick answer. You spent the time to sit with me and to make sure I understood an issue. Somehow your talks usually segued to something to do with overlapping Gaussians, which surprisingly had a lot of applications. Thank you for making me laugh and reminding me why I am happy to not have had any brothers. Seriously, thank you for your time, your encouragement and your support.

Maria del Mar Quiroga, thank you for your constant encouragement and reality checks. Thank you for making sure I stayed awake with mate and helping me to hide the additional grays I got from the stress of graduate school. Your friendship has been a blessing and thank you for joining the lab to help offset the guy gender bias.

Jeroen Joukes (office buddy), thank you for helping me to stay grounded in this process. I always valued our talks about life and science. I will miss sharing in your new discoveries and being able to turn around and have someone relate to my Matlab, computer or life issues.

Kohitij Kar, thank you for all of your help with my projects over the years. Thank you for teaching me more about tES and taking the time to help me set up my experiment. I appreciated your insight with getting everything set up downstairs. Thank you for always being a subject as well. I will miss our walks for coffee or smoothies and impromptu trips to Tops Diner.

Jon Guez, thank you for your feedback over the years and helping me to think outside of the box about science and other things. Thank you also for introducing me to pistachios and making sure that in my times of stress I still had something to eat. I will miss returning the favor.

To every current and former member of the KLab, there are too many to list, thank you for all your input in lab meetings and at other times throughout this process. Thank you for answering my questions, for celebrating accomplishments and for introducing me to the love of Trader Joe's. I will always fondly remember our enlightening lunch conversations.

To my thesis committee, thank you all for being a part of this journey with me. I thank you for the investment of your time and for your encouragement over the years. Dr. Mauricio Delgado, thank you for agreeing to be my thesis committee chair. I appreciate your help with my fMRI questions and connecting me to others in your lab for support. Dr. April Benasich, I enjoyed my time rotating in your lab. Thank you for sharing your love of research with me. Dr. Kevin Pang, thank you for agreeing to be a part of this group. I still remember getting to know you from the Foundations in Neuroscience class we won't say how many years ago. Dr. David Whitney, thank you for your feedback and your

willingness to be my external committee member. I will miss connecting with you and others at VSS.

There are a few friends whose support has been critical over the years. Anushree Karkhanis, thank you for your friendship and encouragement over the years. Thank you for including me in your family celebrations and treating me like an extended family member. Thank you for the laughs, for showing me around the electrophysiological setup upstairs and always being there for a science question or just to talk about life. Arielle Selya, thank you for all the coffee talks and for your help over the years with statistics or other questions. It has been a blessing to stay in contact with you. Thank you also for always trying to motivate me with school and also with the gym. I could still use some motivation on the latter one. To both of you, your dedication and commitment to your work has always inspired me and in part helped to keep me moving forward these past years.

To my roommate, Lillian, thank you for opening your home to me and for your support over these past couple of years. It has been great bonding over our thesis work and I appreciate your understanding when I have “thesis brain.” Thank you for giving me a break on chores these past couple months as I approached this finish line. You have brought peace to a very stressful time and I will always be thankful.

Thank you to my spiritual families. To Liquid Church and my friends there, thank you for your love and encouragement over the years. Thank you for teaching me about Jesus and how to truly walk with the Lord. A special thanks to

Toni Bunkley, Douglas Keane and Vanessa Waszaj, my JF Crew. Our late nights of coffee, Bible convos and worship will forever be in my heart. Thank you for your encouragement in all aspects of my life. To my Relief Bus family, thank you for your patience and encouragement over this past year. It has been a blessing during these final stages and times of transition. Cathe & Caitlin, thank you for helping to bring peace during some times of stress. Yaz, thank you for understanding when I couldn't come out on the bus and always asking me how I was really doing. Johanna, your friendship and spontaneous outings have been such a blessing and have helped to keep me sane during these final months. Thank you for seeing me and loving me.

To my family, thank you for encouraging me in everything I do. Mom, thank you for showing me how to be a strong independent woman. You have shown me that no matter the struggle, you can always make it through. Thank you for your love and support. To my dad thank you for the endless encouragement and love. No matter what I have done, you have always been there to support me. Thank you for believing in me. Thank you also for the endless supplies of chili, tuna melts and other sustenance that has always kept me going. To my beautiful and loving sister, your love and support has been such a blessing. Thank you for your endless encouragement, for all the laughs and for seeing me to my core. You see what others don't and you love me all the more for it. These accomplishments I dedicate to you so you know to keep going towards your dreams. Know also that dreams may change, but each experience

brings us wisdom and prepares us for the steps ahead. To my immediate and extended family, I love you all dearly.

This time has also brought a renewal of my faith in God and Jesus. They have directed my path during this journey and on to my next step. They have brought me peace and renewed my sense of motivation during these final stages. *“For it is by grace you have been saved, through faith —and this is not from yourselves, it is the gift of God— not by works, so that no one can boast. For we are God’s handiwork, created in Christ Jesus to do good works, which God prepared in advance for us to do.”* Ephesians 2:8-10

Table of Contents

List of Illustrations

Chapter 1: **General Introduction**

Each day we view, explore, interact with, and navigate our environments with little thought to how our minds construct the complex scenes around us. Much of our world relies on where things are in space so that we may avoid obstacles as we walk, or know where and how to reach and pick up objects. In order to do this, we must identify individual objects either physically present or from memory and determine their location, many times in reference to other landmarks. However, each object consists of many parts with their own relationship to each other, which must be associated with the proper object within a scene. Therefore, we need to combine all this information, determine the boundaries for each object and construct a visual scene. While there are many questions focused on these topics, which can be collectively referred to as visuospatial perception, the following experiments address key issues in this field: How stimulus and cognitive factors influence visual object localization and how different cortical areas contribute to this localization.

As may be expected, under many circumstances target localization is typically accurate and the perceived position is close to the physical position of the target (He & Kowler, 1991; Kowler & Blaser, 1995). However, there are various conditions that result in errors in spatial perception. Discrepancies between the physical location of a target and the perceived location of a target have been shown to result from: eye movements (Honda, 1989, 1991; for a review see Ibbotson & Krekelberg, 2011; Kaiser & Lappe, 2004; Matin & Pearce, 1965; Ross, Morrone, Goldberg, & Burr, 2001), object motion (De Valois & De

Valois, 1991; Krekelberg & Lappe, 1999, 2001; Lappe & Krekelberg, 1998; Whitney & Cavanagh, 2000; Wilson & Anstis, 1969), changes in frame of reference (Bridgeman, Peery, & Anand, 1997; Roelofs, 1935), adaptation (Whitaker, McGraw, & Levi, 1997) and attentional cueing (Kerzel, 2003; Suzuki & Cavanagh, 1997; Tsal & Bareket, 1999, 2005). In addition, the retinal eccentricity of the target (Müsseler, van der Heijden, Mahmud, Deubel, & Ertsey, 1999) and the duration of the target (O'Regan, 1984; Rose & Halpern, 1992; van der Heijden, van der Geest, de Leeuw, Krikke, & Musseler, 1999) yield changes in localization accuracy and variability in response. These perceptual errors highlight the limits of visual processing in humans and provide insight to the underlying neural mechanisms supporting visuospatial localization.

For simplicity, object localization can be understood in three main stages: input (local processing), integration, and output (global processing), see Figure 1-1. To determine the position of a spatially extended target in the visual field it is first necessary to identify and localize the features and components of the target (local processing). We know many visually responsive neurons respond to stimuli that appear within a small region of the visual field, i.e. their spatial receptive field (RF). Figure 1-1 represents these cells as detectors (black dots) that respond to the viewed object (orange shape). These detectors provide information about the local features and fine details of the component(s) of an object within their RF. To determine the location of the object as a whole, the integrator combines the component representations, which may differentially contribute to the perceived position. We model these different levels of contribution with specific weights, ω_i,

for each detector (early bias). This results in an intermediate position estimate. The intermediate position estimate may be biased during the global processing stage (B_g, late bias) resulting in the final perceived position of the target.

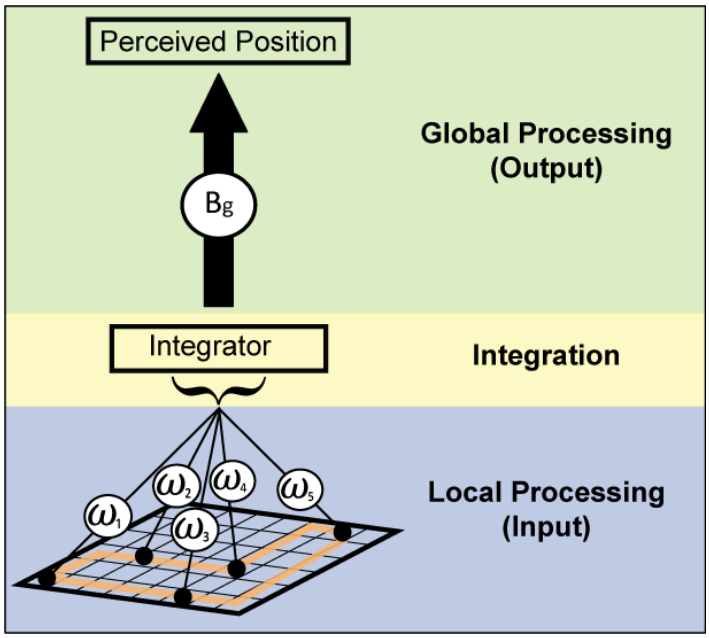

Figure 1-1: Conceptualized model of object localization with three main stages. The first stage (blue) includes the local processing of the visual input (orange shape) by detectors (grid with five detectors highlighted by black dots) that respond to a specific region of the object, i.e. the object components. This local information must be combined in an integration process (yellow) to gain information about the object as a whole. The result of this integration is then processed to yield the final percept of position (green), which we term as global processing. A mislocalization may result from a bias in local processing (early bias) as a result of differential weighting (ω) of cell responses, from a bias in global processing (late bias, B_g) on the output of the integrator or some combination of both.

We know that one or more of these stages of processing are imperfect due to the above mentioned errors in visual localization. In the following experiments, we focus on perceptual localization errors induced by transient stimuli combined with attentional cueing and/or modulations in neural excitability via transcranial electrical stimulation. Since observers must integrate position information from the object's components; such as edges, borders and other

structural elements, to determine the spatial position of an object, mislocalization may result from errors in the local processing of object components. Errors may also be introduced in the global processing stage as the brain transforms the post-integration estimate of position to a motor command or final percept of position. The main goals of this research are to determine how attention and retinal eccentricity influence target localization and investigate the neural mechanisms that govern position perception.

To provide a context for the conducted experiments, we first review visual localization with an emphasis on the behavioral effects of retinal eccentricity and attentional manipulations. We then address a potential theory of position perception followed by proposed neural mechanisms and cortical networks for spatial processing as well as attention. We conclude with the neural mechanisms of transcranial direct current stimulation (tDCS). For clarity, we highlight significant experimental motivations and findings from our experiments in italics as we address relevant topics from the literature.

Visual Localization: Influences of Retinal Eccentricity

Localization of Single Targets

When asked to locate a single target in space, subjects will first make an eye movement to the target and then make a localization response to achieve the greatest accuracy. This process takes 200 ms on average (Adam, Ketelaars, Kingma, & Hoek, 1993). If the target appears briefly, such that the target disappears prior to the completion of an eye movement, or the task restricts eye movements, localization accuracy decreases (Adam et al., 1993; Adam, Paas,

Ekering, & van Loon, 1995). Studies have shown that these mislocalizations are typically in the direction of the fovea (foveopetal) and that the magnitude of this error increases with greater retinal eccentricities of the target (Mateeff & Gourevich, 1983; O'Regan, 1984; Rauk & Luuk, 1980; van der Heijden et al., 1999). These mislocalizations are consistent for absolute (Adam et al., 1993; Adam et al., 1995) and relative localization judgments (Müsseler et al., 1999; van der Heijden et al., 1999), however, the magnitude of error may be reduced in the presence of other anchor points in the display (Rauk & Luuk, 1980). Therefore, the retinal eccentricity of a single target directly contributes to a human observer's ability to localize that target and induces a bias in localization. *While this thesis dissertation does not address localization accuracy of single targets directly, each experiment utilizes a stimulus consisting of multiple targets, each of which may be subject to a specific eccentricity-dependent bias, which we have termed the local processing of the object.*

Localization of Spatially Extended Stimuli

Unlike localization of single targets, objects do not have a distinct point as the target position. The localization of spatially extended stimuli requires knowledge about the components of these stimuli, which then must be integrated to result in a final percept of position as illustrated in Figure 1-1. Under certain conditions, human observers localize spatially extended targets at the center of mass (centroid), which suggests an unbiased (all ω_i equal in Figure 1-1) integration of the target components (He & Kowler, 1991; Kaufman & Richards, 1969; Kowler & Blaser, 1995; Richards & Kaufman, 1969; Vishwanath & Kowler,

2003). Prior studies on visual search have shown that subjects serially fixate on the center of mass of targets as they scan objects across the visual field (Findlay, 1982; Najemnik & Geisler, 2005). However, it has also been shown that features of an object such as edges (Landy, 1993), luminance (Whitaker & McGraw, 1998) and spatial frequency (Rose & Halpern, 1992) bias localization. In addition, psychophysical studies have shown that there are also foveopetal mislocalizations when localizing spatially extended stimuli (Stork, Musseler, & van der Heijden, 2010). A study by Musseler and colleagues (1999) has shown that the magnitude of the error in a spatially extended stimulus is greater compared to a single target (see also Ploner, Ostendorf, & Dick, 2004). In addition, the gradient of this effect across increasing eccentricities is steeper for spatially extended stimuli compared to single targets. This suggests that mislocalization may be the result of an imperfect eccentricity-dependent integration (ω_i not equal in Figure 1-1) of the individual components (but see Kowler & Blaser, 1995). A prior study assessed effects of eccentricity on the dot components of random dot patterns (RDPs). They did not find any evidence to suggest a biased eccentricity-dependent integration of target components (McGowan, Kowler, Sharma, & Chubb, 1998). This suggests that the foveopetal mislocalizations are a result of a late bias in global processing (B_g in Figure 1-1). However, a more recent study (Drew, Chubb, & Sperling, 2010) has shown biased integration dependent on the distance of an object component relative to the center of the object itself. Interestingly, they found two patterns of responses across subjects: those biased more by components at the center of the target

and others with the reverse pattern. This suggests different strategies or mechanisms involved in localization. Given this controversy, *it remains uncertain in what direction and on what level (local or global) localization perceptual errors will occur as a result of varying retinal eccentricity. Experiment 1 provides evidence for eccentricity affecting the local processing of position perception.*

Visual Localization: Influences of Attentional Factors

Prior research has supported (Goldberg & Wurtz, 1972; Rafal, Calabresi, Brennan, & Sciolto, 1989; Remington, 1980; Shepherd, Findlay, & Hockey, 1986) the claim that a "shift of attention appears to function as a way of guiding the eye to an appropriate area of the visual field" (Posner & Petersen, 1990). Given that the natural response to localizing a target is to fixate on it, it is intuitive that attentional mechanisms may provide a coarse localization of the target followed by an eye movement to yield fine localization (Adam et al., 1993). Common experimental manipulations linked to attention have been shown to influence position perception, ultimately resulting in increased accuracy (Adam, Davelaar, van der Gouw, & Willems, 2008; Bocianski, Müsseler, & Erlhagen, 2010; Fortenbaugh & Robertson, 2011; Newby & Rock, 2001), and reduced uncertainty (Prinzmetal, Amiri, Allen, & Edwards, 1998; Tsal & Bareket, 1999, 2005). However, studies have also shown that attentional cueing may introduce biases in localization (Kosovicheva, Fortenbaugh, & Robertson, 2010; Suzuki & Cavanagh, 1997; Tsal & Bareket, 1999). Many of these studies used single targets, therefore, it is unclear how these attentional manipulations alter the localization of an object. Evidence for attentional influences on the components

of a stimulus includes previous studies that have shown that feature-based attention can be used to select a subset of components within an object (E. H. Cohen, Schnitzer, Gersch, Singh, & Kowler, 2007; Drew et al., 2010). This suggests that subjects have the ability to encode, select and act on individual components of a stimulus in part through attentional mechanisms. Another study has shown that spatial attention alters the perceived size of an RDP (Anton-Erxleben, Henrich, & Treue, 2007), potentially through mislocalizations of target components. In summary, *the research literature shows ample effects of attentional cueing on the perceptual localization of single targets, however, it fails to address how attentional cueing alters object localization. Experiments 1 - 4 utilized visual cueing towards subregions of a target and showed evidence for attentional cueing effects in the local processing stage of position perception.*

Position Encoding: Labeled Line Theory

It is well known that many of the cortical and subcortical visual structures have a retinotopic organization. Therefore, these structures encode the visual field in such a way that neighboring regions within a visual structure represent neighboring regions of the retina and have neighboring RFs. Given that there is an orderly representation of the visual field throughout visual cortex, one may suggest that this organization is functionally relevant. Therefore, it has been proposed that neurons within a particular modality may have a “specific energy” (Norrsell, Finger, & Lajonchere, 1999) which can be considered a detector for a specific stimulus attribute (Watson & Robson, 1981), or in the case of spatial perception, a specific retinal location. The labeled line theory states that specific

subpopulations of cells indicate probabilistically whether or not a stimulus appeared in a specific retinal location. Each subpopulation's response could then be integrated to achieve the final percept of position, similar to that shown for the local processing stage in Figure 1-1.

However, this suggests that the quality of retinotopic organization in the visual areas should directly correlate with improved position perception, which has not been shown in the literature (but see Michel, Chen, Geisler, & Seidemann, 2013). The coding of position perception is far more complex with multiple visual structures concurrently encoding a representation of the visual field. In addition, our eyes move on average three times per second (Carpenter, 1988), therefore, the visual input from the retina to these regions constantly changes. To account for this, the encoding of position in retinal coordinates must be transformed to world coordinates for us to interact with surrounding objects. To reduce the complexity induced from multiple eye movements and different frames of reference (i.e. eye-, head- and body-centered) we tested the labeled line theory in human subjects as they maintained fixation. If position perception truly utilizes a labeled line model, then we hypothesize that behavioral responses will be best described by an integration of detectors that respond to specific regions in the visual field. Therefore, the "label" of a detector remains yoked to a specific region of the visual field regardless of changes in cell firing rate or RF properties. *It remains uncertain how well the labeled line theory explains position perception. Using quantitative models, we show that a weighted combination of*

the object components best describes the perceived position of a stimulus, which suggests the integration of labeled detectors (Experiment 1).

Neural Correlates of Visuospatial Processing and Attention

Cortical Visuospatial Processing

It is well known that cortical visual processing is divided into two anatomically and functionally distinct pathways; dorsal (spatial processing) and ventral (object recognition). However, these pathways do not encode stimuli in isolation (Keizer, Colzato, & Hommel, 2008; Mahon et al., 2007; Schenk & Milner, 2006) and are connected reciprocally (Borra et al., 2008; Felleman & Van Essen, 1991; Goodale & Milner, 2010; Zanon, Busan, Monti, Pizzolato, & Battaglini, 2010). While our research incorporates the processing of specific targets, we are most interested in how the spatial positioning of target components influences global localization. Therefore, we will focus primarily on regions in the dorsal processing stream.

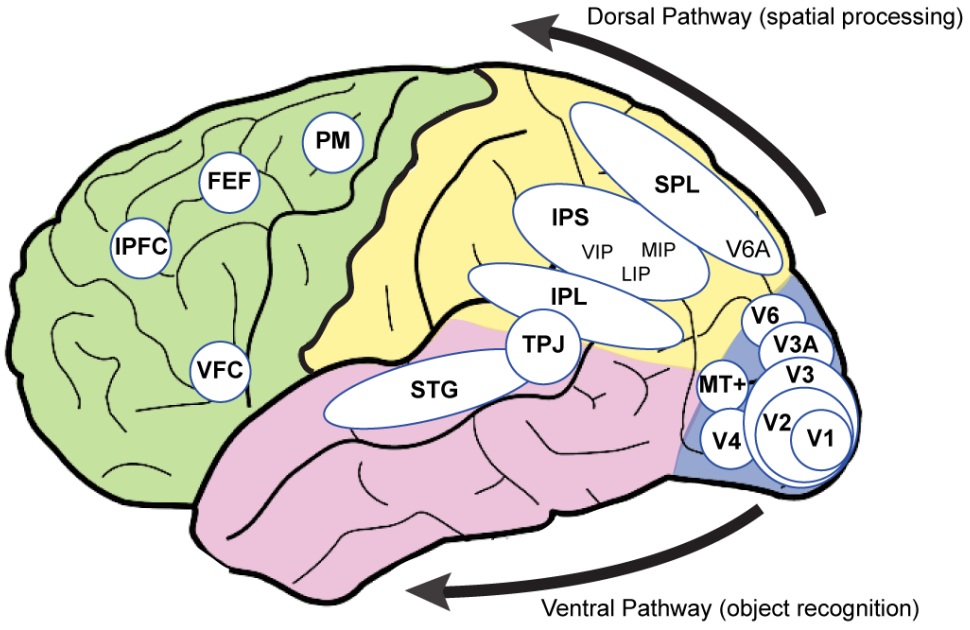

Figure 1-2: Coarse organization of cortical regions implicated in visuospatial processing and spatial attention The early visual cortical areas include V1, V2, V3, V3A, V4, MT+ and V6. The temporoparietal junction (TPJ) includes some portions of the superior temporal gyrus (STG) and inferior parietal lobule (IPL). The intraparietal sulcus (IPS) contains medial intraparietal area (MIP), lateral intraparietal area (LIP) and ventral intraparietal area (VIP). Other abbreviations: Superior parietal lobule (SPL), which includes V6A caudally, premotor cortex (PM), frontal eye field (FEF), lateral prefrontal cortex (lPFC) and ventral frontal cortex (VFC) which includes portions of the inferior and medial frontal gyri.

The earliest visual cortical areas (V1 and V2) provide input to both processing streams, however, information remains somewhat segregated within distinct subregions or layers. The dorsal stream then continues to include other regions organized retinotopically, V3, V3A & V6 (for a review see Kravitz, Saleem, Baker, & Mishkin, 2011). Given the organization of these regions and their specialization in processing visual input, modulations in neural activity within these areas may drive alterations in local processing and influence the localization of an object. For purposes of this thesis, we will refer to cortical areas in the occipital lobe (V1-V6, including hMT+) as the early visual cortical areas, see Figure 1-2.

Moving forward in cortical hierarchy there are two main projections to posterior parietal cortex (PPC), which includes the superior and inferior parietal lobules (SPL and IPL, respectively) and the intraparietal sulcus (IPS) (for a review see Kravitz et al., 2011). PPC has been linked to both attention (Corbetta & Shulman, 2002) and spatial processing (Fink et al., 2000; Morris, Chambers, & Mattingley, 2007 ; Morris, Kubischik, Hoffmann, Krekelberg, & Bremmer, 2012; Szczepanski & Kastner, 2013). The subregions within IPS have different functional specializations. The ventral intraparietal region (VIP) is a site for cross modal integration. VIP receives input from MT and MST (referred to as hMT+ in

humans), regions known for processing motion, as well as input from somatosensory, auditory and vestibular areas. The lateral intraparietal area (LIP) has been implicated in the initiation and execution of eye movements, as well as attention (see *Spatial Attention Networks* section). LIP neurons respond to a flashed stimulus and remain active until a saccade is made to the remembered location (Gnadt & Andersen, 1988). Whereas motor planning in LIP focuses on eye movements, the medial intraparietal area (MIP) and V6A constitute the parietal reach region and have been implicated in planning, execution and monitoring of reaching movements. These regions then project to regions in the frontal lobe including: the frontal eye field (FEF), that has a role in top-down control of eye movements and attention; lateral prefrontal cortex (lPFC), that has a role in spatial working memory; and premotor cortex (PM), that mediates various forms of visually guided action, see Figure 1-3.

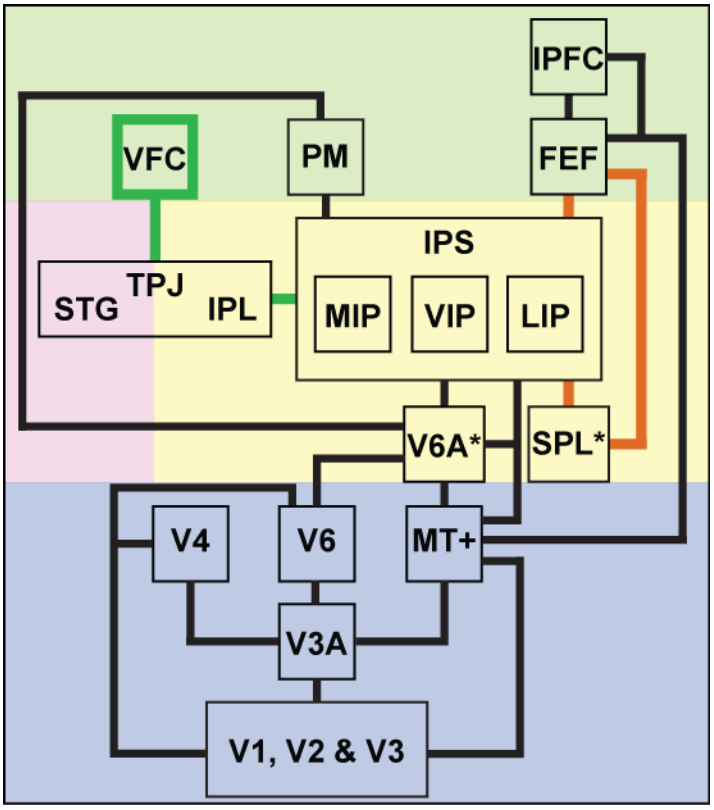

Figure 1-3: Connections between selected cortical areas implicated in visuospatial processing and/or spatial attention. Areas are the same as those identified in Figure 1-2: (occipital (blue), parietal (yellow), temporal (pink) and frontal (green)); and organized by cortical hierarchy (bottom → top corresponds to low → high in hierarchy). All lines represent reciprocal connections. However, feedforward connections represent direct input to regions higher in the cortical hierarchy, whereas the feedback connections represent direct or indirect input from higher cortical areas to lower ones. The connections highlighted in orange indicate the dorsal frontoparietal attention network, whereas the ones in green indicate the ventral frontoparietal attention network. VFC is also green since it is more involved in attentional processing as opposed to visuospatial processing. *It is unclear if the SPL, when mentioned in the context of attention, also includes V6A and whether V6A truly projects to FEF directly. Therefore, they are shown as separate boxes. V6A is in the caudal region of the SPL.

Spatial Attention Networks

Many cortical and subcortical structures have been implicated in allocating spatial attention. Corbetta and Schulman (2002) propose a model of attention that highlights two distinct, but interconnected, cortical networks mediating endogenous (top down) and exogenous (bottom up) attention; the dorsal

frontoparietal (IPS, SPL and FEF) and ventral frontoparietal (temporoparietal junction (TPJ), including the IPL and the superior temporal gyrus (STG); and ventral frontal cortex (VFC), including inferior/middle frontal gyrus) networks (Figure 1-3). Interestingly, the dorsal frontoparietal network has a large degree of overlap with the dorsal processing stream including regions in PPC (such as IPS) and FEF. Modulations of neural activity during attentional tasks have been shown in regions within the IPS, such as LIP (Goldberg, Bisley, Powell, & Gottlieb, 2006) and VIP (Cook & Maunsell, 2002). In particular, LIP shows sustained responses to a visual cue, increases in baseline firing in anticipation of a cue onset, increased responses for behaviorally relevant visual transients (Colby, Duhamel, & Goldberg, 1996), and responses to the locus of attention (Bisley & Goldberg, 2003).

Previous studies, including those with spatial neglect patients, have suggested that the allocation of attention by the above mentioned cortical regions towards each visual field is not balanced. Spatial neglect is a multifaceted debilitating disorder described by a subject's inability to act on or perceive multimodal stimuli typically in the left hemifield. These impairments cannot be explained solely by a deficit in primary sensory or motor processing and have been linked to attention, intention, spatial memory, and reference frame deficits. Less than 10% of patients with neglect exhibit damage in the left hemisphere with concurrent right visual field deficits (for a review of spatial neglect see Karnath, Milner, & Vallar, 2002). The preponderance of left hemifield neglect as a result of damage in the right hemisphere has led to various attentional allocation

theories. The hemispatial theory, for instance, proposes that the right hemisphere directs attention to both visual fields, whereas the left hemisphere directs attention solely to the right visual field (Heilman & Van Den Abell, 1980; Mesulam, 1981). In further support of this, Silvanto and colleagues (2009) show that increases in right PPC activity yield bilateral increases in cortical excitability in V1/V2, whereas increases in left PPC activity only yield significant increased cortical activity in left V1/V2.

Another theory, although not mutually exclusive from the hemispatial theory, is the interhemispheric competition theory (ICT). The ICT states that homologous frontal and/or parietal cortical regions across hemispheres function as opponent processors through reciprocal inhibition (J. D. Cohen, Romero, Servan-Schreiber, & Farah, 1994; Kinsbourne, 1977). It is the asymmetry of these activation levels that drives the allocation of attention such that the more activated hemisphere biases attention towards its contralateral visual field (Reuter-Lorenz, Kinsbourne, & Moscovitch, 1990; Szczepanski & Kastner, 2013). In healthy subjects, the right hemisphere is thought to be more dominant which explains pseudoneglect, a condition where healthy human subjects have a leftward bias in line bisection tasks (Bowers & Heilman, 1980; but see Jewell & McCourt, 2000). The ventral frontoparietal attention network (Corbetta, Kincade, Lewis, Snyder, & Sapir, 2005) shows a right lateralization, which is consistent with damaged regions that most notably yield spatial neglect. Szczepanski and Kastner (2013) show that specific cortical regions display asymmetries in

contralateral attentional biases across hemispheres, versus an average bias across multiple regions in a cortical hemisphere.

Many questions remain about the structure of attentional networks and the connections between cortical regions both intra- and interhemispherically. We reasoned that if an asymmetrical allocation of attention towards each visual field influenced localization, then we may be able to alter the balance of attention with tDCS and predicted that this would yield corresponding changes in visual localization. Within the hierarchy of cortical function, posterior parietal regions rest in between the encoding of visual input (early visual cortical areas) and even higher cognitive functions such as intention and working memory in frontal cortex. One might hypothesize that perceptual errors in localization could be introduced in PPC, given its role in coordinate transformations (eye- to body-, head- or even attention-centered (McCloskey & Rapp, 2000), sensorimotor transformations, visuospatial processing and attention. Therefore, we decided to examine the role of PPC in position perception. The more recent utilization of brain stimulation techniques, such as tDCS, allow us to modulate the neural activity in a particular area and examine its causal role in a behavior, such as localization. *In Experiments 3 - 5, we show that tDCS over PPC alters localization in a polarity-dependent manner consistent with interhemispheric competition confirming PPC's causal role in visual localization.*

Modulating Neural Activity with Transcranial Stimulation

Transcranial direct current stimulation modulates neuronal activity, noninvasively, with long lasting aftereffects up to 2 h (Nitsche & Paulus, 2001).

Current literature suggests that tDCS induces weak electrical fields that modulate the membrane potential predominantly in neurons with their axo-dendritic axis oriented parallel to the electromagnetic field. Rather than induce action potentials directly, studies have shown that application of these weak electrical currents instead yield small depolarizations or hyperpolarizations in cells, which effect cells' overall excitability (for a review see Ukueberuwa & Wassermann, 2010). The most prominent effects of tDCS are in regions near and directly under the stimulation electrodes (Utz, Dimova, Oppenlander, & Kerkhoff, 2010), however far reaching changes have also been shown using fMRI (Antal, Polania, Schmidt-Samoa, Dechent, & Paulus, 2011; Biswal, Van Kylen, & Hyde, 1997; Meinzer, Lindenberg, Antonenko, Flaisch, & Floel, 2013). The placement of the electrodes determines which type of polarization is expected in the stimulated region. In general, the anode (positive electrode) placed over the region of interest yields depolarization and enhanced excitability of a cortical region, whereas the cathode (negative electrode) placed over the region of interest yields hyperpolarization (Chan, Hounsgaard, & Nicholson, 1988; Lopez, Chan, Okada, & Nicholson, 1991).

It has been suggested that the proposed tDCS-induced changes in neural excitability mediate changes in a variety of behaviors: motor (Elbert, Lutzenberger, Rockstroh, & Birbaumer, 1981; Jaeger, Lutzenberger, & Birbaumer, 1987; Vines, Nair, & Schlaug, 2006), tactile perception (Matsunaga, Nitsche, Tsuji, & Rothwell, 2004; Ragert, Vandermeeren, Camus, & Cohen, 2008; Rogalewski, Breitenstein, Nitsche, Paulus, & Knecht, 2004), auditory

perception (Mathys, Loui, Zheng, & Schlaug, 2010; Vines, Schnider, & Schlaug, 2006) and visual perception (Antal, Nitsche, & Paulus, 2001; Korsakov & Matveeva, 1982). Prior studies have also shown visual perception changes with tDCS applied over PPC (Ko, Han, Park, Seo, & Kim, 2008; Sparing et al., 2009; Stone & Tesche, 2009). In spatial neglect patients, Sparing and colleagues (2009) showed that placement of the anode over the damaged hemisphere combined with the cathode over the unaffected hemisphere reduced rightward biases in line bisection. *Experiments 3- 5 showed that tDCS over PPC also biased localization in healthy subjects in a polarity-dependent manner.*

Although consistent tDCS-induced behavioral changes have been shown, the behavioral effects of tDCS can vary based on multiple factors: electrode size, placement, current amplitude, current duration, etc. (for a review see Nitsche et al., 2008; Zaghi, Acar, Hultgren, Boggio, & Fregni, 2010). Therefore, it is common to see differences in effects across experiments. In addition, current flow within the brain depends on idiosyncratic brain folding (A. Datta, Baker, Bikson, & Fridriksson, 2011; Wagner, Fregni, et al., 2007), which may lead to variability in the effects of tDCS across different subjects. *Experiments 3-5 showed that tDCS over PPC resulted in inconsistent changes in localization behavior relative to baseline, as well as in BOLD signal changes in PPC. However, when comparing tDCS conditions with reverse polarity we show consistent behavioral effects across most subjects. The general assumptions of tDCS may explain differences due to reversing the polarity of tDCS over PPC,*

but they are insufficient to explain the variability in behavior relative to baseline and in the BOLD signal across subjects.

Many of the behavioral tDCS experiments including our own (Experiments 3 and 4) base conclusions on the assumption that tDCS alters neural activity in regions below the electrode. Recent studies support the focality of transcranial electrical stimulation to a particular brain region by showing specific behavioral and/or BOLD signal changes related to the stimulated area (Antal et al., 2004; Antal, Polania, Schmidt-Samoa, Dechent, & Paulus, 2011; Meinzer et al., 2012). However, behavioral experiments alone cannot disprove that the spread of current to regions beyond those under the electrodes may contribute to behavioral changes (Wagner, et al., 2007). To determine the extent of neural changes with the application of tDCS, we performed fMRI experiments with concurrent tDCS. However, studies only recently began combining tDCS and MRI concurrently (Antal et al., 2011; Holland et al., 2011; Kwon et al., 2008; Stagg, O'Shea, et al., 2009); therefore, there are still many questions concerning how tDCS alters the BOLD signal. The BOLD signal measured with fMRI is proportional to changes in regional cerebral blood flow (rCBF). Some studies have shown tDCS-induced increases in rCBF (Zheng, Alsop, & Schlaug, 2011) and the BOLD signal (Stagg, O'Shea, et al., 2009) in regions under the electrode, regardless of polarity. However, other studies examining rCBF or the BOLD signal have shown varying changes in regions near and far from the electrode (Antal et al., 2011; Holland et al., 2011; Lang et al., 2005; Meinzer et al., 2012; Paquette, Sidel, Radinska, Soucy, & Thiel, 2011; Wachter et al., 2011). *Although*

we predicted increases in the BOLD signal under the anode in our task, Experiment 5 revealed varying effects of tDCS on the BOLD signal across subjects. However, this variability predicted the variability in behavior.

Summary

To determine the impact of attentional cues and retinal eccentricity on localization and define the neural correlates underlying position perception, we used three approaches: behavioral studies, transcranial electrical stimulation and brain imaging.

In order to identify the neural mechanisms of position perception, we must first quantify the process behaviorally. Therefore, Aim 1 (Experiments 1 and 2) quantified visuospatial integration in object localization behaviorally in healthy human subjects and examined how two factors, target component eccentricity and attentional visual cues, altered localization judgments of an RDP. In particular this aim focuses on the following questions:

- Do these two factors influence the local processing of the object components or the global position of the target?
- What patterns of bias are present in the local processing of target components and/or global position of the target?
- Do our results support a labeled line model of position perception?

If cueing induced its effect through attentional mechanisms modulating neural activity in regions implicated in attention should also systematically alter localization. In Aim 2 (Experiments 3 and 4) and Aim 3 (Experiment 5), we applied tDCS to alter neural excitability in posterior parietal cortex (PPC), a

region implicated in attention networks and spatial processing. This sought to answer the following questions:

- How do modulations of neural activity in PPC alter localization of a target?
- Does tDCS over PPC alter localization biases seen in Aim 1 in a polarity-dependent manner?
- Do our results support any of the current theories of attentional allocation?

Aim 2 does not conclusively implicate the PPC in position perception since we do not have direct evidence that PPC activity changes with the application of tDCS. Although we placed the electrodes over PPC in Aim 2, the spatial extent of modulation is unknown. Therefore, Aim 3 combined tDCS and fMRI to examine which cortical regions have task dependent tDCS-induced alterations of the BOLD signal. In particular, we sought to answer the following questions:

- Does tDCS induce widespread or more localized changes in the BOLD signal?
- Do voxels in PPC or other regions exhibit tDCS-induced polarity-dependent changes in the BOLD signal that predict perceived position?
- Do our results support any of the current theories of attentional allocation?

Each of these methods provides a specific contribution to the main goals of this research and all are necessary to show how different factors influence

position perception and which regions within the network of spatial processing control different aspects of visuospatial localization.

Chapter 2: **General Methods**

These studies consisted of five main experiments. All experimental conditions assessed centroid estimation under slightly different paradigms and each aim focused on a specific aspect of position perception. Aim 1 focused on specific factors that could influence centroid determination: retinal eccentricity (Experiment 1 – Bilateral-Cue), lateralized spatial attention (Experiment 1 – Unilateral-Cue), and motor-response bias (Experiment 2). Aim 2 focused on the influence of tDCS over PPC on centroid localization before (Experiment 3) and during (Experiment 4) the experimental task. Aim 3 focused on identifying neural correlates of position perception with fMRI (Experiment 5).

All experimental procedures were approved by the Institutional Review Board of Rutgers University and followed international guidelines for the ethical treatment of human subjects as expressed in the Declaration of Helsinki. All subjects provided written informed consent and reported normal or corrected-to-normal vision. The below section covers topics applicable to multiple experiments. Methods specific to individual aims and experiments will be discussed in the following applicable chapters.

Stimulus Display Apparatus

Experiments 1 – 5A

Stimuli appeared on a Sony FD Trinitron (GDM-C520) CRT monitor at a refresh rate of 120 Hz using custom software, Neurostim (http://neurostim.sourceforge.net), and viewed from a distance of 57 cm. The

display measured 40° (width) by 30° (height) and had a resolution of 1024 x 768 pixels.

Experiment 5B

As in the previous experiments we used Neurostim to present the visual stimuli. A Canon REALis SX80 Mark II LCOS projector back-projected the stimuli onto a screen located at the end of the MRI bore at a refresh rate of 60 Hz. Subjects viewed the stimuli via a mirror attached to the head coil. The combined distance of the screen to the mirror and the mirror to the subjects' eyes was 103 cm. The display measured 22° (width) by 12° (height) and had a resolution of 1920 x 1080 pixels.

Eye Tracking

Experiments 1 – 5A

A head-mounted Eyelink II eye tracker system (SR Research, Mississauga, Canada) recorded eye movements by tracking the pupils of both eyes at a sample rate of 500 Hz. Individually molded bite bars or a chin rest were used to reduce head movement.

Subjects were required to maintain fixation within a 3° × 3° or smaller square at the center of the display for the duration of each trial. Experiments 3 and 4 did not require fixation during the response epochs, but all other experiments did. Trials in which subjects failed to fixate appropriately were terminated immediately and repeated randomly at a later time within the block.

Experiment 5B

An MR compatible Eyelink 1000 eye tracker system (SR Research, Mississauga, Canada) recorded eye movements by tracking the pupils of the left eye at a sample rate of 250 Hz. We asked subjects to maintain fixation until they made their response.

Transcranial Direct Current Stimulation

Experiments 3 – 5A

We applied tDCS using an STG4000 series stimulus generator (Multi Channel Systems, Reutlingen, Germany) with a pair of saline-soaked sponges attached to conductive rubber electrodes (7.6 cm diameter). We placed the two electrodes (anode and cathode) over the locations of P3 and P4 (in accord with the international 10-20 method for EEG electrode placement). There was no separate reference electrode in this dual montage. Given the large size of the electrodes, the spread of current from these electrodes (A. Datta et al., 2009; Kar & Krekelberg, 2012), and the nominal location of the PPC (Dambeck et al., 2006; Herwig, Satrapi, & Schonfeldt-Lecuona, 2003; Hilgetag, Theoret, & Pascual-Leone, 2001; Pourtois, Vandermeeren, Olivier, & de Gelder, 2001; Sack et al., 2002), these montages are expected to generate significant electric fields in each subjects' PPC.

We had two tDCS experimental conditions; one for each polarity (anode over P3 and cathode over P4 or cathode over P3 and anode over P4). For Aim 2, the current was 1 mA for 15 minutes prior (Experiment 3) or during (Experiment 4) the presentation of visual stimuli. In Aim 3 (Experiment 5A) we increased the

current to 1.6 mA and only applied tDCS during the presentation of the stimuli. This resulted in current densities below 0.04 mA/cm^2, which is within current safety guidelines (Iyer et al., 2005; Nitsche, Liebetanz, et al., 2003). We increased and decreased the current linearly over a period of 10 s at the start and end of tDCS respectively, which has been shown to reduce subject discomfort (Nitsche, Liebetanz, et al., 2003). The majority of subjects were unable to distinguish the polarity direction significantly across all experiments.

The application of tDCS will generate tactile sensations. Therefore, if we used a condition without tDCS as our baseline condition it is likely subjects will be able to determine whether it was a baseline or experimental condition. Ideally, we wanted to have subjects blind to the tDCS condition type. To mask the tactile effects of tDCS we increased the current linearly to the applicable magnitude for each experiment over 10 s and then decreased the current back to 0 mA. This resulted in a total of 20 s of tDCS during the sham condition. This mimics the initial sensation of tDCS using a short duration of tDCS that should not influence behavior. We applied the sham tDCS using the same electrode montage. The majority of subjects could not distinguish the sham conditions from the experimental conditions, although additional subjects are needed in Experiment 5 to test the significance of these results. Another type of control paradigm used with noninvasive stimulation methods is to apply stimulation for the full duration over an area presumed to be uninvolved in the task. However, given the resolution of tDCS it is difficult to stimulate another region of cortex thought to be uninvolved in our experiments. Therefore, we did not use this method.

Experiment 5B

In this experiment we combined tDCS with MRI acquisition, which has previously been shown to be safe with minimal artifacts in MR images (Antal, Bikson, et al., 2012; Holland et al., 2011). However, one study has shown a reduction in the BOLD signal to noise ratio of 3 – 8 % (Antal et al., 2011). We followed setup similar to previous experiments (Antal et al., 2011; Holland et al., 2011). The stimulus generator was in the control room and connected to the MR compatible cables in the scanner room via a wall mounted connection equipped with a radio frequency (RF) filter. We then connected the MR compatible cable to the electrode leads each equipped with a 5.6 kΩ resistor to reduce transient increases in temperature as a result of induction voltages from the RF pulses. We placed each lead in a plastic covering to avoid overlapping wires and loops to prevent current induction (Brocke, Schmidt, Irlbacher, Cichy, & Brandt, 2008; Stagg, O'Shea, et al., 2009), and passed these leads out the side of the head coil and along the bore towards the back of the scanner.

We applied tDCS using an STG4000 series stimulus generator (Multi Channel Systems, Reutlingen, Germany) with conductive gel covered electrodes (7.6 cm diameter). We applied a current of 1.6 mA for 15 minutes while subjects completed the experimental task in the MRI machine. We again increased (decreased) the current linearly over a 10 s period at the start (end) of the stimulation period. For the sham (baseline) condition we increased the current to 1.6 mA experiment over 10 s and then decreased the current back to 0 mA. This resulted in a total of 20 s of tDCS during the sham condition. We placed the two

electrodes (anode and cathode) over the locations of P3 and P4 (in accord with the international 10-20 method for EEG electrode placement) as in the previous experiments with tDCS.

Chapter 3: **Quantifying Spatial Processes Using Behavioral Paradigms in Healthy Human Subjects (Aim 1)**

The experiments included in this aim have been published in the Journal of Vision (Wright, Morris, & Krekelberg, 2011). The Association for Research in Vision and Ophthalmology holds the copyright for this published work. We adapted this chapter from the published article.

Introduction

The purpose of Aim 1 is to quantify visuospatial integration in object localization behaviorally in healthy human subjects. Although multiple factors influence localization, we focused on the role of the retinal eccentricity of object components and attentional cues in a centroid estimation task. Given the conflicting results of the effects of retinal eccentricity on object localization and the limited research on the influence of spatial attention on object localization*, the main goal of Aim 1 was to determine whether and in what way these factors influence the local or global processing of centroid estimation.*

To better understand position perception, integration, and the roles of retinal eccentricity and spatial attention in these processes, we developed quantitative, descriptive models of visual target localization. We then used these models to analyze behavioral data from an experiment in which human observers localized the centroid of RDPs. While an RDP is not a natural stimulus, it has a complexity between that of a single dot and true extended objects, and is well suited to study spatial integration in a quantitative manner. Our results showed that subjects indicated the centroid of the RDPs reliably, but also had systematic,

eccentricity-dependent biases in this localization process. Moreover, attentional cues shifted the centroid toward the locus of attention. Our modeling results showed that both the effect of eccentricity and the effect of attention are explained most parsimoniously by assuming that the location of an extended object is determined as the weighted sum of its components. Each subject assigned weights to the components that varied with eccentricity: either higher or lower weights near the fovea. In addition, a non-predictive attentional cue led to a local increase in weights combined with an overall gradient toward the hemifield with the cue. This is consistent with the idea that attention acts on a representation of component positions (i.e., the dots), and not only on the outcome of the spatial integration process (i.e., a centroid estimate). Taken together these data suggest that spatial integration and its attentional modulation may take place in early visual representations and support the labeled line theory for position perception.

Methods

Participants

Nine subjects participated in Experiment 1. We excluded two subjects because they could not complete the minimum number of trials (see *Experimental Procedure* section) or could not perform the task. The remaining seven subjects ranged in age from 18 to 34 years. Two subjects were male and two subjects reported being left-handed. Subject 1 was an author (JMW); all remaining subjects were naïve to the purpose of the experiment.

Four subjects participated in Experiment 2. Subjects ranged in age from 21 to 34 years. One subject was female. All subjects were right-handed and two out of the four subjects also completed Experiment 1. All four subjects were naïve to the purpose of the experiment.

Visual Stimuli

The main stimulus was an RDP consisting of 25 small white (50 cd/m^2) squares (0.16° x 0.16°) on a black (0.4 cd/m^2) background. On each trial, 25 unique dot positions were selected randomly from a grid of 712 possible dot positions within a radius of 15° from the fixation point. Each potential dot location in the grid was 1° away from its nearest horizontal and vertical neighbor. In addition, no dots appeared within a 2° × 2° square region surrounding the fixation point (Figure 3-1A). The actual centroids of the RDPs across all trials approximated a normal distribution with a horizontal and vertical mean of 0° and a standard deviation of 1.5°.

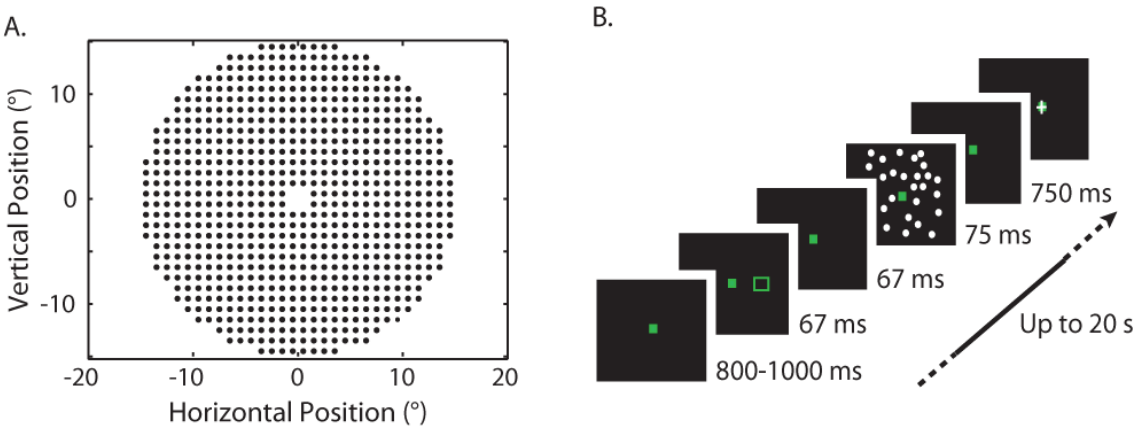

Figure 3-1: Experimental paradigm (Experiment 1). (A) Array of all possible dot positions. 25 positions were selected at random on each trial. (B) Sample trial from Experiment 1 (Right-Cue condition). Subjects fixated centrally for the duration of the trial. A non-informative cue appeared at an eccentricity of 7.5° just before the onset of the RDP. Shortly after the offset of the RDP, a cursor appeared at the point of fixation and subjects moved the cursor to the perceived centroid location.

In separate trials, the cue(s) appeared on the left, right, or on both sides of the visual display.

A green square outline (1° × 1°; line width: 0.12°) appeared at an eccentricity of 7.5° along the horizontal meridian. This non-informative cue appeared to both the left and right of fixation (Bilateral-Cue) or only on one side of the visual display (Unilateral-Cue) to cue attention exogenously. The central fixation stimulus was a small green square (0.12° × 0.12°), which remained visible for the duration of the trial at the center of the display.

Trial Presentation

Each block consisted of 200 trials. Blocks of Bilateral-Cue trials were interleaved with blocks of Unilateral-Cue trials within a session. Blocks of Unilateral-Cue trials contained both Left-Cue and Right-Cue trials presented randomly within the block. Typically, subjects completed three blocks of experimental trials per hour. All subjects received between 1 to 2 h (3 to 6 blocks) of training on the task prior to completing experimental trials. Data collected during the training blocks were not analyzed. Subjects completed blocks of trials from Experiment 2 in separate sessions.

Experimental Procedure

Experiment 1

The experimental task was to estimate the centroid of an RDP (Figure 3-1). In the Unilateral-Cue conditions, we examined the influence of exogenous attention on performance and cued subjects to one side of the visual display, either to the left (Left-Cue condition) or right (Right-Cue condition) of fixation. The goal of the Bilateral-Cue condition in this experiment was to assess effects of

retinal eccentricity on centroid estimation. Therefore, we balanced the allocation of exogenous attention across both sides of the visual display by presenting non-informative cues simultaneously to the left and right of fixation. We presented Bilateral-Cues instead of no cues to keep the visual display and the temporal structure of the task as similar as possible between the Unilateral- and Bilateral-Cue conditions.

Each trial began when the subject fixated the central fixation point. After a variable delay, the attentional cue(s) appeared for 67 ms (8 frames) just prior (134 ms) to the appearance of the RDP. This cue–target interstimulus interval was chosen to maximize effects of exogenous attention on behavioral performance (Cheal & Lyon, 1991; Muller & Rabbitt, 1989). The RDP remained visible for 75 ms (9 frames). A cursor (white crosshair; 50 cd/m^2, 0.51°) appeared at fixation 750 ms after target offset. Subjects were instructed to locate the centroid, i.e., average position, of all dots presented on a trial by moving a cursor to the centroid using a computer mouse in their right hand (regardless of handedness) and then clicking the left button.

All subjects completed a minimum of 600 experimental trials for the Bilateral-Cue condition and 800 experimental trials for each of the Left- and Right-Cue conditions.

Experiment 2

This experiment reexamined centroid estimates using a different mode of behavioral response (i.e., two-alternative forced choice, 2AFC). The procedure was identical to the Unilateral-Cue trials in Experiment 1 except that instead of a

cursor appearing 750 ms after target offset, a green probe line extending the full height of the display (0.04° width) appeared briefly (250 ms) to the left or right of the actual centroid of the RDP (offsets: −4°, −2.5°, −1.5°, −0.75°, −0.25°, 0.25°, 0.75°, 1.5°, 2.5°, 4°). Subjects indicated whether the perceived centroid was to the left or right of the probe line (Question A) by pressing the left or right arrow keys on each trial, respectively. To control for the possibility that the cue condition biased the subject's key choice rather than their perception per se, subjects also completed blocks in which they were instructed to make the reverse comparison, that is, whether the probe was to the left or right of the perceived centroid (Question B). Subjects first completed all blocks answering one question and then completed all blocks answering the other question. The order was counterbalanced across subjects. All subjects completed a minimum of 600 trials per instruction condition.

Data Analysis

Experiment 1

We conceptualize the estimation of centroids by human observers as a three-stage, weighted integration process with up to two sources of perceptual bias (early and late) in which the individual dot representations are first combined and then transformed into a behavioral response (Figure 1-1). The actual centroid of an RDP is the mean of the horizontal and vertical dot coordinates. Human centroid estimates are inevitably imperfect and include some degree of variable error (noise) as well as constant error (bias).

These sources of error could arise either by altering the local processing of the dot representations themselves (early bias, represented by ω_i) or by altering the output of the integration process within the global processing stage (multiplicative (β) or additive (ε) bias (late bias), represented collectively as B_g in Figure 1-1). To gain insight into the computations that underlie the subjects' centroid estimates, we developed quantitative models that describe the subject's response as a function of the actual centroid position (Equation 1) or in terms of a weighted integration of individual dot positions (Equations 2-5). In the following sections, we show only the equations for the horizontal (X) coordinates, but analogous equations were used for the vertical (Y) coordinates.

Model Descriptions

Bilateral-Cue Condition

Late Bias Model

The late bias model assumes that subjects integrate the dot representations veridically, but the output of the integrator is perturbed by a linear, eccentricity-dependent bias and/or constant bias. Accordingly, the model computes the perceived centroid $\hat{c}_x$ as a simple function of the actual centroid, c_x. Here, we consider a simple linear bias according to

$$\hat{c}_x = \beta_x c_x + \varepsilon_x \quad (1)$$

where β_x is a slope parameter that quantifies the magnitude of the eccentricity-dependent horizontal bias and ε_x is an error term along the horizontal dimension. The value of β in the fitted model for a given subject indicates whether the

observer had an overall linear foveofugal ($\beta > 1$) or foveopetal ($\beta < 1$) bias in their centroid estimates relative to the point of fixation. If $\beta = 1$, then there was no overall linear bias due to the retinal eccentricity of the centroid position. The parameter ε represents a constant bias in the centroid estimates across all trials regardless of the position of the actual centroid. We determined a separate β and ε for the vertical coordinates.

Although we report here only a linear late bias model, we did consider the possibility of other late bias models in which the perceived centroid is computed as a nonlinear function of the actual centroid position (e.g. a sigmoid). Qualitative assessments of the relationship between perceived and actual centroids suggested that approximately linear effects predominated and that the addition of nonlinear components to the late bias model was not necessary.

Early Bias Model – Weighted Average (Weighted Average Model):

The use of weighted average models in prior studies of localization (Landy, 1993; Landy & Kojima, 2001; McGowan et al., 1998) prompted us to also examine this descriptive model in our centroid estimation task. Unlike the late bias model, the weighted average model does not assume equal integration of all dot components. Rather, this model can capture an early bias in which individual dot representations contribute differently to the overall centroid estimate on the basis of their positions in the visual field. The weighted average model implements a normalized weighted sum of all dot positions on a given trial and also allows for a constant late bias, ε. Specifically, the weighted average model for displays containing 25 dots (as used in this study) is

$$\hat{c}_x = \sum_{i=1}^{25} \frac{\omega_i x_i}{\sum_{i=1}^{25} \omega_i} + \varepsilon_x \quad (2)$$

where $\omega_i = \omega(x_i, y_i)$ is a weighting function that assigns a weight to the *i*th dot on the basis of its horizontal and vertical position in the visual field (see below). A dot position with a higher weight contributes more to the centroid estimate, $\hat{c}_x$, compared to a dot position with a lower weight. Preliminary, non-parametric analyses, in which we used a spatially gridded model and allocated weights to specific grid locations (up to 120), showed that the effects of eccentricity were well described by a unimodal, Gaussian-shaped weighting function anchored at the point of fixation. Therefore, we chose the following form to describe the weights:

$$\omega(x_i, y_i) = ae^{-[\frac{{x_i}^2}{2\sigma_x^2} + \frac{{y_i}^2}{2\sigma_y^2}]} + b \quad (3)$$

The free parameters in this function determine the width (σ_x and σ_y) of the Gaussian function and a constant offset across all spatial positions, *b*. The amplitude of the Gaussian, a, was either +1 or -1 to model an upright or inverted Gaussian, respectively. By definition, all weights should be positive in a weighted average calculation, therefore, we constrained the weighting function to prevent negative weights (see below).

Early Bias Model – Weighted Sum (Weighted Sum):

The weighted sum model is similar to the weighted average model in that it allows for an unequal integration of the dot representations, but differs in that it does not include normalization of the weights (Equation 4). While this is a relatively minor mathematical change, the weighted sum model can capture a

wider range of response strategies (see *Discussion* section). We modeled the perceived centroid as:

$$\hat{c}_x = \sum_{i=1}^{25} \omega_i \, x_i + \varepsilon_x \quad (4)$$

We used the same two-dimensional, 2-D, Gaussian function for ω (Equation 3), now allowing the amplitude (a) to range freely. We again constrained the weighting function to only allow positive weights. While this is not imperative in a weighted sum calculation as it is in a weighted average calculation, in the context of our model, a negative weight would alter the sign of the dot component position. This would cause a dot to shift the perceived centroid towards the opposite hemifield. Preliminary (non-parametric) analyses showed that only one subject (S7) had a small subset (< 10%) of negative weights. Therefore, to maximize the similarity between the weighted average and weighted sum models, parameter constraints remained consistent in both cases.

Unilateral-Cue Condition

Late Bias Model

This model is exactly the same as the late bias model for the Bilateral-Cue condition (Equation 1) and we model the Left- and Right-Cue conditions separately, resulting in a unique late bias model for each condition. This model captures whether attention yields a constant bias in the centroid estimates across trials, ε, or modulates an eccentricity-dependent bias, β. We hypothesized that ε_x would differ between the Left- and Right-Cue conditions and, specifically, would be greater in the Right-Cue condition.

Early Bias Model – Weighted Sum (Weighted Sum):

The weighted sum model is the only early bias model we considered for the Unilateral-Cue conditions because it performed consistently better than the weighted average model in the Bilateral-Cue condition (see *Results* section). Here, we used an identical weighted sum model (Equation 4) but modified the weighting function (Equation 3) to account for lateralized attentional effects. Specifically, we hypothesized that attentional differences across the visual field may have altered the peak position or the width of the Gaussian weighting function from Equation 3. Alternatively, or in addition, attention may have imparted a more global change in which the contributions of dot positions in the attended visual field are enhanced while those on the opposite visual field are attenuated. To account for such effects, we allowed a shift of the peak (or trough) along the horizontal and vertical dimensions (μ_x and μ_y) and extended the weighting function with linear gradients in both the horizontal and vertical dimensions (m_x and m_y):

$$\omega(x_i, y_i) = m_x x_i + m_y y_i + ae^{-\left[\frac{(x_i-\mu_x)^2}{2\sigma_x^2}+\frac{(y_i-\mu_y)^2}{2\sigma_y^2}\right]} + b \quad (5)$$

In addition, we investigated other types of weighting functions including one that used multiple Gaussians to allow for bimodal peaks in weights, but did not find enough evidence to support the use of these alternate models.

Model Fitting

Model parameters were estimated separately for each subject and condition (Bilateral-, Left- and Right-Cue). Least squares fitting methods were used to minimize the model error concurrently across X and Y coordinates.

Pearson's correlation analysis confirmed that each of the fitted models had a significant correlation between the model predictions and subject responses (t (> 500) > 14, $p < 10^{-6}$).

To determine the parameter values in the late bias model, we used the *lsqcurvefit* routine from the Optimization Toolbox in Matlab 7.9 (The MathWorks, Natick, MA). The non-negativity constraint on the weights (see above) required us to use constrained nonlinear optimization to fit the weighted average and weighted sum models. To do this we used the *fmincon* routine from the Optimization Toolbox in Matlab with the following constraint; ($a + b$) > 0. We also constrained the lower and upper bounds for each parameter and set them as follows: μ_x and μ_y to -15 and 15 to keep the center of the Gaussian function within the stimulus display area, a, b and ε to -100 and 100, and σ_x and σ_y to 0 and 7.5 so that the Gaussian function would reach an asymptote level within the stimulus presentation area. Preliminary non-parametric analyses supported the use of 7.5° as the maximum value. We then used repeated curve fits, starting from 1000 random initial parameter choices within these bounds to find the optimal set of parameters. We used this optimal set of parameter estimates for subsequent analysis.

We determined 95% bootstrap confidence intervals (95% CI method) for each of the model parameters using the *bootci* function in Matlab. For each of 1000 bootstrapped sets, we resampled the data with replacement, and reran the *fmincon* procedure with the optimal parameters as initial values.

Comparing Models (AIC Method)

We used the Akaike Information Criterion (AIC) as a measure of relative model performance. This criterion allows the comparison of non-nested models that use different numbers of free parameters and penalizes a model for additional free parameters. Specifically, we used the least squares AIC;

$$AIC = n\ln(\frac{\sum \hat{\epsilon}^2}{n}) + 2\mathrm{K} \quad (6)$$

where n is the number of trials, $\hat{\epsilon}$ is the residuals for each trial, and K is the number of free parameters. This calculation assumes that the errors are normally distributed and have constant variance.

Note that for models with an equal number of parameters, the AIC value is essentially determined by the average squared residual error per trial (i.e., $\frac{\sum \hat{\epsilon}^2}{n}$, Model Prediction Squared Error, MPSE). We use this measure in the main text to provide an intuitive measure of performance. Statistically valid model selection, however, requires comparison of the full AIC values. Models with the lowest AIC value provide the most parsimonious account of the data. We followed the guidelines of Burnham and Anderson (2002) and considered a model to be notably better if its AIC value was less than another model's AIC by four or more units. Models with an AIC difference less than four were considered to be statistically indistinguishable.

Experiment 2:

For each offset of the probe relative to the true centroid position, we calculated the proportion of responses in which subjects judged the probe to be

to the left of the centroid. The data from separate cueing conditions (Left- and Right-Cue) were then fitted with separate cumulative Gaussian functions. The probe offset that corresponded to the inflection point of this psychometric function (point of subjective equality, PSE) was used as an index of the perceived centroid. Psychometric functions were fitted using the *psignifit* toolbox version 2.5.6 (Wichmann & Hill, 2001a, 2001b) in Matlab 7.9. We determined confidence intervals for the PSE using a bootstrapping method and used these confidence intervals to determine whether subject responses differed significantly between cueing conditions (95% CI Method).

Results

Behavioral Results

Centroid Estimation (Experiment 1: Bilateral-Cue)

We first confirmed that subjects were capable of identifying the approximate centroid of the RDPs. The constant error (i.e., bias), defined as the mean of the difference between the subjects' centroid estimates and the actual centroids, was 0.18° horizontally (*SE* = 0.09°) and -0.27° vertically (*SE* = 0.12°) across subjects (Figure 3-2A). Variable error, defined as the standard deviation of subject response error, averaged across subjects was 1.56° horizontally (*SE* = 0.18°) and 1.46° vertically (*SE* = 0.17°). We next calculated the correlation between the behavioral responses and the actual centroid on a trial-by-trial basis for each subject using Pearson's correlation coefficient. All coefficients were significant and ranged from 0.43 to 0.83 (t (> 500) > 14, p < 0.0001). This demonstrates that subjects used the positions of the dots on a trial-by-trial basis

to guide their behavioral responses and did not just click at the center of the screen.

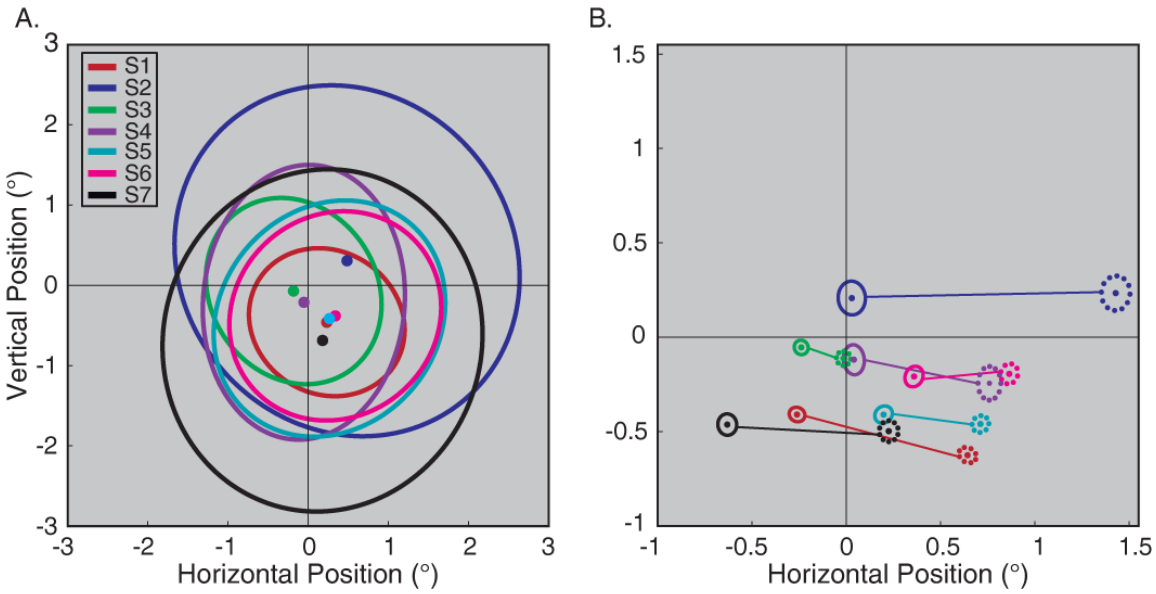

Figure 3-2: Behavioral responses per subject (Experiment 1). (A) Bilateral-Cue condition: Constant error (center of ellipse, dots) relative to the actual centroid (0, 0) and variable error (ellipse = 1 *SD*) for each subject. Negative values indicate a response to the left (x-axis) or down (y-axis) relative to the actual centroid. (B) Experiment 1. Unilateral-Cue conditions: Constant error (center of ellipse, dots) and variable error (ellipse = 1 *SE*) for Left-Cue (solid ellipse) and Right-Cue (dotted ellipse) conditions. Each pair of ellipses denotes 1 subject. For all subjects, the centroid estimate in the Left-Cue condition was significantly to the left (t (> 1500) < -4.5, p < 0.001) of the centroid estimate in the Right-Cue condition. Only S1 showed a significant shift in the vertical direction (t (1797) = 3.45, p < 0.001).

The correlation between subject response and the actual centroid does not eliminate the possibility that subjects may have used a subset of the dots in each trial to determine the centroid location. Previous studies have observed that some subjects place particular emphasis on the boundaries of objects (Findlay, Brogan, & Wenban-Smith, 1993) and localize a dot pattern at the centroid of the implied target shape rather than at the centroid of all the dot positions (Melcher & Kowler, 1999). Therefore, we investigated whether subjects determined the centroid of the implied shape, defined as the polygon formed by the dots along

the convex hull of the RDPs, rather than the centroid of all the dot components. Because the centroid of the implied shape and the true centroid of all the dots are inevitably correlated, we used partial correlation analysis to disentangle these influences on performance. The partial correlation between subject responses and the actual centroid using all of the dots (*Mdn* = 0.60), given the centroid of the implied shape, was significantly higher (rank sum statistic = 110; $p < 0.0001$) than the partial correlation between subject responses and the centroid of the implied shape (*Mdn* = 0.14), given the centroid of all the dots. Using the same methods, we also investigated whether subjects used the average position of the dots on the convex hull, and we found similar results. Therefore, there was no indication that subjects mainly used the outermost dots of the RDP when determining the centroid estimate. We will explore and quantify other behavioral strategies in more detail in the *Model Selection and Analysis* section.

Lateralized Spatial Attention (Experiment 1: Unilateral cue)

The main goal of the Unilateral-Cue condition was to determine how exogenous spatial attention influenced subjects' centroid estimates. In this condition subjects localized a centroid after being cued to either the left (Left-Cue condition) or the right (Right-Cue condition) side of the visual display.

We again found that subjects responded reliably even when cued unilaterally. The Pearson correlation between the centroid estimates and the actual centroid ranged from 0.57 to 0.84 (t (> 700) > 21, $p < 0.0001$). Importantly, attention yielded a significant horizontal bias in the direction of the attended locus for all subjects (t (> 1500) < -4.5, $p < 0.001$; see Figure 3-2B). The constant error,

averaged across subjects, was -0.07° (horizontal; *SE* = 0.13°) and -0.21° (vertical; *SE* = 0.09°) in the Left-Cue condition and 0.66° (horizontal; *SE* = 0.18°) and -0.27° (vertical; *SE* = 0.11°) in the Right-Cue condition. Only one subject (S1) had a significant difference, 0.22°, in the vertical direction (t (1797) = 3.45, p < 0.001). These differences are not due to subjects' eye position as their mean horizontal eye position during presentation of the RDP did not differ significantly between the Left-Cue condition, -0.11° (*SE* = 0.08°), and the Right-Cue condition, -0.12° (*SE* = 0.08°), for any of the subjects.

In addition, attention did not alter subject response variability, which was consistent across all conditions, i.e. Left-, Right- and Bilateral-Cue (one-way repeated measures ANOVA: F = 1.848, p = 0.20). The variable error in the Left-Cue and Right-Cue conditions ranged from 1.28° to 2.74°.

Motor-Response Bias (Experiment 2)

Given that subjects used the computer mouse to indicate the location of the centroid, it is possible that the findings of Experiment 1 were due to an effect of attention on the motor response rather than an effect on visual perception. Specifically, subjects might have simply clicked closer to the attentional cue without a true bias in the location of the perceived centroid. In Experiment 2, we assessed this possibility by repeating the Unilateral-Cue condition using a 2AFC response paradigm rather than a spatially directed motor response. Specifically, subjects were asked to report whether their *perceived centroid was to the left or right of a reference line* that appeared briefly after the offset of the RDP. Even in this paradigm, though, there is the possibility for motor-response bias. To allow

us to determine whether the cue biased the subjects' selection of button presses or their perception, we also reversed the task instructions (in separate sessions); that is, subjects were asked to report *whether the line was to the left or right of the perceived centroid*.

Figure 3-3A plots for one subject the percentage of trials in which the line was reported to be to the left of the centroid as a function of the physical offset of the reference line. For this subject, as for the majority of subjects (Figure 3-3B), the point of subjective equality (PSE) shifted in the direction of spatial attention and remained consistent in direction regardless of the specific task instructions. Thus, Experiment 2 confirms that the perceived centroid of RDPs shifts toward the locus of attention, regardless of the specific modality of motor response.

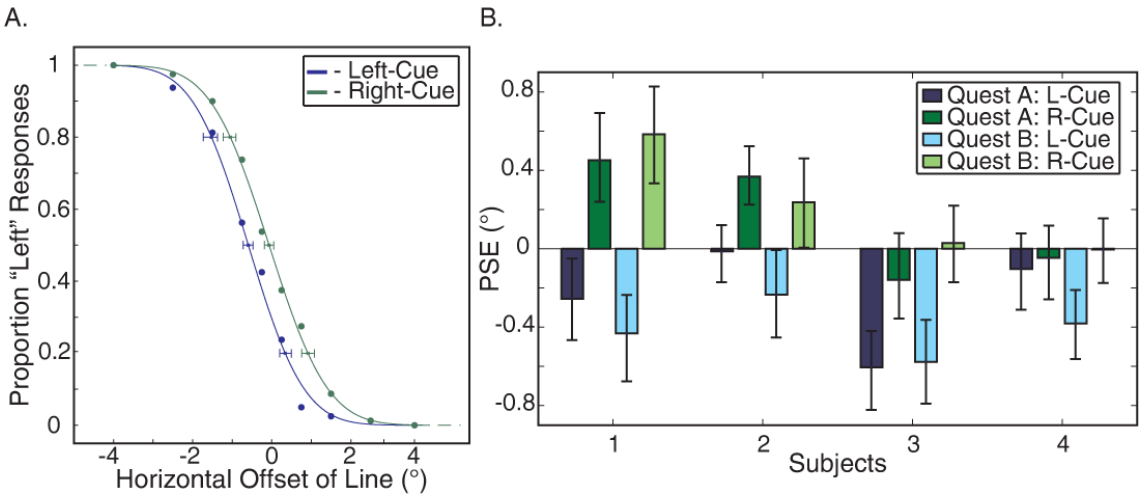

Figure 3-3: Centroid estimates in a 2AFC variant of the localization task (Experiment 2). (A) Psychometric functions for one subject. Each data point is the proportion of trials in which the subject chose the line as being left of the centroid for Left- (blue) and Right-Cue (green) trials. Horizontal axis indicates the physical offset between the reference line and the actual centroid. Error bars depict 95% confidence intervals for 25%, 50% [point of subjective equality (PSE)], and 75% thresholds. In this plot, data from trials in which subjects were asked to report whether the centroid was to the left of the line (Question A) and whether the line was to the left of centroid (Question B) are combined. This subject has a perceived centroid (PSE) significantly to the left in the Left-Cue condition relative to the Right-Cue condition. (B) Constant error (PSE) relative to the actual centroid for each subject. Each bar shows the PSE for a specific combination of cue condition (Left-Cue: blue bars; Right-Cue: green bars) and question type (A: darker bars; B: lighter bars). Negative values indicate perceived centroids to the left of the actual centroid. Error bars depict 95% confidence intervals. For both question types, the predicted perceived centroid in the Left-Cue condition was significantly to the left relative to the Right-Cue condition (t (1797) = 3.45, p < 0.001) for all but 1 comparison (Subject 4, Question A).

Model Selection and Analysis

In the *Behavioral Results* section, we showed that subjects localized centroids accurately though imperfectly, and spatial attention introduced further biases in this process. The goal of this section is to describe and understand these results in the context of a three-stage, weighted integration model (Figure 1-1). In this scheme, inaccuracies in centroid estimates could arise from improper weighting of the individual dot representations (early bias), from a bias in the output of the integrator (late bias), or both. To assess these possibilities, we

analyzed the data using three quantitative models that each implemented a different operation for the computation of centroids. In each case, the models were used to predict subjects' centroid estimates on a trial-by-trial basis using knowledge of the RDP dot positions.

Retinal Eccentricity (Experiment 1: Bilateral-Cue)

We first assessed the performance of a late bias model in which observers are assumed to compute a veridical centroid at an early stage of processing but then subject the output of this operation to a late bias that is a linear function of its retinal eccentricity (Equation 1). The slope parameter of this function, β, characterizes the eccentricity-related bias across the horizontal or vertical dimensions of the visual field. A β significantly less than one indicates an overall foveopetal bias in subjects' centroid estimates, and thus subjects tended to report the centroid to be closer to the fovea than its true position. A value of β significantly greater than 1 indicates that the observer had an overall linear foveofugal bias. Four out of the seven subjects had a significant foveopetal bias in the perceived centroid in both the horizontal and vertical dimensions (i.e., $\beta < 1$ [95% CI Method]; $M = 0.68°$, $SE = 0.03°$; Figure 3-4). In contrast, two out of the remaining three subjects had a significant foveofugal bias in the perceived centroid in both the horizontal and vertical dimensions, therefore their responses exaggerated the true eccentricity of the centroid (i.e., $\beta > 1$ [95% CI Method]; $M = 1.30°$, $SE = 0.1°$). The remaining subject had a significant foveofugal bias ($\beta = 1.20°$) in the horizontal direction and a foveopetal bias ($\beta = 0.78°$) in the vertical direction.

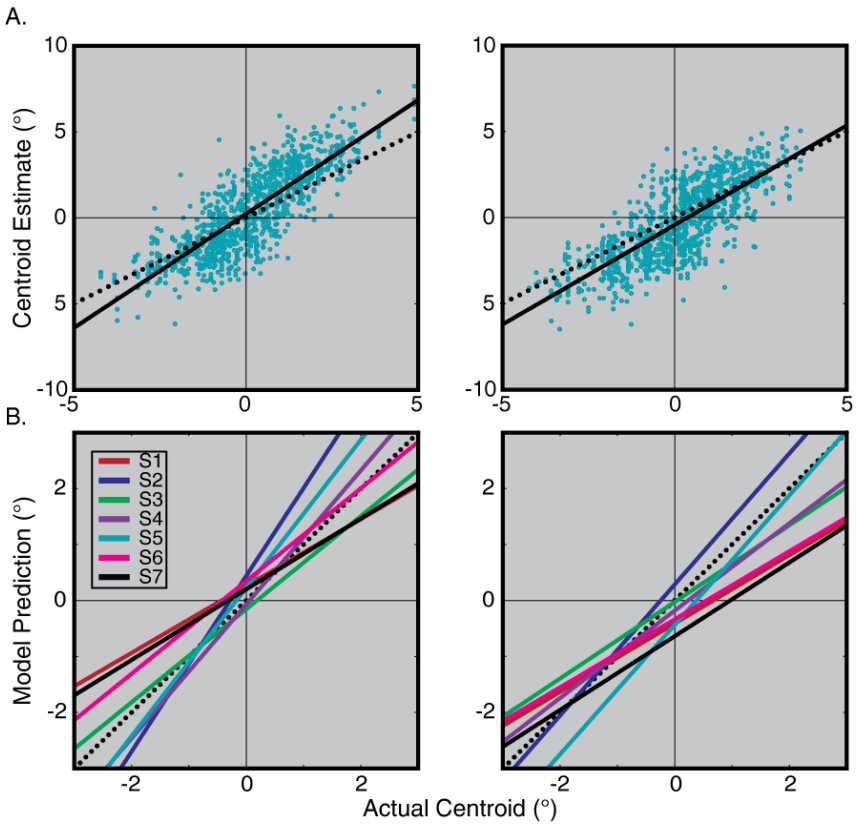

Figure 3-4: Late bias model (Experiment 1). (A) Centroid estimates of a single subject (S5) plotted against the actual centroid position for the horizontal (left) and vertical (right) dimensions. Fitted late bias linear regression model (solid line). This subject shows a foveofugal bias (i.e., $\beta > 1$). (B) Fitted late bias model for all subjects along the (left) horizontal and (right) vertical dimensions. Each solid line depicts the estimated behavioral response as a function of the actual centroid position for one subject using the fitted parameters from the late bias model. Four subjects show a significant foveopetal bias in both dimensions (red, black, green and pink), two subjects show a significant foveofugal bias in both dimensions (dark and light blue), and one subject shows a foveofugal bias along the horizontal dimension and a foveopetal bias along the vertical dimension (purple; 95% CI Method). Unity (dotted) line shows where the actual centroid equals the centroid estimate.

To probe for early biases, we evaluated models in which each dot in the RDP was assigned a weight based on its position in the visual field (Equations 2 and 4). In a preliminary analysis, we implemented a nonparametric model using a separate weight parameter for different regions across the visual field in which no assumptions were made about the shape of the underlying distribution of weights

across the visual field. These analyses showed some subjects with higher weights in more foveal locations that gradually decreased toward the periphery and others with the reverse pattern. This suggested that a 2-D Gaussian would provide an appropriate description of the distribution of weights across the visual field using only a small number of parameters. This Gaussian weighting function was used in two separate models: the weighted average (Equation 2) and weighted sum (Equation 4) models. The weighted average model differs from the weighted sum model in that it normalizes the weights assigned to each dot by the sum of the weights for all dots on a given trial (see *Methods* section).

Of these three models, the weighted sum model clearly performed best. For a more intuitive comparative measure of model performance, we calculated the squared residual error per trial for each model. We refer to this measure as the model prediction squared error (MPSE; see *Comparing Models (AIC Method)* section). The median MPSE across subjects for the weighed sum model was 3.48 deg^2 (1.03 deg^2 < MPSE < 7.69 deg^2), whereas the median MPSE for the late bias model was 3.94 deg^2 (1.09 deg^2 < MPSE < 8.57 deg^2) and 4.16 deg^2 for the weighted average model (1.24 deg^2 < MPSE < 9.28 deg^2). These comparisons of relative model performance, however, do not take into account the fact that each of the models: late bias, weighted average and weighted sum, has a different number of free parameters. We used the AIC to overcome this limitation. Lower AIC values indicate a more parsimonious model, and one model is considered to outperform another model significantly if its AIC value is lower than the comparison model by four or more units (Burnham & Anderson, 2002).

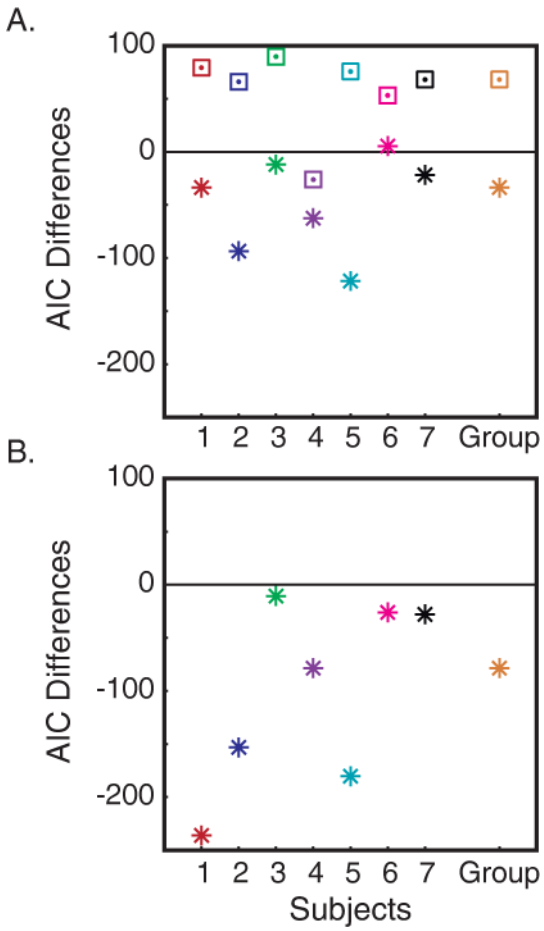

Figure 3-5: Comparison of relative model performance using the AIC (Experiment 1). The AIC values for each model, weighted average (squares) and weighted sum (asterisks), are plotted as difference scores relative to that observed for the late bias model (horizontal black line) for individual subjects (columns, color and number consistent with prior figures) and group median. Negative values indicate AICs lower than the late bias model. Lowest AIC value indicates best model. (A) Bilateral-cue. Weighted sum model has the lowest AIC in all but 1 case (S6) by four or more units. (B) Unilateral-cue. The AIC value for the weighted sum model was lower than the late bias model by four or more in all but 1 case (S6).

Figure 3-5A reports the AIC values for the early bias models (symbols) relative to that of the late bias model (horizontal line at zero). Thus, negative values indicate early bias models that outperform the late bias model. Using this criterion, the late bias model outperformed the weighted average model for six out of seven subjects. The weighted sum model, however, outperformed the late

bias model for six out of seven subjects (AIC differences; weighted average *Mdn* = 66.12, *SE* = 14.66; weighted sum *Mdn* = -33.62, *SE* = 17.43). Hence, this statistical analysis shows strong support for the weighted sum model.

Given that the weighted sum model best described the data, we next examined the subject-specific weight distributions from this model to assess the contribution of each dot component to subjects' centroid estimations. Four out of the seven subjects exhibited higher weights closer to the fovea (Figure 3-6, A-D), while the remaining three subjects displayed an opposite pattern, albeit with a smaller effect size (Figure 3-6, E-G). These weight patterns suggest that dot positions closer to the fovea influenced the centroid estimation more or less than would be expected from an equal integration of all dot positions. We confirmed that although some effects were small, the majority of subjects (six out of seven) displayed significant differential weighting: the amplitudes of the Gaussian weight functions differed significantly from zero (95% CI Method).

It is important to note that the pattern of weights across the visual field (i.e., an upright or inverted Gaussian function) does not map directly onto an overall foveopetal or foveofugal bias in performance. For example, Subject 5 has an overall foveofugal bias, but higher weights at the fovea (Figure 3-6B). This may seem counterintuitive, but in the weighted sum model, the overall magnitude of the weights indicates whether there is a general bias towards or away from the fovea. To understand this, consider a subject who calculates the true centroid of the dots; this subject's weights should be 0.04, since there are 25 dots presented on a trial. However, if the subject weighted the majority of dot positions below

0.04 there will be an overall foveopetal bias (Figure 3-6, D-G), whereas if the majority of weights are above 0.04 there will be an overall foveofugal bias (Figure 3-6, A & B). The relative magnitude of the foveal and peripheral weights only modulates this bias depending on the number of dots presented in each of those regions. For instance, a subject with the majority of weights above 0.04 and an upright Gaussian will overestimate the centroid of an RDP with many dots near the fovea less than an RDP with many dots in the periphery. The ability to capture such effects is a qualitative difference between the weighted sum and the less flexible weighted average model. We expand on this idea further in the *Discussion* section.

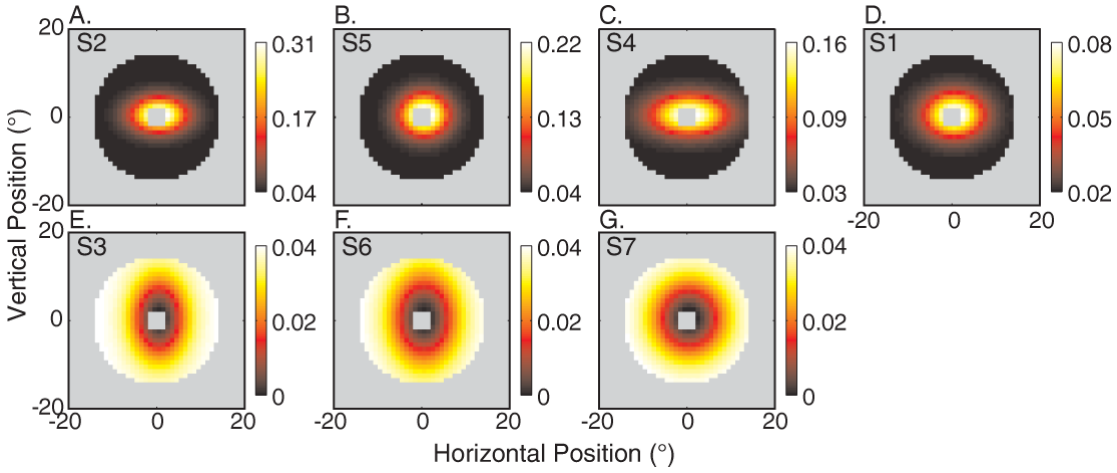

Figure 3-6: Eccentricity weight maps (Experiment 1: Bilateral-Cue condition). Weight maps were determined with the weighted sum model (Equation 3). The color maps indicate the weight at a particular spatial location with white being largest and black being lowest. Gray regions depict areas without any dot positions. (A–D) Weight maps showing higher foveal weights. Ordered from greatest effect size to smallest effect size. (E–G) Weight maps showing lower foveal weights for the remaining three subjects. Each panel has its own color map to allow the visualization of all subject weight patterns, even when idiosyncratic effect sizes were small. All subjects except one (S3), however, had a significant eccentricity-dependent weight gradient (see main text for details).

The significant parameters of the Gaussian weighting function and the superior performance of the weighted sum model relative to the late bias model

suggest that there is an influence of eccentricity on the encoding of individual dot positions, and hence an early bias. However, this does not imply there is not also a late bias. The error term, ε, in Equation 4 of the weighted sum model represents an additive late bias. For the majority of subjects (six out of seven) this term differed significantly from zero in both the horizontal (M = 0.17°; SE = 0.08°) and vertical directions (M = -0.25°; SE = 0.12°). This suggests the application of a rightward and downward bias after the integration of dot components.

Lateralized Spatial Attention (Experiment 1: Unilateral-Cue)

We next examined how spatial attention altered perceived centroids, again in the context of our three-stage spatial localization framework (Figure 1-1). Just as inaccuracies in baseline performance due to retinal eccentricity could have arisen from early or late computational biases, so too could our observed attentional effects. Because the weighted average model fared poorly in the previous section, we did not consider it here. We did, however, compare model performance of the late bias model and the weighted sum model. In the late bias model attention induces a linear bias on the actual centroid (Equation 1). In the weighted sum model attention could shift the Gaussian weighting functions (to model localized attraction by the exogenous cues), or induce a linear gradient within the weighting function (to model a more global attraction towards the attended side) (Equation 5). Across subjects, the MPSE per trial for the weighted sum model was 3.77 deg^2 (1.91 deg^2 < MPSE < 10.03 deg^2), whereas the median MPSE was 3.89 deg^2 for the Late Bias model (1.95 deg^2 < MPSE < 11.08

deg^2). To determine whether the weighted sum model is truly a better model given the additional free parameters, we compared the AIC values for the weighted sum model to the late bias model for the Unilateral-Cue conditions (Figure 3-5B). In all subjects, the weighted sum model significantly outperformed the late bias model (AIC difference; *Mdn* = -78.58, *SE* = 33.41). Therefore, we conclude that the weighted sum model gave the most parsimonious account of the influence of attention on visuospatial localization.

The specific pattern of weights in the weighted sum model during the lateralized attentional conditions provides insight into the mechanisms of spatial attention. To visualize the attention-induced changes in weights, we determined the differences between weights in the Left-Cue and Right-Cue conditions across the stimulus presentation area (Figure 3-7). While each subject's weight map showed an idiosyncratic pattern, there were clear commonalities that were also reflected in the population weight map (Panel H): A peak in weight differences in the left visual field and a trough in weight differences in the right visual field. This qualitative understanding of the weight maps was confirmed by a statistical analysis of the free parameters in the model. The slope of the horizontal gradient (m_x) in the Right-Cue condition was higher than that of the Left-Cue condition for all subjects (individually significant in four out of seven subjects, 95% CI Method). This shows a coarse effect of attention; weights in the attended visual field were generally greater than weights in the unattended field. At the same time, the peak of the weighting function (μ_x) was shifted rightward in the Right-Cue compared to the Left-Cue condition in five out of seven subjects (individually significant in

two subjects, 95% CI Method). This shows a more focused shift of attention towards the exogenous cue. Lastly, and unexpectedly, the late constant horizontal bias, ε_x, was larger in the Left-Cue compared to the Right-Cue condition in all subjects. This difference was individually significant in four out of seven subjects (95% CI Method). While this late bias is opposite to our expectation, additional analyses in which we omitted this term from the model generated qualitatively similar weight maps and had little effect on overall model performance.

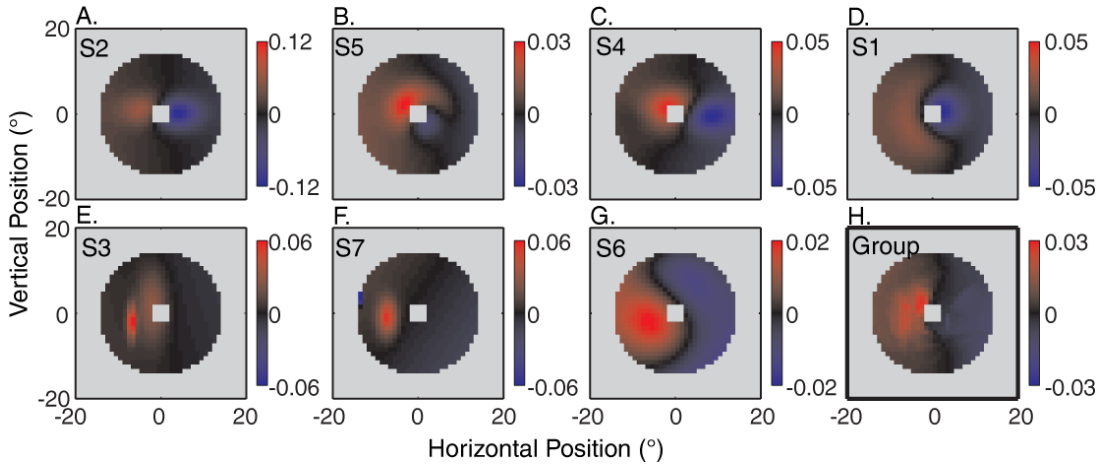

Figure 3-7: Attentional weight maps (Experiment 1: Unilateral-Cue conditions). Attentional weight maps were determined as the difference maps between the Left-Cue and Right-Cue conditions using the weighted sum model (Equation 5). Red indicates a location where the Left-Cue weight was higher and blue indicates a location where the Right-Cue weight was higher. Gray regions depict areas without any dot positions. (A–G) Subject-specific weight difference maps ordered the same as in Figure 3-6. In all cases, weights were enhanced in one or both of the visual fields that contained the exogenous cue. The local structure of these differences varied considerably across subjects. (H) Group weight difference map, obtained using the median of each weight difference at a specific spatial position across subjects.

Discussion

Our experiments and models investigated the role of retinal eccentricity and the locus of spatial attention in visuospatial localization. Although subjects

were reasonably accurate when determining the centroid of an RDP, our weighted sum model revealed systematic differences in the utilization of specific dot positions. First, subjects put significantly different weight on foveal regions compared to more peripheral regions of the visual field. Second, attentional cues yielded spatially specific increases in weights surrounding the focus of attention, as well as global increases in weights in the attended visual field. We conclude that the localization of extended objects consisting of multiple components is modulated by retinal eccentricity and attentional cues, and that the influence of attention includes a modulation of the eccentricity-dependent influence on the components.

We first discuss why the weighted sum model outperformed the weighted average model, then discuss our work in the light of earlier research on the localization of visual objects, and end with a speculative proposal for a neural implementation of the weighted sum model.

Weighted Sum Versus Weighted Average

If subjects calculated the true centroid, then both the weighted sum model using weights of 0.04 and the weighted average model using weights of 1 would have predicted their performance accurately. Our data, however, clearly showed that there are systematic errors in the localization of centroids due in part to differential weighting of specific dot positions. These errors were most parsimoniously captured by the weighted sum model, and not by the weighted average model. The difference between these models is the normalization across all weights in the weighted average model. Consider the subjects with

lower weights surrounding the foveal regions; the normalization of the weighted average model would inevitably lead to a foveofugal bias. Contrary to this intuition, some of our subjects with this inverted Gaussian weighting pattern nevertheless showed a foveopetal bias. Hence at an abstract level of description one can speculate that the subjects did not perform an appropriate normalization in their centroid calculation.

Retinal Eccentricity

All subjects showed differential weighting of dot positions depending on retinal eccentricity. Higher foveal weights might have been expected given earlier reports of foveal biases in localization tasks (Mateeff & Gourevich, 1983; O'Regan, 1984; van der Heijden et al., 1999), and lower foveal detection thresholds (Johnson, Keltner, & Balestrery, 1978). We hypothesized initially that the three subjects with higher peripheral weights may have placed particular emphasis on the dots along the boundary of the stimulus (Findlay et al., 1993). However, we eliminated the possibility that subjects actually calculated the centroid of the implied shape of the RDP using partial correlation analysis. In addition, there was no evidence to indicate that subjects with an inverted Gaussian pattern showed a higher partial correlation between the subject responses and the centroid of the implied shape given the actual centroid of the dots. Alternatively, enhanced sensitivity to transient stimuli for more peripheral targets may have contributed to this pattern. Given that the RDP was displayed very briefly, peripheral positions may have exerted greater influence on behavioral responses than foveal dots. An interesting prediction of this

hypothesis is that individual variations in sensitivity should correlate with idiosyncratic localization weight patterns. Lastly, we examined whether gender or handedness predicted the type of weight pattern. We found no relationship between these factors and the weight pattern, however, our sample size is limited.

A previous study reported similar weighting patterns (Drew et al., 2010) relative to the true centroid of an RDP. Since eye position was not restricted in that study, however, it is not possible to assess how the retinal eccentricity of each dot position influenced the final weighting, and how that may have played into the weighting relative to the true centroid. Conversely, because our true centroid positions were relatively close to the fovea, the eccentricity bias we observed could also reflect these “object-centered” effects of Drew et al. (2010). However, when we examined weighting relative to the true centroid of each RDP, we did not find similar weight patterns across subjects. To further disentangle centroid-centered and fovea-centered weighting a future study would need to both control eye position and vary centroid position systematically and over a wider range than in our study.

Related to this, even though we interpret our finding as an effect of eccentricity, we acknowledge that the subjects could have developed a bias to respond closer to the fovea because that was the average location of the centroid over all trials, or because they had to maintain fixation at the center of the display throughout the entire trial. Such effects, however, would depend only on the location of the centroid, not the positions of the individual dots; hence, our

finding that an early bias model outperformed the late bias model speaks against this interpretation.

In contrast to our results, McGowan and colleagues (1998) found no evidence of differential weighting due to dot position. We believe this can be attributed to the small size of their RDPs; even in our experiments the weighting was relatively constant on a small scale. McGowan et al. (1998) also found a strong nonlinear effect of dot proximity, such that isolated dots had a stronger influence on the centroid than clustered dots. Although we found some support for such effects in our data, they were weak and not consistent across subjects. This may also be the consequence of our larger RDPs and concomitant larger spacing between the dots.

Lateralized Spatial Attention

Consistent with earlier reports of attentional mislocalization of single dots (Tsal & Bareket, 1999), we showed that centroid estimates were shifted in the direction of (exogenously cued) attention. Our modeling results showed that this was most parsimoniously captured as a change in the weighting function in the weighted sum model such that locations near the cue received larger weights than locations remote from the cue. This enhancement was not restricted to the location of the cue as we also found a more general increase in weights across the attended side of the visual field.

To our knowledge ours is the first study to show that spatial attention differentially alters the usage of the components of a target in a localization task. One way to interpret these findings is that attentional modulation acts, at least in

part, on early visual representations. Consistent with this, the weight patterns that our behavioral data reveal are similar to those found using functional imaging (R. Datta & DeYoe, 2009), which leads us to speculate about possible neural mechanisms.

Neural Mechanisms

While the weighted sum model used in our experiments is a descriptive model, we speculate that it may be implemented neurally as distortions in the population activity of early visual neurons. In this view, the input layer in Figure 1-1 would correspond to an early retinotopic area where receptive fields correspond to specific locations on the retina; these neurons are labeled lines for position. If a downstream area performs the centroid computation by computing the inner product of each neuron's label and its firing rate, then any distortion or inhomogeneity in the population firing rate would lead to a misperception. In terms of neural mechanisms, eccentricity-dependent weighting (i.e. distortions or inhomogeneities in the neural response) may result from differences in receptive field size, cortical magnification, latency differences, or other differences in local circuitry (Roberts, Delicato, Herrero, Gieselmann, & Thiele, 2007).

To account for a late bias, the region that computes the centroid or a region further downstream may further bias the centroid computation to yield the final perceived centroid. Given that our data show that subjects perform an imperfect normalization across all dots when performing the centroid task, one way to interpret these data is that they reflect changes in the neural activity

normalization process (Heeger, 1992) with eccentricity or changes in attention (Reynolds & Heeger, 2009).

Alternatively, the bias due to attention could be the result of well-known attentional modulation of neuronal activity of early visual areas (for a review see Kastner & Ungerleider, 2000; Reynolds & Chelazzi, 2004), attentional modulation of receptive field location (Womelsdorf, Anton-Erxleben, Pieper, & Treue, 2006; Womelsdorf, Anton-Erxleben, & Treue, 2008), or the eccentricity-dependent attentional modulation of spatial integration (Roberts et al., 2007). Our behavioral data are too coarse to distinguish among the relative contributions of these processes; future studies using functional imaging or electrophysiological recordings are required to determine how visual cortex integrates spatial information and generates a percept of position.

Chapter 4: **Manipulating Spatial Processes Using Transcranial Direct Current Stimulation (Aim 2)**

The experiments included in this aim have been published in the Journal of Vision (Wright & Krekelberg, 2014). We adapted this chapter from the published article.

Introduction

If the effects of attentional cueing on localization, as shown in Aim 1, were due to attentional mechanisms then modulating neural activity in PPC, a region implicated in attention, could systematically alter localization. We reasoned that an imbalance in the activity of the PPC in the two hemispheres could induce spatial mislocalization as suggested by theories of interhemispheric competition (J. D. Cohen et al., 1994; Kinsbourne, 1977; Szczepanski, Konen, & Kastner, 2010). Therefore, *the main goal of Aim 2 is to investigate the causal involvement of PPC in visual localization*.

We used tDCS over PPC of healthy human volunteers and investigated how the stimulation affected the centroid estimation of a one-dimensional (1-D) horizontal RDP. Given the lateral placement of the attentional cues and the large behavioral effect specific to the horizontal dimension in Experiment 1, see Figure 3-2, we changed from a 2-D stimulus to a 1-D stimulus for this aim and also Aim 3. We placed one electrode over left PPC and the return electrode over right PPC (dual tDCS) to maximize the imbalance between left and right PPC excitability (Giglia et al., 2011), and thereby maximize a potential behavioral

effect. Specifically, we reasoned that an **a**node placed over the **r**ight **PPC** combined with a cathode over the left PPC (we refer to this montage as rPPCa) should increase excitability of the right PPC and decrease excitability of the left PPC. If the allocation of attention was driven by a linear combination of the activation levels across both PPCs, the rPPCa montage would increase the allocation of attention to the left visual field and, based on our previous behavioral findings (Wright et al., 2011), induce leftward localization compared to stimulation with the reverse polarity (rPPCc). Both Experiments 3 and 4 confirmed this hypothesis.

The same, admittedly somewhat simplistic, logic predicts that the rPPCa (rPPCc) montage should induce leftward (rightward) localization when compared to a more traditional sham stimulation control. However, neither Experiment 3 nor 4 confirmed this prediction, and we present possible explanations for this finding in the *Discussion* section.

A final motivation for the experiments in this aim was a recent finding that alternating current stimulation reduces visual adaptation and is particularly effective when applied during but not before the presentation of a visual stimulus (Kar & Krekelberg, 2014). This inspired us to not only use a typical tDCS design that measured the after-effects of stimulation by applying stimulation before the start of the behavioral trials, but also a design in which stimulation was applied during the behavioral experiment. We found that the behavioral effect was similar in amplitude regardless of whether the stimulation was applied before or during task performance. However, this experiment revealed a novel and

interesting time course: the behavioral effects had a rapid onset and then dissipated over ~10 minutes, even with continuing stimulation. After tDCS offset the behavioral effects resurfaced and then dissipated again in ~10-15 min.

Methods

This study consisted of two main experiments. In the first experiment, we applied tDCS prior to all experimental trials (tDCS-Before) and in the second experiment we applied tDCS concurrently with experimental trials (tDCS-During).

Participants

12 subjects (all right-handed; six male; age range 18-34 years) participated in both experiments. Subject 1 was an author (JMW); all other subjects were naïve to the purpose of the experiments. In the tDCS-Before experiment, the performance of one subject deviated largely from the remainder of the subjects. This subject had an effect of tDCS that was opposite in sign to 9 of the remaining 11 subjects and more than 3 *SD*s from the population mean. Therefore, we excluded this subject from all further data analysis for the tDCS-Before experiment.

Visual Stimuli

The 1-D RDP consisted of seven small white (76 cd/m^2) squares (0.20° x 0.20°) on a black (0.4 cd/m^2) background. On each trial, seven unique dot positions, selected from a grid of 32 possible dot positions, appeared on the display. The grid extended from -15.5° to 15.5° relative to the vertical midline at a constant height of 3° above the horizontal midline. Each dot location in the grid was 1° away from its nearest horizontal neighbor(s). The actual centroids of the

RDPs across all trials approximated a normal distribution with a mean of 0° and a standard deviation of 1.5°.

A green square outline (1° × 1°; line width: 0.12°) served as an exogenous cue for attention. This cue appeared at an eccentricity of 8.08° in either (or both) the left or right visual field and was centered over two grid locations; (-7.5°, 3°) and (7.5°, 3°), respectively.

The central fixation stimulus was a small red square (0.16° × 0.16°), which remained visible for the duration of each trial at the center of the display. One block contained a minimum of 120 trials with the three cue conditions interleaved.

Experimental Procedure

Centroid Localization Task

In each of the experiments, the task was to estimate the centroid of a 1-D RDP (Figure 4-1B). We manipulated exogenous attention by cueing subjects to one side of the visual display: either to the left (Left-Cue condition) or right (Right-Cue condition) of fixation. In a baseline condition, we cued subjects to both sides of the display (Bilateral-Cue condition). This kept the visual display and the temporal structure of the task as similar as possible between the cue conditions thus avoiding confounding the influence of spatial attention with temporal uncertainty (Morris et al., 2010).

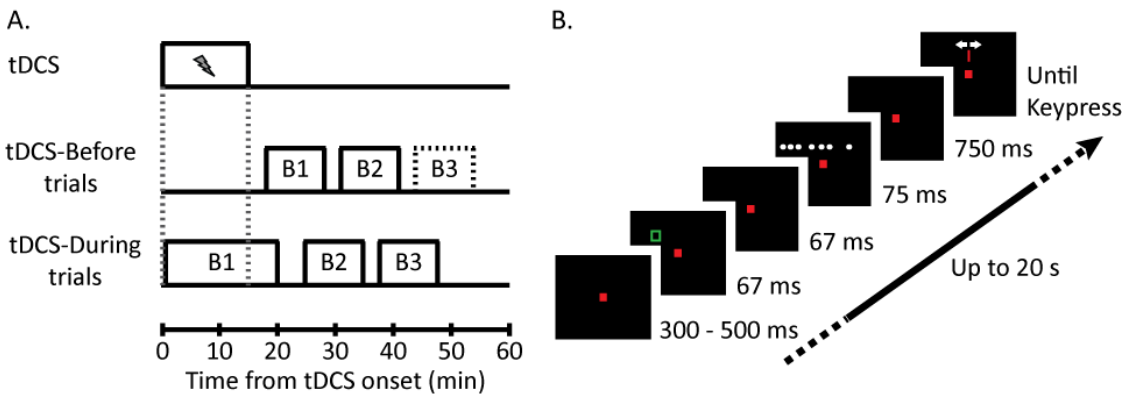

Figure 4-1: Experimental paradigm (Experiments 3 and 4). (A) In both experiments tDCS was applied for 15 min at the start of a session (top trace). In the tDCS-Before experiment (middle trace) subjects completed at least two blocks of trials following tDCS offset. In the tDCS-During experiment, trials began 20 s after tDCS onset and subjects completed an additional two blocks of trials after tDCS offset. (B) Example trial (Left-Cue condition). Subjects fixated centrally until the RDP disappeared. A non-informative cue appeared at an eccentricity of 8.08° just prior to the onset of the RDP. After 750 ms from the offset of the RDP, a cursor appeared at the center of the grid and subjects moved the cursor to the perceived centroid location.

Each trial began when subjects fixated the central fixation point. After a variable delay (300 – 500 ms), the attentional cue(s) appeared for 67 ms (eight frames) just prior (134 ms) to the appearance of the RDP. This cue-target interstimulus interval maximizes effects of exogenous attention on behavioral performance (Cheal & Lyon, 1991; Muller & Rabbitt, 1989) and induces shifts in perceived centroid location (Wright et al., 2011). The RDP remained visible for 75 ms (nine frames). A cursor (red vertical line 0.04° x 0.5°) appeared at the center of the grid of dots (0°, 3°) 750 ms after target offset. Subjects then located the centroid of all dots presented on a trial by moving the cursor to the centroid using a computer mouse in their right hand and then clicking the left button (Figure 4-1B).

Experiment 3: tDCS-Before

Each session began with subjects seated in a darkened room for 15 minutes while receiving rPPCa, rPPCc, or sham tDCS. During tDCS, subjects viewed a black visual display (0.4 cd/m^2) and were allowed to listen to music. After the stimulation period, subjects performed the centroid localization task in a minimum of two blocks of trials for a total of at least 200 trials (Figure 4-1A).

Experiment 4: tDCS-During

In these sessions, subjects received 15 minutes of tDCS (rPPCa, rPPCc, or sham) while they performed the centroid localization task after a short delay (20 s) at the beginning of the session to avoid interference from the initialization of stimulation. Subjects continued completing experimental trials for 5 minutes following tDCS offset (approximately 400-500 trials in total). After this 20 min period for each stimulation type, subjects completed two blocks of experimental trials without stimulation for a total of at least 200 additional trials (Figure 4-1A). The experimental task was the same as in Experiment 3.

Session Ordering

All subjects completed a minimum of 12 sessions: six tDCS-Before and six tDCS-During sessions. We used a repeated measures design, therefore, for each experiment, subjects completed two sessions per stimulation condition, i.e. rPPCa, rPPCc, and sham. Six subjects completed all tDCS-Before sessions prior to tDCS-During sessions. We used the same randomized order of stimulation conditions per subject in each of these experiments so that differences could not be attributed to session ordering. However, we recognized that there could be a

training effect by completing all tDCS-Before sessions prior to the tDCS-During sessions. Therefore, in the remaining subjects we interleaved the tDCS-Before and tDCS-During sessions and assigned the stimulation conditions randomly across subjects and experiments. We did not find any qualitative differences due to session ordering between subject groups, therefore, we analyzed all subjects together.

Initially, subjects received between 1 to 2 h (three to six blocks) of training on the localization task. Data collected during these training blocks are not reported here, however, we ensured that accuracy and the correlation of subject responses to the actual centroid at the end of training were comparable to subsequent measures during the experiment. After these practice runs, subjects participated in only one session per day.

Data Analysis

Population Response Error Functions Over Time

We first determined the mean response error relative to the actual centroid as a function of time per stimulation session and subject. To do this, we grouped behavioral responses in a single session into non-overlapping time bins of 250 s. We then determined the mean response error for each time bin that contained at least 30 trials. To account for time gaps introduced by breaks between sessions, we used the *interp1* function in Matlab 7.14 (The MathWorks, Natick, MA) to interpolate between the bins using a shape-preserving piecewise cubic spline. We did not extrapolate beyond the first or last time point in a session. We then

used the interpolated functions and averaged the mean responses per time point across sessions to generate one time course per subject and montage.

To determine the difference in behavioral responses between rPPCa and rPPCc stimulation, we subtracted the subject-specific rPPCa interpolated time course from the rPPCc interpolated time course. Therefore in the resultant time course, positive values indicate that the perceived centroid in the rPPCc stimulation condition was more to the right relative to the rPPCa stimulation condition. We performed a similar analysis between the rPPCa (rPPCc) and sham conditions where positive values indicate that the perceived centroid during rPPCa or rPPCc stimulation was more to the right relative to the sham condition. To view the effect of stimulation across the population, we determined the median response across subjects at each time point. We only included time points with data from nine or more subjects. The error bars represent the median absolute difference between the subject response and the population median scaled by the square root of the number of subjects, and significance of individual data points was tested with Wilcoxon signed-rank tests.

Significance Tests

We first verified if our sample met conditions of normality using the Jarque-Bera method (*jbtest* function in Matlab 7.14). If the sample violated assumptions of normality we used nonparametric significance tests and report the median and range of the data in lieu of parametric measures. The main population level analysis of significance was based on a repeated measures ANOVA (rmANOVA) with the following within-subject factors: stimulation type

(rPPCa, rPPCc), cue location (Left-, Right-, Bilateral-Cue) and centroid position (more than 2.5° left, less than 2.5° left, less than 2.5° right, more than 2.5° right of fixation).

Partial Correlation Difference (PCD)

The location of the centroid and the bisection point of the outermost dots are correlated in our stimulus. Hence, even if subjects actually performed a bisection task, they could still perform reasonably well on the centroid task. To disentangle the influence of the centroid from the bisection point on the behavioral responses of each subject we calculated the pairwise partial correlations between the behavioral response, the centroid, and the bisection point. We reasoned that the partial correlation with the highest value identified the response strategy that subjects most likely utilized across trials. To assess the statistical significance of the difference between these partial correlation values, we compared the actual difference in partial correlations with a null distribution created by 1000 random shuffles of the behavioral responses per subject. A PCD was considered statistically significant if it exceeded the 95^{th} percentile of this null distribution.

Results

Subjects reported the centroid of a briefly presented 1-D RDP. We applied tDCS through electrodes placed over the left and right PPC. There were three stimulation conditions: anode over right PPC combined with the cathode over left PPC (rPPCa), anode over left PPC combined with the cathode over right PPC (rPPCc) and sham stimulation.

Before showing the influence of tDCS, we first present an analysis of the subjects' performance on the behavioral task that confirms they can reliably assess the centroid of our 1-D dot stimulus, and that their localization behavior is consistent with previous reports.

Task Performance – Sham

As a general measure of task performance, we determined subject response bias and variability relative to the actual centroid for the sham condition regardless of cue condition. The response bias, defined as the mean of the absolute difference between subject responses and the actual centroid across trials, was 0.38° (*SE* = 0.10°) across subjects. The variable error, defined as the standard deviation of the subject response error across subjects, was 1.81° (*SE*: 0.06°). Across subjects, the Pearson correlation between the behavioral responses and the actual centroid ranged from 0.74 to 0.91 ($p < 0.001$). This confirms that –similar to 2-D dot displays (Wright et al., 2011) – subjects reliably estimated the centroid of the 1-D stimulus. We also analyzed the subject response error while maintaining the sign of the error and found that most subjects showed a rightward bias, which was individually significant in six subjects ($t (\geq 700) > 2.85$, $p < 0.01$, $d > 0.11$). Three subjects showed a significant leftward bias ($t (\geq 700) < -5.09$, $p < 0.01$, $d < -0.19$). This is similar to the variability seen in previous line bisection studies (Jewell & McCourt, 2000).

Consistent with our previous findings using 2-D RDPs (Wright et al., 2011), we found that the attentional cue significantly shifted perceived location as revealed by a main effect of cue location (rmANOVA; $F (2, 20) = 4.22$, $p = 0.03$,

η_p^2 = 29.68, see *Significance Tests* section). Subjects' responses were more leftward in the Left-Cue condition (*M* = 0.06, *SE* = 0.09) relative to either the Bilateral-Cue (*M* = 0.25, *SE* = 0.10) or Right-Cue conditions (*M* = 0.29, *SE* = 0.10). One of our goals was to investigate whether this pattern of mislocalization induced by exogenous cues could also be generated by transcranial stimulation of PPC. Finally, subjects had a foveal bias as revealed by a main effect of centroid position (F (3, 30) = 8.35, $p < 0.001$, η_p^2= 45.50). The magnitude of this foveal bias increased for more peripheral centroids (*M* = 0.97, *SE* = 0.05) compared to more foveal centroids (*M* = 0.56, *SE* = 0.04). Such a foveal bias has been reported previously (Mateeff & Gourevich, 1983; O'Regan, 1984; Stork et al., 2010; van der Heijden et al., 1999).

tDCS-Before (Experiment 3)

Next, we investigated how tDCS over PPC affected localization. As discussed previously, current views of tDCS suggest that excitability is increased underneath the anode and excitability is decreased underneath the cathode. Furthermore, the current evidence supports the view that each PPC mainly allocates attention and responds predominantly to visual stimuli in the contralateral visual hemifield (see *Discussion* section). Given these assumptions, the most sensitive analysis to detect whether tDCS of left and right PPC affects localization is to compare the sessions where the anode was placed over right PPC and the cathode over left PPC (rPPCa condition) with the sessions in which the anode and cathode were reversed (rPPCc condition). Below we will present

those results first, and then drill down to further comparisons between stimulation and sham.

In this experiment stimulation was applied before subjects completed experimental trials. We subtracted the average response error in the rPPCa condition from the average response error in the rPPCc condition for each subject. Positive differences indicate a shift in the perceived centroid to the right under rPPCc stimulation relative to rPPCa stimulation. A population level rmANOVA (see *Significance Tests* section) revealed a significant main effect of stimulation (F (1, 10) = 10.86, p = 0.008, η_p^2 = 52.06). At the single subject level, 9 out of 11 subjects had a positive difference (M = 0.09, SE = 0.03) and the effect was individually significant in three subjects (t (≥ 720) ≤ -1.99, p < 0.05, d ≤ -0.1, Figure 4-2).

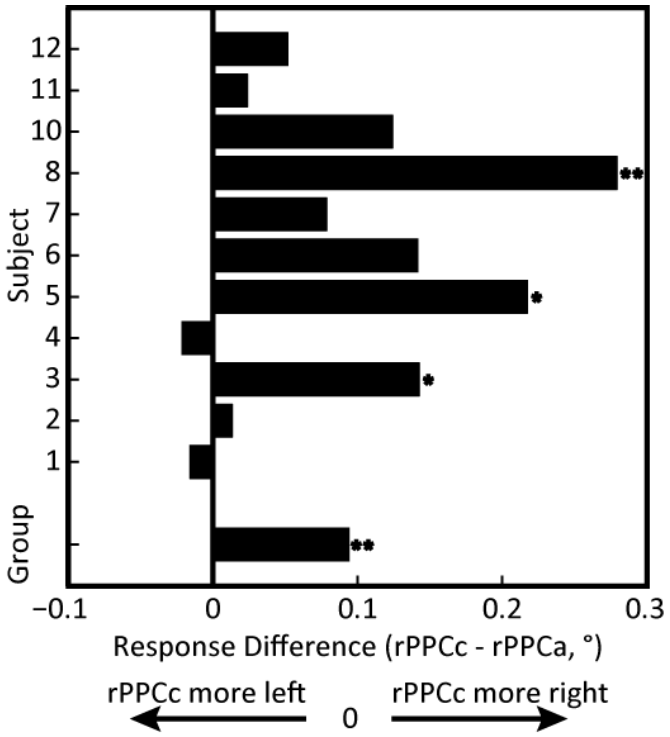

Figure 4-2: tDCS-induced mislocalization after tDCS comparing rPPCc and rPPCa stimulation (Experiment 3). Bars show the difference in average response errors

between the rPPCc and rPPCa conditions for each subject and the group average (bottom bar). Positive values indicate rPPCc responses that were shifted more to the right relative to the rPPCa responses. Asterisks indicate significance (*$p < 0.05$; **$p < 0.01$). The rPPCc montage shifted the perceived centroid location rightward compared to the rPPCa montage, supporting the involvement of the PPC in localization.

We did not find a significant interaction between montage and cue-location (F (2, 20) = 0.92, p = 0.42, η_p^2 = 8.39), hence we found no evidence that stimulation was more or less effective depending on the locus of attention. This was further supported by a control analysis in which we investigated only the Bilateral-Cue condition and found that the influence of stimulation was qualitatively the same as in the full data set. Similarly, there was no significant interaction between montage and centroid position (F (2, 20) = 1.58, p = 0.22, η_p^2 = 13.61). Given this lack of significant interactions we pooled the data across cue-location and centroid location for all further analyses.

Figure 4-3 shows the time course of the behavioral effect of tDCS (see *Population Response Error Functions Over Time* section). As before, positive values indicate that the perceived centroid shifted more rightward under rPPCc stimulation compared to rPPCa stimulation. The aftereffects of stimulation dissipated within approximately 15 min. In principle, this dissipation could be confounded by fatigue or other stimulation-independent factors that affected overall performance on the task. To exclude this possibility, we compared performance in the first and second block of trials in the sham condition and found no significant differences in the mean response error (Wilcoxon signed-rank test; Z = -0.78, p = 0.43) or the variable error (Z = -1.33, p = 0.18). We

conclude that the temporal dissipation shown in Figure 4-3 can be ascribed to the waning influence of the tDCS stimulation.

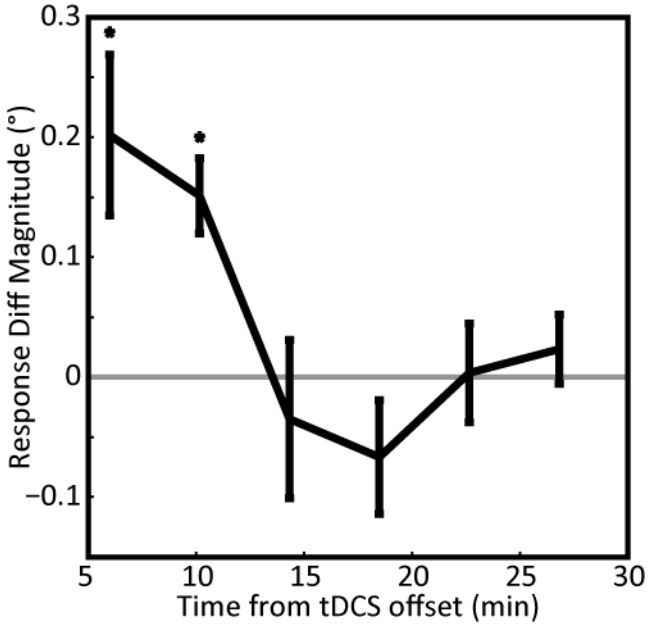

Figure 4-3: Time course of response errors after tDCS (Experiment 3). The black curve shows the response differences, rPPCc – rPPCa, as a function of time, averaged across all subjects. Positive values indicate that rPPCc stimulation shifted the perceived centroid rightward relative to rPPCa stimulation. Asterisk denotes significance at $p < 0.05$. The graph shows that the aftereffect of tDCS dissipated over a period of approximately 15 min.

The above-described mislocalizations may also result if tDCS affected subject's eye position. We monitored fixation and aborted trials in which eye movement strayed beyond 1.25° from the fixation point, but this leaves a window of error that allows for small deviations in eye position. For example, if rPPCc caused the eye position to deviate slightly to the left, dot positions could appear more rightward yielding a rightward mislocalization relative to rPPCa especially if rPPCa induced opposite effects in eye position. We therefore examined the horizontal displacement in eye position during the presentation of the RDP. A population level rmANOVA (see *Significance Tests* section) revealed no main

effect of stimulation (F (1, 10) = 0.37, p = 0.56, η_p^2 = 3.24), attention cue (F (2, 20) = 1.93, p = 0.17, η_p^2 = 14.95) or centroid position (F (3, 30) = 0.85, p = 0.48, η_p^2 = 7.19) on eye position. Limiting the analysis only to trials within 15 minutes of tDCS offset also did not reveal any significant effects. Therefore, we conclude that our results are not a result of changes in eye position.

Figure 4-4 compares performance in the rPPCa and rPPCc conditions to sham stimulation. Somewhat surprisingly, we found that the sign of the directional bias was the same in the rPPCa and rPPCc conditions for most subjects. Across the population this effect was highly significant (sign test; p < 0.01). Given that the subjects also had idiosyncratic biases in the sham condition (see *Task Performance – Sham* section) we investigated whether those biases could predict the effect of tDCS. The correlation between the sign of the bias in the sham condition (left/right) and the sign of the effect of tDCS, however, was not significant (r (9) = 0.24, p = 0.48).

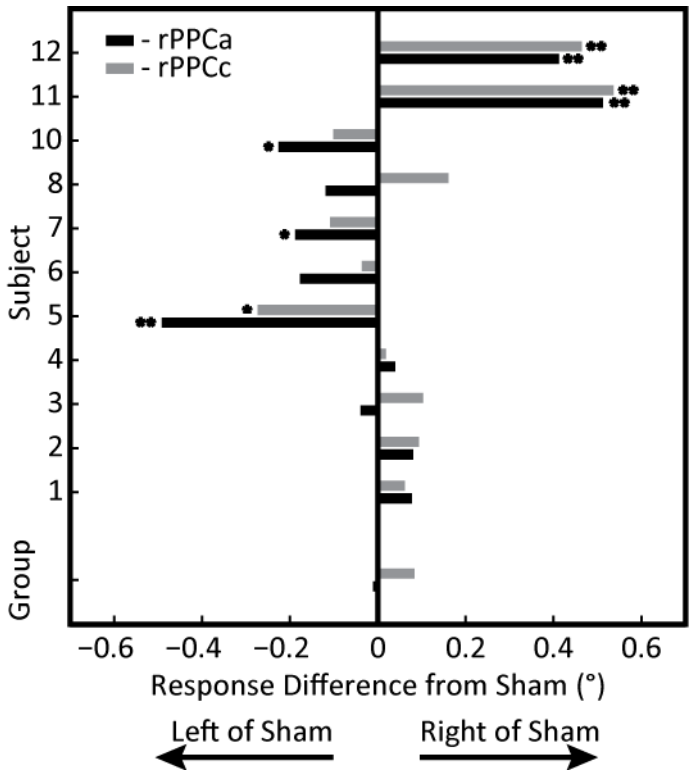

Figure 4-4: tDCS-induced mislocalization after tDCS comparing rPPCa and rPPCc to sham stimulation (Experiment 3). rPPCc (gray) and rPPCa (black) mislocalization relative to sham stimulation for each subject and the group average (bottom bars). Positive values indicate rightward shifts in response relative to sham. Asterisks indicate significance (*$p < 0.05$, **$p < 0.01$) for a specific subject and stimulation condition compared to sham. This graph shows that the sign of the behavioral effect differed across subjects, but that rPPCc effects were typically more rightward than rPPCa effects (see also Figure 4-2).

tDCS-During (Experiment 4)

In the first set of experiments, tDCS was applied before the subjects performed the task. In other words, the behavioral effects we reported were aftereffects of tDCS. This mimics the typical use in many clinical studies, but there is increasing evidence that tDCS specifically targets populations of neurons that are active (Kar & Krekelberg, 2013). Based on this we performed a second set of experiments in which tDCS was applied concurrently with the task.

Following the analysis of Figure 4-3 we again determined the time course of the stimulation effect, subtracting the effect of rPPCa from rPPCc stimulation (Figure 4-5). The behavioral effect was largest at the start of tDCS and dissipated over approximately 8 min of ongoing stimulation. The behavioral effect increased again once stimulation had ended, and lasted approximately 10 min following stimulation. Even though the latter phase of the tDCS-During experiment is not an exact replication of the tDCS-Before experiment, its time course (including the magnitude) is similar to that shown in Figure 4-3.

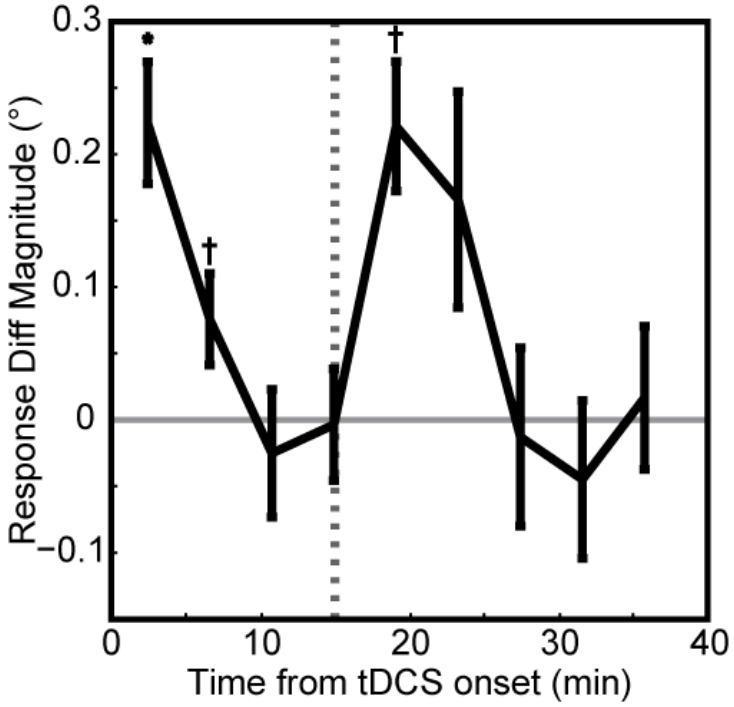

Figure 4-5: Time course of response errors during and after tDCS (Experiment 4). The black curve shows the response differences, rPPCc – rPPCa, as a function of time, averaged across all subjects (see *Population Response Error Functions Over Time* section). Positive values indicate that rPPCc stimulation shifted the perceived centroid rightward relative to rPPCa stimulation. The dashed line indicates tDCS offset. One asterisk denotes significance with $p < 0.05$ and a cross denotes a trend at $p < 0.10$. This figure shows that tDCS induced both short-term effects which dissipated even while current was applied and an aftereffect which lasted ~10 min (as in Figure 4-3).

Figure 4-6 shows the response error differences for individual subjects in the early (A) and late (B) phases. This graph shows that the rightward shift when comparing rPPCc to rPPCa is found consistently across subjects both during tDCS and immediately after tDCS (F (1, 10) = 10.69, p = 0.008, η_p^2 = 49.29). However, separate population rmANOVAs on each phase revealed a significant effect of stimulation in the early (F (1, 10) = 15.67, p = 0.002, η_p^2 = 58.75) but not in the late phase (F (1, 10) = 0.83, p = 0.38, η_p^2 = 7.03) due to Subject 2 who displayed a large deviation, more than 2 *SD*s, from the rest of the group. Given the consistency in the overall direction of the effect, the large intersubject variability in the comparison with sham stimulation (Figure 4-7) is remarkable.

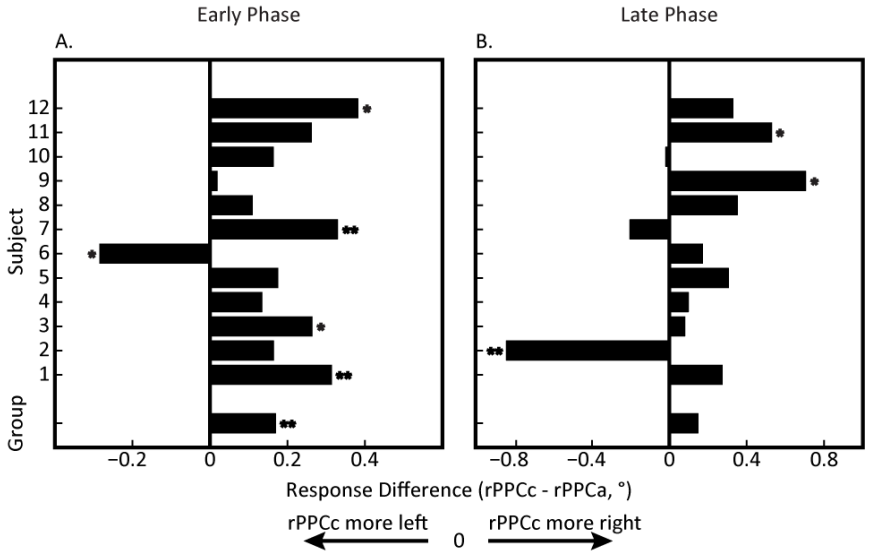

Figure 4-6: tDCS induced mislocalization during and after tDCS comparing rPPCc and rPPCa stimulation (Experiment 4). (A) Early phase during tDCS: 0-8 min after tDCS onset and (B) late phase after tDCS offset: 2-10 min after tDCS offset. Positive values indicate rPPCc responses that were shifted more to the right relative to rPPCa responses. These graphs show that rPPCc tDCS typically induced rightward shifts compared to rPPCa tDCS across both the early and late phase. Asterisks indicate significance (*p < 0.05, **p < 0.01).

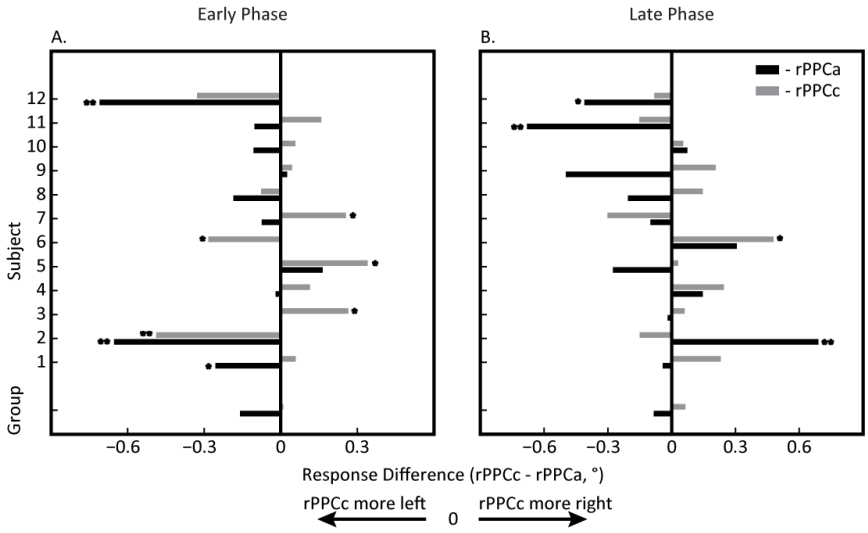

Figure 4-7: tDCS induced mislocalization during and after tDCS comparing rPPCc and rPPCa to sham stimulation (Experiment 4). (A) Early phase during tDCS: 0-8 min after tDCS onset and (B) Late phase after tDCS offset: 2-10 min after tDCS offset. Positive values indicate rightward shifts in rPPCc (gray) and rPPCa (black) responses relative to sham. These graphs show a large degree of intersubject variability when comparing stimulation to sham, but –as shown in Figure 4-6– a consistently rightward shift when comparing rPPCc and rPPCa. Asterisks indicate significance (*$p < 0.05$, **$p < 0.01$).

Similar to the tDCS-Before experiment there were no systematic deviations in eye position that would explain these behavioral effects. We performed two population level rmANOVAs (see *Significance Tests* section) to demonstrate this. The first used trials in the early phase (0 – 8 min following tDCS onset) and the second in the late phase (2 – 10 min following tDCS offset). Both analyses showed no main effect of stimulation (F (1, 10) < 0.47, $p > 0.51$, $\eta_p^2 < 4.04$), attention cue (F (2, 20) < 2.04, $p > 0.15$, $\eta_p^2 < 15.62$) or centroid position (F (3, 30) < 2.07, $p > 0.12$, $\eta_p^2 < 15.81$) on eye position.

Task Strategy – Control Analysis

Although we instructed subjects to determine the centroid of each RDP, it is possible that subjects instead utilized only the positions of the two outermost dots and localized the bisection point. This would make our task similar to

traditional line bisection tasks. Because the bisection point is correlated with the centroid location, accurate performance on the centroid task (shown above) does not exclude a bisection strategy. The strategy followed by the subject is relevant for our definition of localization error. For instance, if a subject actually performed bisection, but we defined errors with respect to the true centroid, our measure could be insensitive, or even biased. We performed a number of analyses to rule out such possible confounds.

To determine which of the two strategies subjects employed we used a partial correlation analysis (see *Partial Correlation Difference (PCD)* section). We first used the sham trials regardless of cue condition. In four subjects the partial correlation between the behavioral responses and the actual centroid was higher than the partial correlation between the responses and the bisection point ($0.40 < PCD < 1.05$, $p < 0.001$). We infer that these subjects most likely adopted a true centroid localization strategy. Three subjects showed the reverse pattern ($-0.44 < PCD < -0.36$, $p < 0.001$). It is possible that these subjects adopted a bisection strategy. The remaining four subjects showed no significant difference ($|PCD| < 0.09$, $p > 0.10$). Analyzing the partial correlation values across the rPPCa and rPPCc conditions showed that the response strategies typically remained consistent across montages (8 out of 11 subjects).

Finally, we investigated whether a subject-specific definition of localization error (i.e. relative to the bisection point for subjects that appeared to follow a bisection strategy, and to the centroid for subjects that appeared to follow a centroid strategy) affected any of our results. It did not; neither for the tDCS-

Before nor for the tDCS-During experiment. For simplicity, we therefore defined error for all subjects as the mismatch between the actual and the reported centroid for all analyses.

Discussion

Our experiments investigated the causal involvement of PPC in visual localization. We show that tDCS with electrodes placed over the left and right PPC alters visual localization. Specifically, placing the anode over left PPC and the cathode over right PPC induces a rightward shift in perceived centroid location relative to the reverse montage. This finding was consistent across subjects and occurred whether the stimulation was applied well before or during the performance of the localization task. Surprisingly, behavioral effects dissipated during the application of tDCS, but resurged after stimulation offset to dissipate again over a period of ~10-15 min.

Below we first discuss the novel insight our experiments provide about tDCS, and how uncertainties inherent in tDCS affect our interpretation of the data. Finally, we discuss a number of potential mechanisms that could underlie the behavioral effects induced by tDCS.

The tDCS Method

The behavioral effects of tDCS vary based on multiple factors; electrode size, placement, current amplitude, current duration, etc. (for a review see Nitsche et al., 2008). For example, a recent study has shown that 2 mA of tDCS for 20 min over the right IPS altered selective attention, whereas 1 mA of current did not (Moos, Vossel, Weidner, Sparing, & Fink, 2012). Sparing and colleagues

(2009), on the other hand, found differences in visual detection and line bisection with only 1 mA of tDCS for 10 minutes over PPC. A direct comparison is difficult since effects may be task specific, other stimulation parameters, such as electrode size, differed between the experiments and because current flow within the brain depends on idiosyncratic brain folding (A. Datta et al., 2011; Wagner, Fregni, et al., 2007). We interpret these findings as showing that a relatively large degree of variability is expected both within and across tDCS studies.

In addition, the little that is known about the modes of action of tDCS at the neural level leads one to expect a high degree of complexity. For instance, cell morphology, and cell orientation with respect to the applied field affects the outcome in terms of membrane depolarization measured in-vitro (Radman, Ramos, Brumberg, & Bikson, 2009). Our previous behavioral findings (Kar & Krekelberg, 2014) as well as unpublished observations in the macaque monkey (Kar & Krekelberg, 2013), furthermore suggest that electrical stimulation affects cells in a state dependent (inactive/active/adapted) manner. As a consequence, the net effect of stimulation in-vivo is not easy to predict and may well include neural changes that are not well described by changes in excitability.

One specific potential explanation for the large intersubject variability when comparing stimulation to sham is that the electrical fields induced by tDCS are idiosyncratic due to individual differences in brain folding (A. Datta et al., 2009; A. Datta, Zhou, Su, Parra, & Bikson, 2013; Wagner, Fregni, et al., 2007). If the orientation of the induced field in a critical subregion of PPC is opposite to that induced in another subject, one would predict quite different (potentially

opposite) changes in excitability and therefore potentially opposite behavioral effects. The finding that the difference between our two stimulation conditions is nevertheless consistent across subjects can be attributed to the fact that the fields generated in the rPPCa condition are oriented approximately opposite to those generated in the rPPCc condition (limited only by the accuracy of electrode placement). Hence, for each subject, if excitability in a subregion of PPC increased during rPPCa, one would expect it to decrease during rPPCc. This neural consistency should be reflected in behavioral consistency, which is indeed what we found (Figure 4-2 and Figure 4-6). Taken together this analysis suggests that due to the idiosyncratic nature of induced electric fields a comparison of tDCS and sham conditions across subjects should be interpreted with caution, but that some intersubject variability can be removed by comparing montages in which the anode and cathode are reversed.

Effects of tDCS Over Time

Previous studies have shown that the aftereffects of tDCS can last for a few minutes up to 2 hr (Mielke et al., 2013; Nitsche & Paulus, 2001; Nitsche, Schauenburg, et al., 2003). The duration appears to depend on the behavioral paradigm, the electrode montage, as well as other stimulation parameters. In our experiments the aftereffects were relatively short-lived (<15 min) and, even more interestingly, we observed that the behavioral effects dissipated during the application of tDCS. This time-course points to mechanisms other than pure excitability changes and is consistent with the idea that different mechanisms may underlie the effect of tDCS applied during and before a task (for a review

see Stagg & Nitsche, 2011). We speculate that the decline of the behavioral effect during stimulation is due to homeostatic mechanisms that compensate for the effects of tDCS by returning network activity to its baseline levels after a sustained increase in excitability (Iyer, Schleper, & Wassermann, 2003; Turrigiano, Leslie, Desai, Rutherford, & Nelson, 1998). This clearly has implications for the use of tDCS in a therapeutic setting.

If these homeostatic mechanisms are indeed triggered by tDCS, one might expect to see an aftereffect of opposite sign after tDCS offset. Instead, we found a behavioral effect with the same sign after tDCS offset (in both experiments). It is possible that our ability to resolve behavioral effects temporally is too coarse to see a negative aftereffect (especially because some homeostatic mechanisms operate on a scale of seconds (Benucci, Saleem, & Carandini, 2013)). In addition, other mechanisms such as synaptic plasticity have been implicated in the aftereffects of tDCS (Liebetanz, Nitsche, Tergau, & Paulus, 2002; Nitsche, Fricke, et al., 2003; Nitsche et al., 2005), and these may mask any aftereffects of homeostatic regulation. Direct investigations at the cellular level are needed to resolve these issues of mechanism.

Clearly, uncertainty about the mode of action of tDCS limits the forcefulness with which we can draw conclusions from our experiments and it is possible that some of our conclusions (and those of others) may have to be revisited once a better mechanistic understanding of tDCS has been developed. With that caveat, we continue the discussion based on the common, but

simplifying, assumption that excitability is typically increased beneath an anode and decreased beneath a cathode (Nitsche & Paulus, 2000).

Motor Control

We placed the electrodes at P3 and P4 to maximize the induced electric fields in the PPC, and to maximize behavioral effects by increasing excitability in one hemisphere and decreasing it in the other hemisphere. Even though recent studies support the focality of transcranial electrical stimulation to a particular brain region by showing specific behavioral and/or BOLD signal changes related to the stimulated area (Antal et al., 2004; Antal et al., 2011; Meinzer et al., 2012), we cannot eliminate the possibility of current spread to regions beyond PPC (Wagner, Fregni, et al., 2007). Of particular relevance in this context is the possibility that current spread to motor cortex may have altered the subject's localization response (without changing their percept). However, if current spread to motor cortex were the sole cause of the behavioral effects, one would expect to see changes in reaction time (Gandiga, Hummel, & Cohen, 2006) or in the accuracy of the movements (Vines, Nair, et al., 2006). We found no evidence for this. Alternatively, if tDCS changed excitability in the motor region of the right hand, one may expect, for instance, that anodal stimulation over left PPC would generate larger amplitude responses. Instead, we found an overall foveal bias regardless of centroid position. Therefore, we conclude that our effects are not simply due to changes in the motor response but reflect changes in perception driven by the modulation of PPC.

Mechanisms Underlying the Behavioral Effect

Our data show that tDCS over PPC induced changes in perceived centroid position. Since the involvement of PPC in spatial localization is complex, our stimulation protocol may have affected a number of neural mechanisms that affected the perceived centroid position. In our view a modulation of the mechanisms underlying attention is the most likely because the tDCS-induced mislocalization was similar to the mislocalization induced by exogenous attentional cues, but we also discuss alternative or additional explanations here.

The ICT provides a useful framework to interpret our findings. Previous studies have shown that the disruption of the right PPC with TMS induces leftward errors in line bisection (Brighina et al., 2002; Fierro et al., 2000) and anodal stimulation of the lesioned hemisphere in neglect patients (or cathodal stimulation of the nonlesioned hemisphere) reduces spatial deficits in a line bisection task (Ko et al., 2008; Sparing et al., 2009). Our main findings (Figure 4-2, Figure 4-3, Figure 4-5 and Figure 4-6) provide additional support in healthy observers by showing that dual (anodal/cathodal) stimulation of the PPC in the two hemispheres induced mislocalization towards the hemifield contralateral to the anode. In our experiments there was no statistically significant interaction between the location of the attentional cue and the effect of tDCS. In other words, tDCS' putative effect on the attentional opponency was additive. We note, however, that the ICT also predicts that mislocalization with rPPCa stimulation should have the opposite sign of the mislocalization induced with rPPCc relative to baseline (sham). This prediction was rejected by our findings (Figure 4-4 and

Figure 4-7). If tDCS indeed only generates an additive change in excitability (see above), this implies that the competition/interaction between the two hemispheres is not well described by a simple linear subtraction. Given the large number of parietal regions that are potentially involved in the allocation of attention, and the complexity of their interaction (Szczepanski & Kastner, 2013; Szczepanski et al., 2010), this may not be too surprising.

A second possible mechanism is that tDCS may have interfered with a pre-attentive visual representation of the dot stimuli in PPC. For instance, altering the balance of activation between left and right PPCs may have boosted signal or reduced noise (Vicario, Martino, & Koch, 2013) in a lateralized manner, which could result in mislocalization.

Finally, neurons in PPC are known to have eye-centered receptive fields (Hartmann, Bremmer, Albright, & Krekelberg, 2011), which are modulated by eye position (Andersen, Essick, & Siegel, 1985). Recent work in the macaque monkey has demonstrated that these representations can account for a foveal bias (Morris, Bremmer, & Krekelberg, 2013), as well as mislocalization during eye movements (Morris et al., 2012). This implies that modulating the activity of PPC by tDCS also modulates an internal eye position signal (but not eye position itself, as shown above). For instance if higher firing rates in right PPC correspond to eye positions to the right of the midline, then increased excitability of the right PPC (rPPCa montage) would result in a rightward error in the eye position signal and therefore rightward mislocalization (Morris et al., 2012). This argument hinges on the assumption of a particular hemispheric bias in the eye position

signal. Such biases have been found in primary visual cortex (J. B. Durand, Trotter, & Celebrini, 2010), but not in parietal cortex of the macaque (Bremmer, Distler, & Hoffmann, 1997). A more quantitative assessment of the viability of this mechanism therefore requires more insight into the nature of eye position signals in the human PPC (Merriam, Gardner, Movshon, & Heeger, 2013).

Conclusions

Applying dual tDCS to the right and left PPC generated mislocalizations similar to those found after the presentation of an exogenous visual cue. This supports the causal involvement of the PPC in visual localization and suggests that the balance of activation between the hemispheres is a determining factor in localization. We also found a novel time course for tDCS-induced behavioral effects; there were short-term effects which dissipated while tDCS was still being applied, and aftereffects that arose after the offset of tDCS.

Chapter 5: **Identifying Neural Correlates of Position Perception (Aim 3)**

Introduction

We show support that PPC plays a causal role in visual localization in Aim 2, however, this is contingent on tDCS modulating neural activity in PPC. Behavioral studies alone do not provide enough evidence to determine how tDCS modulates PPC (or surrounding regions). In this aim, we use fMRI to noninvasively measure tDCS-induced changes in PPC neural activity indirectly by assessing changes in the BOLD signal. Therefore, one of the main goals of Aim 3 is *to investigate tDCS modulation of PPC by analyzing the tDCS-induced changes in the BOLD signal within PPC.* Aim 2 also suggested that the lateralized changes in localization due to different tDCS montages may result from the influence of attention networks in a manner consistent with the ICT. Therefore, the second main goal of Aim 3 is *to investigate whether interhemispheric differences in the BOLD signal in PPC predict localization behavior.*

However, independent from any experimental task, there are many questions concerning how tDCS affects the BOLD signal. Previous studies have suggested that tDCS produces localized changes in the BOLD signal in regions under the electrode presumably due to changes in neural activity (for a review see Turi, Paulus, & Antal, 2012). However, increases (decreases) in neural excitability as a result of tDCS may not yield increases (decreases) in the BOLD signal especially if tDCS effects are a result of nonlinear mechanisms. In support of this, previous studies have shown variability in the BOLD signal changes in

regions under the electrodes (Antal et al., 2011; Holland et al., 2011; Stagg, O'Shea, et al., 2009). Previous studies have also shown far reaching changes in the BOLD signal, presumably due to anatomical/functional connectivity (Antal et al., 2011; Meinzer et al., 2013). However, tDCS also yields changes in the BOLD signal from non-neural mechanisms, we expand on this further in the *Discussion* section (S. Durand, Fromy, Bouye, Saumet, & Abraham, 2002; Vernieri et al., 2010). Since there are a limited number of studies combining tDCS and fMRI and still many questions related to how tDCS modulates the BOLD signal, the last main goal of Aim 3 is *to investigate whether tDCS over PPC yields localized and/or widespread changes in the BOLD signal independent of (or dependent on) a visual localization task.*

Similar to Experiment 4 in Aim 2, we applied tDCS over PPC of healthy human volunteers while subjects completed a 1-D centroid estimation task in the MRI scanner. Given the many unknown variables when combining tDCS and fMRI, it is difficult to optimize the experimental design to properly address the applicable scientific questions. Therefore, the data presented in Aim 3 is pilot data that is necessary to direct future experiments. We present this exploratory analysis to identify patterns that appear consistent across subjects, but a proper statistical analysis to fully address the goals presented in this aim will require additional data and experiments. In the *Future Research* section we highlight some potential future experiments.

Methods

This aim consisted of one experiment (Experiment 5) with two parts: One outside the MRI scanner (Experiment 5A) and the other inside the MRI scanner (Experiment 5B). In both parts the experimental task was to locate the centroid of a 1-D RDP with different applications of tDCS over PPC similar to Experiment 4. In the first part, subjects completed the behavioral task in a small darkened room. In the second part, subjects completed the same task in the MRI scanner with the trial timing and response method adapted for suitability with the MRI. We collected data outside the MRI scanner in Experiment 5A to acquire the necessary number of trials to analyze the behavioral data. The optimized timing for MRI limited the number of trials collected during one session in Experiment 5B. We set up the behavioral task to mimic the task within the scanner as best as possible, however, there may remain a small margin of error between the size/eccentricity measurements across both parts of Experiment 5. Experiment 5B also included separate scans used to localize voxels visually responsive to the RDP. We later used this data for selection of voxels in occipital cortex (OC).

Participants

Three subjects (two right-handed; one male; age range 18-25 years) participated in both parts of the experiment. Subjects completed a minimum of four sessions from Experiment 5A, including behavioral training, prior to starting Experiment 5B.

Visual Stimuli

In the centroid localization task, the 1-D RDP consisted of small circles (0.5° in diameter) each with four alternating black and white equal-sized wedges on a gray background. The orientation of each circle was randomized on every trial to one of two orientations; white wedges aligned vertically or horizontally. These stimuli were chosen to generate larger BOLD signal changes in visual cortex. For consistency with the previous chapters, we will refer to these elements as ‘dots’. On each trial, we presented 1 out of 24 configurations that consisted of 10 unique dot positions out of 16 possible dot positions that ranged from 0.56° to 8.3° from the vertical midline and were 1.67° above the horizontal midline. We presented three different configurations for each of eight centroid positions (0.33°, 0.67°, 1° and 1.33° to the left or right of the vertical midline). We optimized the configurations both within one centroid position and across all centroid positions to minimize differences in the probability of a dot appearing at a specific spatial position. We minimized this difference for all positions except the outermost circles (± 8.3° from the vertical midline), which were present in every configuration. Therefore, the bisection point between the two outermost dots remained the same, however, the centroid of the RDP differed depending on the position of all the dots. This avoided confounds between the bisection point and the actual centroid that were present in Experiments 1-4.

To limit analysis to relevant voxels that showed visual responses we presented a leftward or rightward moving (0.5°/second) bar (3° width by 2° height) of natural images on a gray background. We selected 25 different images

randomly from a collection of 100 images for each run. The bar changed images at a rate of 4 Hz. The mid position of the bar was 1.67° above the horizontal midline at the same height as the RDP and traversed 20° horizontally.

The fixation stimulus was a small red square (0.09° × 0.09°), which remained visible for the duration of each trial at a position (0°, -1.67°) relative to the center of the display.

Experimental Procedure

Centroid Localization Task (Experiment 5A and B):

Each trial began with a variable delay until the RDP appeared. In Experiment 5A we used 300 – 500 ms to maximize the number of trials collected. In Experiment 5B we increased the delay to optimize the timing for fMRI such that the time between RDPs was 5 – 8 s for each subject. The RDP remained visible for 117 ms (7 frames). A cursor (red vertical line 0.5° in length) appeared at fixation 1000 ms after target offset. Subjects then located the centroid of all dots presented on a trial by using the left and right arrows keys (Experiment 5A) or by moving the cursor to the centroid using an MR compatible trackball in their right hand and then clicking the left button (Experiment 5B), see Figure 5-1.

Similar to Experiment 4 in Aim 2, in both parts of Experiment 5 subjects received 15 min of tDCS (rPPCa, rPPCc, or sham). Subjects performed the centroid localization task after a short delay (20 s) at the beginning of the session to avoid interference from the initialization of stimulation. Subjects continued completing experimental trials for 5 min following tDCS offset (approximately 350-550 trials in part A and 100-200 in part B). After this 20 min period for each

stimulation type, subjects completed two (Part A) or three (Part B) blocks of experimental trials without stimulation for a total of at least 140 additional trials.

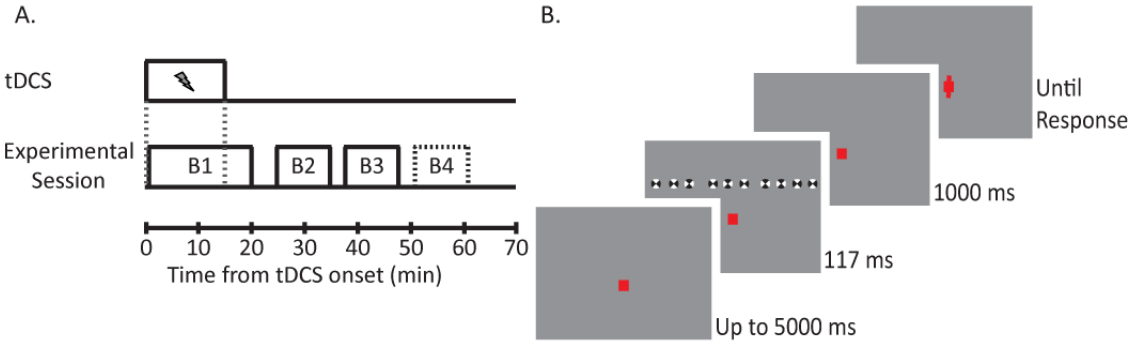

Figure 5-1: Experimental paradigm (Experiment 5). (A) In both Experiment 5A and B, tDCS was applied for 15 minutes at the start of a session (top trace). Trials began 20 s after tDCS onset and subjects completed an additional 2 – 3 blocks of trials after tDCS offset. (B) Example trial from Experiment 5B. Trials in Experiment 5A were similar, but had a different delay time at the start of a trial. We instructed subjects to fixate until they made their response. After 1000 ms from the offset of the RDP, a cursor appeared at fixation and subjects moved the cursor to the perceived centroid location.

Visual Response Localizer (Experiment 5B):

Subjects passively viewed the leftward or rightward moving bar without a concurrent experimental task. We asked subjects to maintain fixation for the duration of the run (~5.5 min). During one run subjects viewed three repetitions of each of the alternating leftward and rightward moving bars beginning with the leftward direction. Subjects completed three runs in total.

Session Ordering

Experiment 5A:

Initially, subjects received between 1 to 2 hr (three to six blocks) of training on the localization task. Data collected during these training blocks are not reported here. However, we ensured that the correlation of subject responses to the actual centroid at the end of training were comparable to subsequent

measures during the experiment. After these practice runs, subjects participated in only one session per day. Each session began with a short training (24 trials) block.

Subjects completed up to two sessions for each stimulation condition (rPPCa, rPPCc and sham). S1 and S2 completed all rPPCa and rPPCc conditions prior to sham. S3 had each type interleaved randomly. The order of the sessions is a concern due to subject training and tDCS carryover effects from prior sessions. With three subjects it is impossible to control for all possible effects, however, we gave subjects ample training and spaced sessions a minimum of 24 h apart. Future data collection will need to optimize session order across subjects. Prior studies have used balanced Latin square designs, although, they do not assume repetition of the same condition as in this experiment. Therefore, we developed a least squares optimization routine in Matlab 7.14 to balance the position of each tDCS session type within the order of the six sessions and balance the number of times a specific type of session occurred before or after another type. With more subjects this algorithm will generate the required counterbalancing across tDCS conditions.

Experiment 5B:

Subjects completed one preliminary MRI session that did not use tDCS to collect an anatomical scan, the visual response localizer runs and to practice the task in the MRI scanner. Subjects then completed one session per tDCS type (rPPCa, rPPCc and sham) for a total of four MRI sessions. We scheduled MRI

sessions a minimum of 48 hr apart from all other sessions. Each session began with a short behavioral training (24 trials) block.

fMRI Data Acquisition

We conducted all imaging at the Rutgers University Brain Imaging Center (RUBIC) using a 3T Siemens TRIO scanner. We placed the subject's head in a 32-channel head coil with padding around the head to minimize movement. We used a T1-weighted MPRAGE sequence to collect high resolution (voxel resolution = 1 mm^3) anatomical images from each subject. For functional scans we used a T2*-weighted echo planar imaging sequence (repetition time = 2000 ms, echo time = 25 ms, flip angle = 90°, matrix = 64 x 64). The 35 slices (in plane resolution = 3 x 3 mm; slice thickness = 3 mm) covered the entire brain and were oriented approximately parallel to the anterior commissure and posterior commissure (ACPC) line.

Data Analysis

We conducted all preprocessing and GLM analyses with Brain Voyager QX 2.6 (Brain Innovation, Maastricht, Netherlands). For all subsequent analysis we utilized Matlab 7.14 (The MathWorks, Natick, MA).

fMRI Preprocessing

We included a linear trend removal, slice scan time adjustment, 3-D motion correction with alignment to the first volume within an MRI session and temporal filtering using a high-pass fast fourier transform filter with a 0.0078 Hz cut-off. We include the linear trend removal because it is known that there may be substantial fluctuations in the mean BOLD signal across all voxels over time

independent of any experimental paradigm. This analysis removes those linear drifts in the BOLD signal. However, if the effects from tDCS simply induced a linear nonspecific widespread change in the BOLD signal across all voxels this analysis would also remove those effects. The output from this preprocessing analysis quantifies how much the mean intensity across all voxels of a brain volume deviated from the mean intensity of a reference volume over time. Therefore, we also examine this output to determine if there are any changes in the mean intensity dependent on tDCS timing. For simplicity, we refer to these changes in the mean intensity of the fMRI signal relative to a reference volume and other measures of the mean of the BOLD signal as mean intensity (see *Current Spread* section).

We aligned the images from each functional run to the high-resolution anatomical image for each subject. We then transformed the data into Talairach space.

Linear Regression

We performed linear regression on the fMRI time course for each voxel and used the timing of the RDP as a predictor. The output from this analysis is a beta value, β_{RDP}, that indicates how well the predicted BOLD time course relates to the actual BOLD time course within each voxel. To generate the predicted BOLD time course, we convolved the RDP timings with a two-gamma hemodynamic response function (HRF, onset = 0 s, response to undershoot ratio = 6, time to response peak = 5 s, time to undershoot peak = 15 s, response and undershoot dispersion = 1). Therefore, a positive β_{RDP} indicates voxels that have

an increase in the BOLD signal after the RDP stimulus, whereas a negative β_{RDP} indicates voxels that show a decrease in the BOLD signal after the RDP stimulus. We created a separate predictor for RDPs during the different tDCS sessions (rPPCa, rPPCc and sham). The linear regression also included the following confounds: a constant for each functional run and the six motion predictors generated from fMRI preprocessing for each functional run.

Voxel Cluster Selection

PPC:

Since we placed electrodes over the P3 and P4 positions of the 10-20 EEG electrode placement system, we examined the BOLD signal in voxels within a cluster (20 mm^3) centered on the mean Talairach coordinates for P3 (x = -38, y = -62, z = 47) (Herwig et al., 2003) and P4 (x = 38, y = -62, z = 47). This generated 2 clusters per subject each with 200-450 voxels that contained functional data.

Occipital Cortex (OC):

Since we did not have a priori knowledge of a specific location to use within OC, we selected voxels within OC that showed significant BOLD modulation as a function of the visual response localizer task. To complete this analysis we used a similar linear regression method as described previously except we used the 24 unique bar positions from the localizer stimulus as predictors. We selected voxels in left and right OC that had a significant positive beta value for one or more of the 24 predictors. We created two separate clusters for voxels within the left and right hemispheres.

Results

Current Spread

We first analyzed whether tDCS produced widespread changes in the BOLD signal across all voxels. To do this we examined whether the mean of the BOLD signal, which we refer to as mean intensity, across all voxels changed as a function of tDCS timing (see *fMRI Preprocessing* section). We examined the change in the mean intensity as a function of time during the first run of each (rPPCc, rPPCa and sham) session. The first run in the rPPCa and rPPCc sessions included 15 min of tDCS (only 20 s of tDCS in the sham condition) and included brain volumes collected for up to 5 min after tDCS offset. If tDCS altered the BOLD signal across all voxels during stimulation, then the mean intensity across all voxels should depend on the timing of tDCS. For example, we may expect to see an increase in the mean intensity that drops after tDCS offset. However, our data show a steady increase (except in the sham condition for S2 that remains stable with large variability) in the mean intensity across all voxels independent of tDCS (Figure 5-2). Therefore, we conclude that tDCS does not generate a consistent widespread change in the BOLD signal across all voxels.

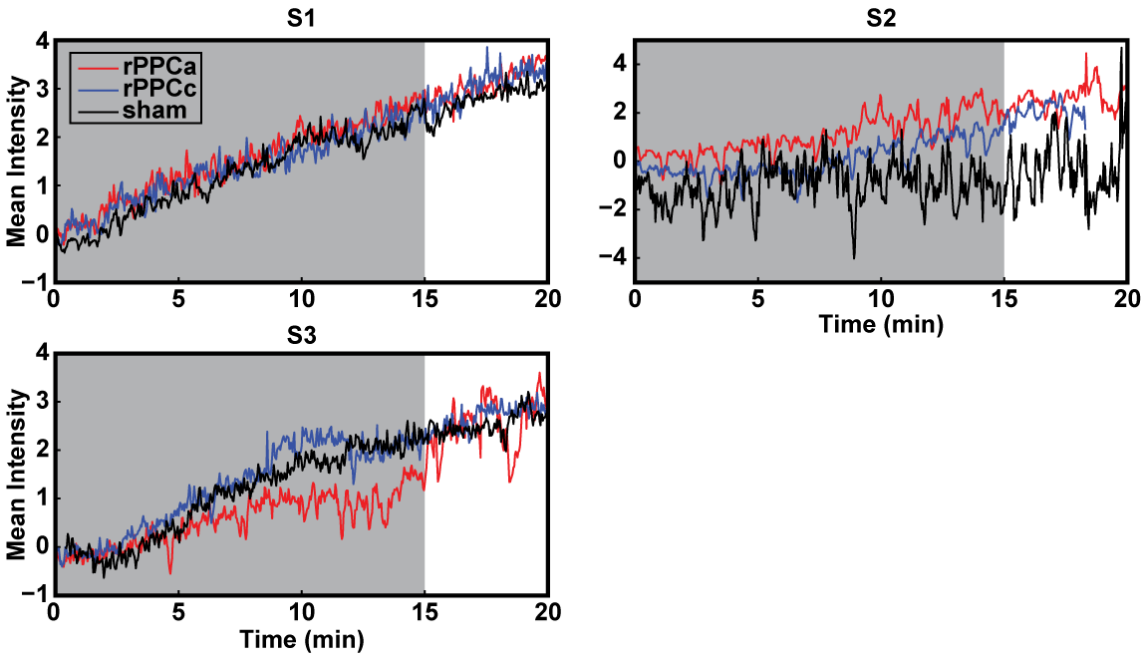

Figure 5-2: Changes in mean intensity across all voxels over time. Separate graphs for each subject (S1, S2 and S3) with line traces for each session: rPPCa (red), rPPCc (blue) and sham (black). Traces adjusted to all start at a 0 mean intensity value at time 0. Mean intensity continues to increase or remain steady with similar variability both during (gray region) and after (white region) tDCS. Therefore, tDCS does not change the mean BOLD signal across all voxels dependent on tDCS timing.

Since we applied tDCS bilaterally, one may expect lateralized tDCS-induced changes in the BOLD signal rather than similar changes across all voxels. Therefore, we calculated the mean intensity separately for voxels within the left and right cortical hemispheres after correcting the data for the above shown changes in mean intensity across all voxels (Figure 5-3). We again examined the data from the first run within a session. The results do not show a change in the magnitude or variability of the mean intensity across voxels within the left or right hemisphere during the first scan. Although there are differences in the magnitudes of the mean intensity of the BOLD signal seemingly linked to tDCS type, we cannot make claims about tDCS montage effects from this since we collected data from different tDCS conditions across different sessions. The

differences in the mean intensity magnitudes may result from various factors including differences in MRI scanner usage prior to each session and subject placement within the magnetic field.

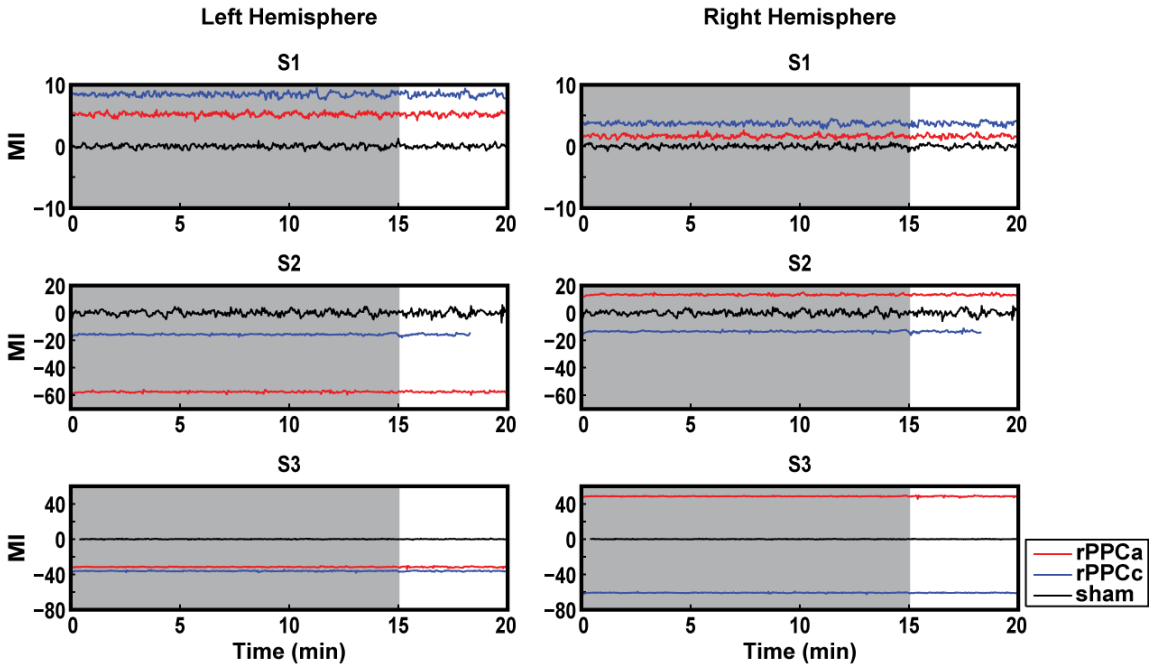

Figure 5-3: Changes in mean intensity in cortical hemispheres over time. Mean intensity (MI) from voxels in the left (left column) and right (right column) cortical hemispheres. Rows show data from different subjects (S1, S2 and S3). Data traces shown for each tDCS session: rPPCa (red), rPPCc (blue) and sham (black). Values have been normalized per subject and hemisphere to the average MI in the sham condition. tDCS does not change the mean BOLD signal across voxels within cortical hemispheres dependent on tDCS timing (gray region: during tDCS; white region: after tDCS).

Averaging the BOLD signal across voxels within a hemisphere may mask more localized changes in the mean BOLD signal. Since we placed the electrodes over PPC, we examined mean intensity changes in voxels within PPC (see *Voxel Cluster Selection* section) but again did not find any evidence for tDCS-induced changes in the mean intensity dependent on tDCS timing (Figure 5-4). We found similar results in selected voxels in OC (not shown).

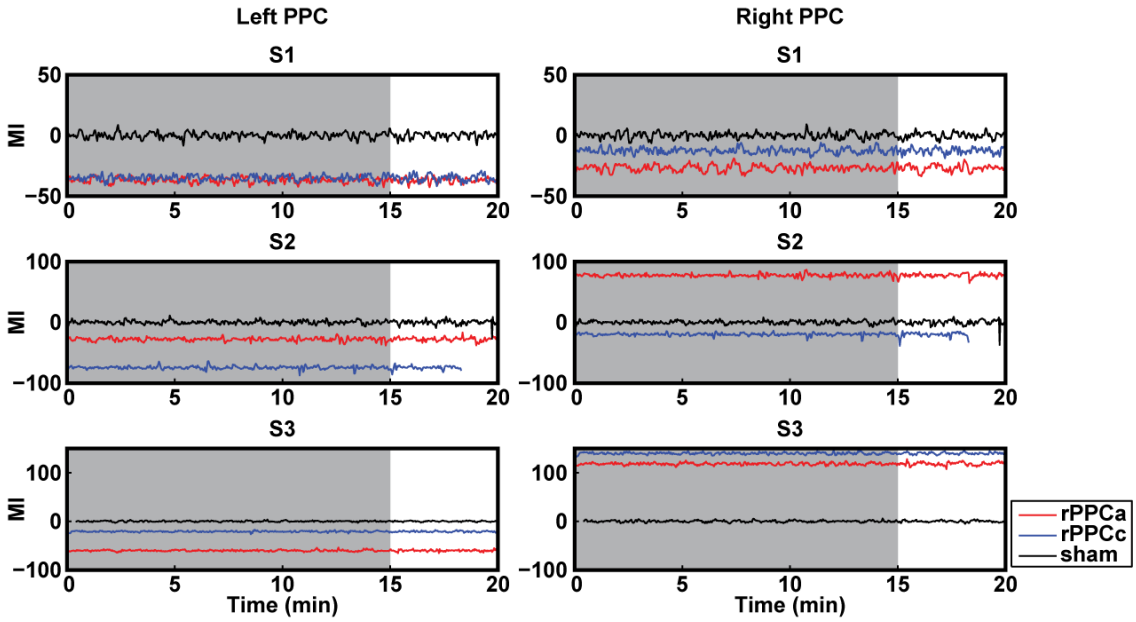

Figure 5-4: Changes in mean intensity in PPC over time. Mean Intensity (MI) from voxels in the left (left column) and right (right column) PPC. Rows show data from different subjects (S1, S2 and S3). Data traces shown for each tDCS session: rPPCa (red), rPPCc (blue) and sham (black). Values have been normalized per subject and PPC cluster to the average MI in the sham condition. tDCS does not change the mean BOLD signal across voxels within PPC dependent on tDCS timing (gray region: during tDCS; white region: after tDCS).

The above results examined mean BOLD signal changes across voxels independent of the visual task. However, there is evidence that tDCS acts on active populations of cells (Kar & Krekelberg, 2013). Therefore, BOLD signal changes due to tDCS may be yoked to the presentation of the RDP. We examined the beta value from a linear regression, β_{RDP}, that indicated whether the fluctuations of the BOLD signal within a voxel were correlated with the predicted BOLD time course determined from the RDPs for each tDCS session. The magnitude of the β_{RDP} represents the visual response of a voxel. We did not find any consistent changes across subjects in β_{RDP}s during the first run of a session (or in subsequent sessions, data not shown) when the anode or cathode was placed over left or right PPC relative to sham (Figure 5-5A). Only the BOLD

signal in OC ipsilateral to the anode was reduced, suggesting that an anode over left PPC decreases the BOLD signal in left OC. This pattern was short lasting and was not found in later scans within the session (i.e. well after tDCS offset).

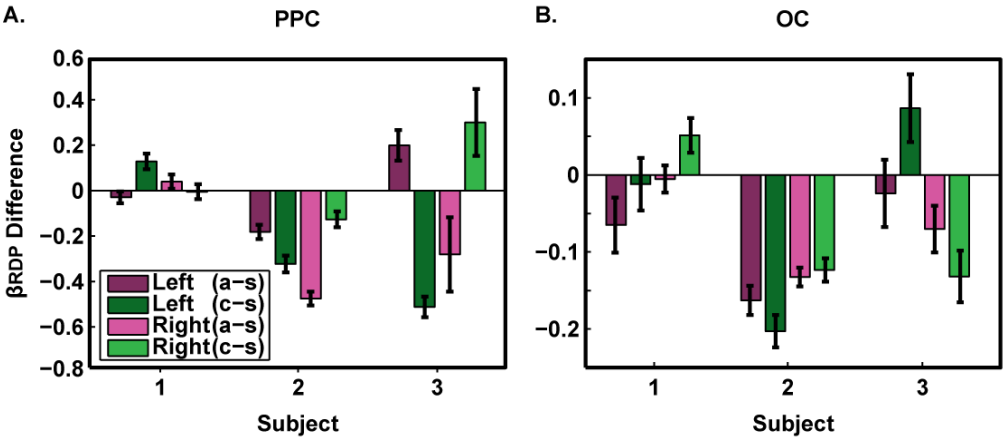

Figure 5-5: Differences in β_{RDP} relative to sham in PPC and OC. Data collected during the first run in a session. Anode (pink bars) or cathode (green bars) over left (darker bars) or right (lighter bars) PPC. Analysis completed on voxels in left (darker bars) and right (lighter bars) PPC (left column) and OC (right column). Error bars depict *SE*. Since we placed electrodes over left and right PPC concurrently, dark green and light pink bars represent differences between the rPPCc and sham condition and dark pink and light green bars represent differences between the rPPCa and sham conditions. PPC shows no consistent changes in the BOLD signal response to the RDP across subjects. OC shows a decrease in the BOLD signal in the same cortical hemisphere as the anode.

We did not find any evidence that tDCS induces widespread nonspecific changes in the BOLD signal. Moreover, tDCS did not induce consistent changes in the BOLD signal response to the RDP in PPC, but there was some evidence for a change in OC based on the anode position. Overall, however, variability across the three subjects was large. One possible explanation is that idiosyncratic patterns in tDCS-induced BOLD changes are due to idiosyncratic differences in brain folding across subjects (A. Datta et al., 2009; A. Datta et al., 2013; Wagner, Fregni, et al., 2007).

Mislocalization and the BOLD Signal

In Aim 2 we argued that the highly variable results when comparing either of the stimulation conditions to sham could be the consequence of subjects' idioysyncratic brain folding. We reasoned that the opposite polarity in the rPPCa and rPPCc conditions cancelled out some of the task-irrelevant neural changes from tDCS, which resulted in consistent differences in behavioral responses across these stimulation conditions. Our fMRI experiments provide additional insight into this hypothesis, which predicts that the difference in the BOLD signal between rPPCa and rPPCc conditions per subject explains that subject's behavioral mislocalization even with quite different tDCS-induced BOLD signal changes across subjects. Specifically we predicted an imbalance in the activation of left and right PPC, as measured by the BOLD signal, would yield mislocalization in a manner consistent with the ICT.

To test this hypothesis we determined interhemispheric differences in the BOLD signal within PPC and compared this to the direction of mislocalization across stimulation conditions. Specifically, we calculated the imbalance of PPC activity, the difference between the mean β_{RDP} for voxels within left PPC and those within right PPC, during rPPCc stimulation ($lPPC_{rPPCc}$ - $rPPC_{rPPCc}$) and during rPPCa stimulation ($lPPC_{rPPCa}$ - $rPPC_{rPPCa}$). We then subtract the imbalance of PPC activity during rPPCa stimulation from the imbalance of PPC activity during rPPCc stimulation, which results in a difference in beta values based on predictions from the ICT, β_{ICT}:

$$\beta_{ICT} = (lPPC_{rPPCc} - rPPC_{rPPCc}) - (lPPC_{rPPCa} - rPPC_{rPPCa}) \quad (7)$$

Based on the ICT and the traditional assumptions of tDCS, we hypothesized that rPPCc stimulation would yield a greater left-right imbalance in the BOLD signal in PPC compared to rPPCa stimulation (positive β_{ICT}) and correlate to more rightward localization during rPPCc stimulation (positive response error difference) as shown in Aim 2. This could be because rPPCc increases the BOLD signal more in left PPC due to increases in neural excitability and less in right PPC due to reductions in neural excitability relative to rPPCa stimulation. However, due to the idiosyncratic brain folding per subject, rPPCc may generate smaller left-right imbalances in PPC relative to rPPCa, a negative β_{ICT}, which should yield more leftward localization during rPPCc stimulation. As predicted, a positive (negative) β_{ICT} coincides with a positive (negative) mislocalization (Figure 5-6). Importantly, the pattern of β_{ICT} was subject-specific; suggesting that the tDCS-induced BOLD changes are idiosyncratic, but that these BOLD changes result in behavioral changes that are consistent with the ICT.

To show this relationship between BOLD signal changes and mislocalization behavior we compared BOLD data (Experiment 5B) and behavioral data (Experiment 5A) from different experimental sessions. Therefore, the relationship between BOLD and behavior cannot be attributed to any tactile or other difference from application of tDCS in the MRI scanner. Therefore, we conclude, that changes in the BOLD signal within PPC predict localization patterns, presumably due to changes in neural activity.

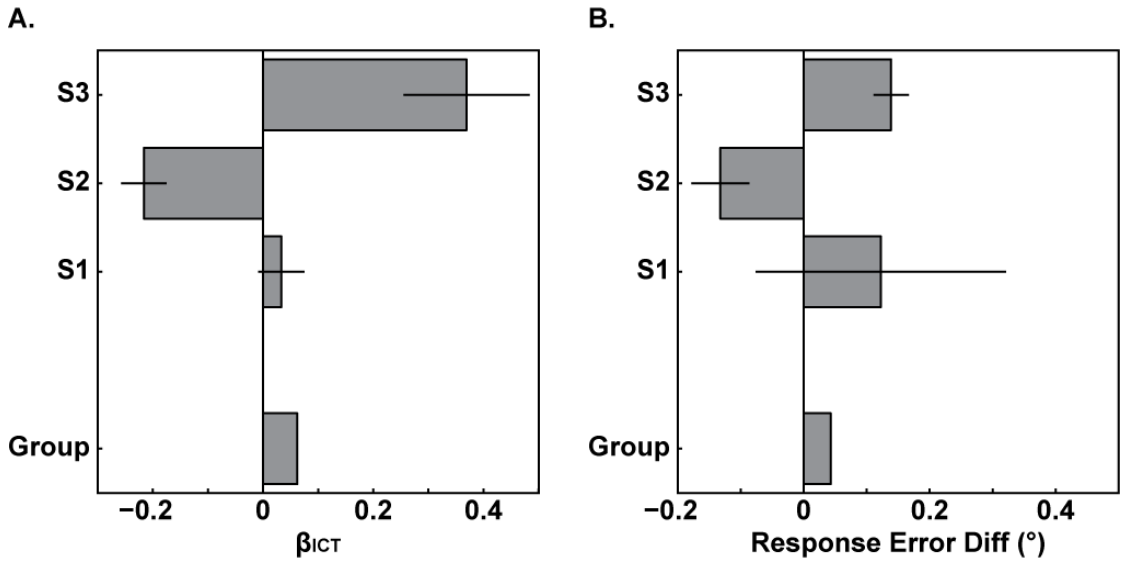

Figure 5-6: Comparison of the BOLD signal changes in PPC and localization responses between rPPCc and rPPCa stimulation (Experiment 5). Error bars depict *SE*. (A) β_{ICT} (Equation 7) magnitudes for each subject (S1, S2 and S3) and the mean across subjects (bottom row). Positive (negative) values indicate a larger (smaller) left-right imbalance in the BOLD signal in PPC during rPPCc stimulation compared to rPPCa stimulation. (B) Response error (response – actual centroid) differences between rPPCc and rPPCa stimulation for each subject and the group mean (bottom row). Positive (negative) values indicate more rightward (leftward) mislocalization during rPPCc stimulation. The pattern of β_{ICT} magnitudes matches the pattern of response error differences.

The above analysis used data across an entire session, however, there may be differences in β_{ICT} or behavior earlier or later in a session due to the timing of tDCS. Therefore, we split the data into trials collected during the first 20 min run, that included 15 min of tDCS, and all later runs. Intriguingly, subject S1's mislocalization was reversed in the later blocks, and this change was also reflected in that subject's β_{ICT}.

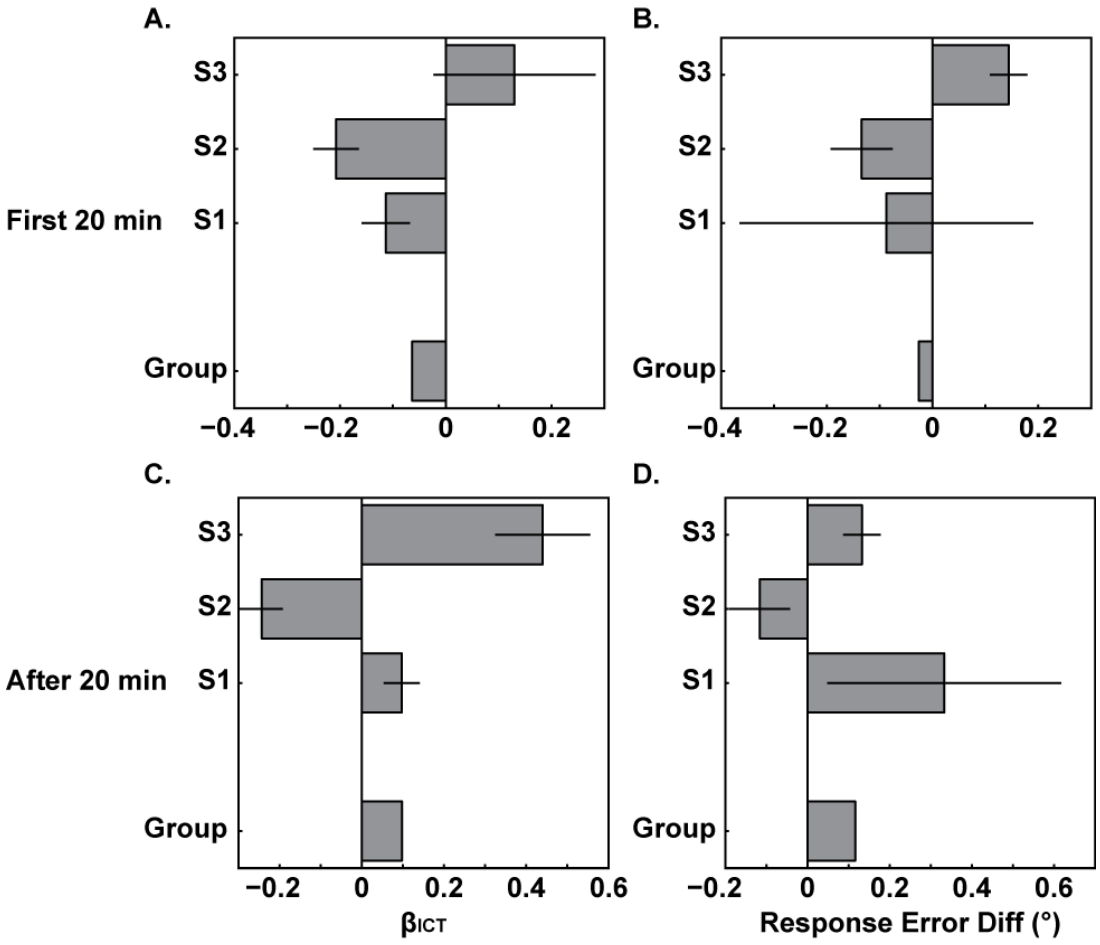

Figure 5-7: Comparison of the BOLD signal changes in PPC and localization responses between rPPCc and rPPCa stimulation relative to tDCS timing (Experiment 5). Error bars depict *SE*. (A & C) β_{ICT} (Equation 7) magnitudes for each subject (S1, S2 and S3) and the mean across subjects (bottom row) from the first 20 min run including 15 min of tDCS (top row) and from later post-tDCS offset runs (bottom row). Positive (negative) values indicate a larger (smaller) left-right imbalance in the BOLD signal in PPC during rPPCc stimulation compared to rPPCa stimulation. (B & D) Response error (response – actual centroid) differences between rPPCc and rPPCa stimulation for each subject and the group mean (bottom row) from the first 20 min run including 15 min of tDCS (top row) and from later post-tDCS offset runs (bottom row). Positive (negative) values indicate more rightward (leftward) mislocalization during rPPCc stimulation. The pattern of β_{ICT} magnitudes matches the pattern of response error differences even when the direction of the behavioral effect differed between the first and later runs (S1).

It remains possible that other brain regions will also show this relationship to behavior, however, a similar interhemispheric comparison of beta values across tDCS conditions in OC did not predict behavior (not shown). Therefore, we find subject-specific differences in the BOLD signal within PPC that correlate

with behavior in a manner consistent with the ICT. This also supports that tDCS yields localized changes in the BOLD signal related to the experimental task.

The above analysis examined differences between the rPPCc and rPPCa stimulation conditions, however, the β_{ICT} may also correlate with the localization differences between the tDCS conditions and sham. We determined the β_{ICT} as in Equation 7, however, we used the interhemispheric differences applicable to the compared conditions, i.e. rPPCa and sham or rPPCc and sham. Our results again show a relationship between β_{ICT} and the response error difference using data from the entire experimental session.

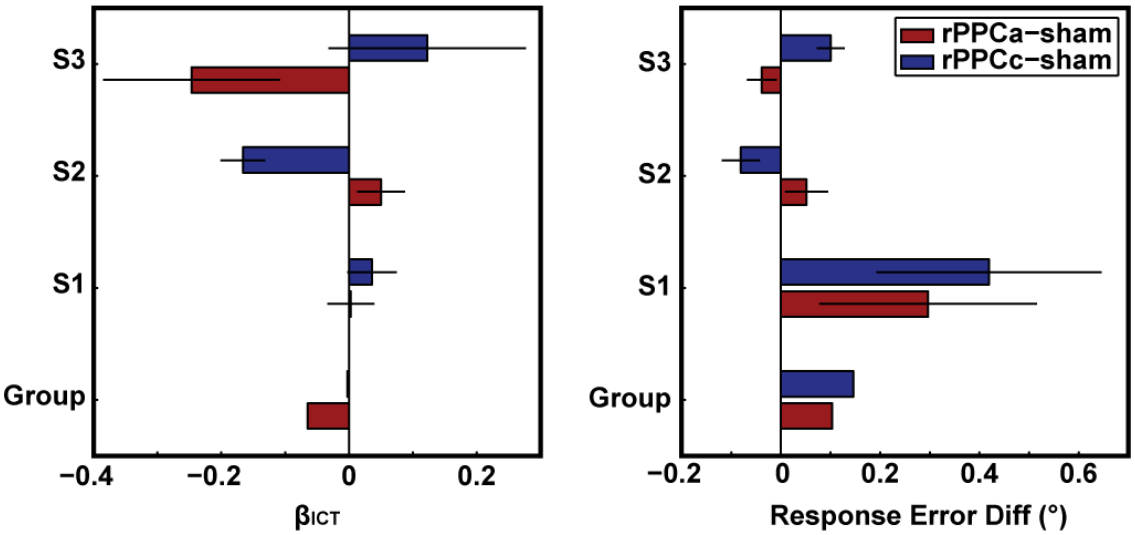

Figure 5-8: Comparison of the BOLD signal changes in PPC and localization responses between rPPCc or rPPCa stimulation and sham (Experiment 5). Error bars depict *SE*. (A) β_{ICT} (Equation 7) magnitudes for each subject (S1, S2 and S3) and the mean across subjects (bottom row). Positive (negative) values indicate a larger (smaller) left-right imbalance in the BOLD signal in PPC during rPPCc or rPPCa stimulation compared to sham stimulation. (B) Response error (response – actual centroid) differences between rPPCc or rPPCa stimulation and sham for each subject and the group mean (bottom row). Positive (negative) values indicate more rightward (leftward) mislocalization during rPPCc or rPPCa stimulation relative to sham. The pattern of β_{ICT} magnitudes matches the pattern of response error differences.

We again split the data into trials within the first 20 min run and those occurring after the first run. Unlike the previous comparison between rPPCc and rPPCa stimulation, the magnitude of the β_{ICT} and response error difference no longer correlated with the split data sets (Figure 5-9). Therefore, although the BOLD differences in PPC carry some information relevant to localization (Figure 5-8), there are changes in behavior that are not fully captured by the BOLD changes in PPC.

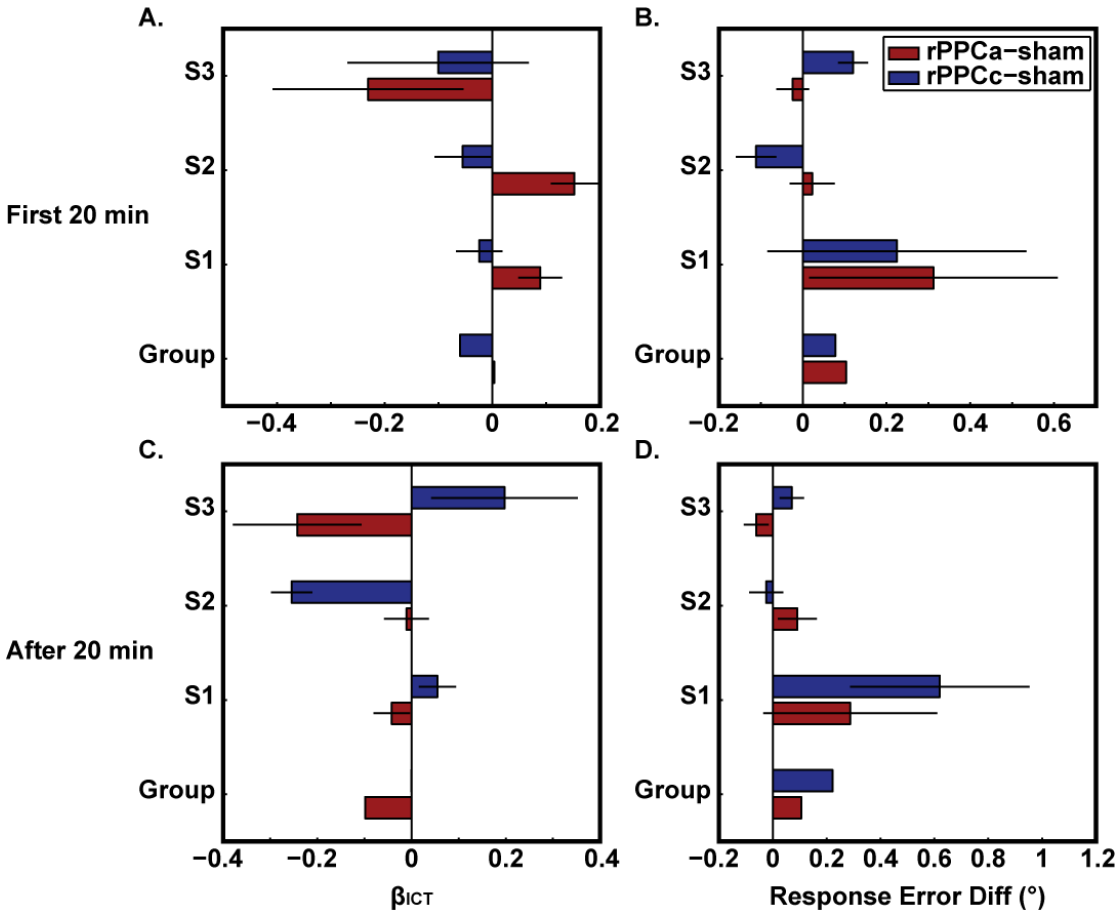

Figure 5-9: Comparison of the BOLD signal changes in PPC and localization responses between rPPCc or rPPCa stimulation and sham relative to tDCS timing (Experiment 5). Error bars depict *SE*. (A & C) β_{ICT} (Equation 7) magnitudes for each subject (S1, S2 and S3) and the mean across subjects (bottom row) from the first 20 min run including 15 min of tDCS (top row) and from later post-tDCS offset runs (bottom row). Positive (negative) values indicate a larger (smaller) left-right imbalance in the BOLD signal in PPC during rPPCc or rPPCa stimulation compared to sham. (B & D) Response error (response – actual centroid)

differences between rPPCc or rPPCa stimulation and sham for each subject and the group mean (bottom row) from the first 20 min run including 15 min of tDCS (top row) and from later post-tDCS offset runs (bottom row). Positive (negative) values indicate more rightward (leftward) mislocalization during rPPCc or rPPCa stimulation relative to sham. The pattern of β_{ICT} magnitudes no longer match the pattern of response error differences.

The above results involved the comparison of two conditions, but we hypothesized that the interhemispheric differences in the BOLD signal between left and right PPC or even the BOLD signal change in either the left or right PPC may predict mislocalization direction within a single condition. However, we found no evidence of this. We also found no consistent relationship between the BOLD signal changes and the direction of localization error when we collapsed data across rPPCa, rPPCc and sham conditions.

Discussion

Experiment 5 investigated the influence of tDCS over PPC on the BOLD signal in voxels both close to and far from the electrodes. Our results suggest that tDCS induces localized BOLD signal changes in PPC that predict the differences in the perceived centroid across tDCS (rPPCa, rPPCc and sham) conditions. We first discuss various mechanisms that may underlie tDCS-induced changes in the BOLD signal followed by a discussion of the relationship between the ICT predicted difference in the BOLD signal (β_{ICT}) and behavioral localization differences between conditions. However, we acknowledge that the generalization of these pilot results remains limited due to the small number of subjects. Therefore, we also highlight factors to consider in future experiments.

Effects and Mechanisms of tDCS on the BOLD Signal

Before we could confirm PPC's role in localization we had to investigate if tDCS induced widespread changes in the BOLD signal, which may confound our analysis and suggest that tDCS influences a large extent of cortex. For example, if the BOLD changes we saw in PPC were the same as those in other regions then our claims about the involvement of PPC with this task are limited. There are only a few studies examining concurrent tDCS and fMRI, therefore, the effects of tDCS on the BOLD signal are largely unknown. Some studies state that tDCS induces more localized or functionally relevant changes in the BOLD signal (Antal et al., 2011; Meinzer et al., 2012), however, many did not look at widespread changes in the mean BOLD signal dependent on tDCS timing independent of a task. Our results further confirm a more localized or functionally relevant tDCS-induced change of the BOLD signal and do not support widespread changes in the mean BOLD signal. Although we did find some artifacts (not shown) in voxels near the skull similar to previous studies (Antal, Bikson, et al., 2012).

We limited our analysis to voxels within the PPC and examined both changes in the mean BOLD signal and changes in the BOLD signal in response to the RDP. Although we found changes in the BOLD signal in response to the RDP under the anode and the cathode the results were inconsistent across subjects. As previously mentioned, the influence of tDCS on neural activity is idiosyncratic due to individual brain folding, which may in turn yield idiosyncratic differences in the BOLD signal. However, it is important to note that changes in

the BOLD signal from tDCS may arise from neural and non-neural mechanisms. One of the non-neural mechanisms is the direct effect of tDCS on the blood vessels, which will alter rCBF and could subsequently alter the BOLD signal. Durand and colleagues (2002) have shown vasodilation after application of tDCS which could increase rCBF and in turn could yield BOLD increases. In addition to this, tDCS generates electromagnetic fields, which may influence the BOLD signal. In brief, the principles of MR imaging rely on the orientation of predominantly hydrogen atoms within a static magnetic field combined with properties of magnetic resonance. The BOLD signal arises because the decay of the MR signal is slower in regions with a greater amount of oxygen in the blood (increase in T2*), which has been shown to be an indicator of underlying neural or synaptic activity. Deoxygenated hemoglobin is paramagnetic, which creates spatial inhomogeneities in the magnetic field that reduce the MR signal (decrease in T2*). The electromagnetic fields induced by tDCS could create more spatial inhomogeneities (decrease T2*) or reduce the influence of spatial inhomogeneities and counter some of the effects of deoxygenated hemoglobin (increase T2*). While the physics of these possible effects have not yet been explored, the latter effect implies that tDCS may reduce the decay of the MR signal and could explain why studies using post-mortem subjects have shown tDCS artifacts in the MR signal in cerebrospinal fluid (CSF) and around the skull in regions under the electrode (Antal, Bikson, et al., 2012). Although our studies support that these non-neural mechanisms are not influencing all voxels or voxels within a cortical hemisphere, the non-neural mechanisms may also

preferentially alter the BOLD signal in voxels with active populations of neurons, hence, voxels that respond to the RDP. However, if the BOLD signal changes resulted simply from non-neural mechanisms then we would not expect the BOLD signal to predict localization behavior as shown in our results.

Interhemispheric Differences in the BOLD Signal and Localization Behavior

The ICT suggests that the balance in activation in frontal and parietal areas generates a lateralized attention vector that we propose influences centroid localization behavior. A previous study has shown that the activation levels summed across frontal and parietal regions responsive to an attention task are comparable across hemispheres however individual subject differences predict responses in a line judgment task (Szczepanski & Kastner, 2013). Asymmetries in interhemispheric activation levels also differ across cortical regions. There is an asymmetry across left and right PPC that favors the left visual field, whereas the asymmetry across left and right FEF favors the right visual field (Szczepanski et al., 2010) and these asymmetries may be altered using TMS with subsequent changes in line judgment (Szczepanski & Kastner, 2013). Our goal was to bias the interhemispheric asymmetry across PPCs using dual tDCS. Based on the ICT and these previous findings we predicted that the interhemispheric differences in the BOLD signal in PPC should predict centroid localization behavior. We confirmed this by comparing the localization error across different tDCS conditions to the interhemispheric difference of PPC BOLD responses across those conditions, β_{ICT}, and found that the β_{ICT} predicts localization behavior. The correlation between β_{ICT} and centroid localization

behavior suggests that tDCS-induced BOLD signal changes in PPC derive, at least in part, from changes in the neural activity in PPC. We acknowledge that the comparison of the rPPCa and rPPCc conditions to sham showed increased variability between the β_{ICT} and behavior when we divided the data set based on earlier/later runs. This suggests that other regions may be influencing behavior outside of the influence of PPC (although we analyzed OC and did not find a correlation between the BOLD signal changes and localization) or that the BOLD signal is not sensitive enough to detect all the underlying changes in the neural activity from tDCS. However, the fact that the relationship between β_{ICT} and behavior was present when we combined all trials and runs suggests that our data set has limited statistical power. Limitations of detecting tDCS-induced BOLD signal changes or our limited statistical power may be why we were unable to find a correlation between the interhemispheric difference in the BOLD signal in PPC and behavior within a specific tDCS condition.

Future Research

Additional experiments are needed to better understand the influence of tDCS on the BOLD signal. Our results do not show any changes in the mean BOLD signal as a result of tDCS, however, since we applied different tDCS montages across different experimental sessions, we are unable to compare the mean BOLD signal changes across conditions. A design that includes tDCS and sham within the same session without an experimental task allows for comparison of the mean BOLD signal across conditions. However, it is imperative to consider tDCS duration and the aftereffects from tDCS. Short

durations may limit detectability of changes in the BOLD signal, however, longer durations may cause carryover effects into subsequent conditions.

Although we used tDCS to maximize the asymmetry in activation across PPCs, our predictions extend to position perception processing independent of tDCS condition. If PPC truly influences localization in a manner consistent with the ICT, then BOLD signal differences across left and right PPC should predict localization behavior. This also suggests that trial by trial fluctuations in the BOLD signal should correlate to the magnitude of the localization error. Future research can target PPC or subregions of PPC and examine the BOLD signal changes in voxels within these areas. The changes in individual voxels or the mean BOLD signal changes in these regions may be used to decode the direction of localization error. This method can be used with or without tDCS to determine which regions carry information related to perceived position. However, tDCS or another stimulation method may be necessary to increase the signal to noise ratio in the BOLD signal to detect the relationships between BOLD signal and behavioral changes.

Conclusions

Our results show that knowledge of tDCS polarity is inadequate to predict BOLD signal changes and perceived centroid position since we do not see consistent results across subjects. However, given the idiosyncratic differences in the expected tDCS induced changes in current density, a homogenous change in a population of neurons may be unrealistic. If the BOLD signal truly captures these idiosyncratic changes in the neural activity and it is these changes in PPC

that drive localization behavior, then regardless of the polarity of tDCS stimulation, the changes in the BOLD signal should predict behavior as we have shown. Therefore, it is imperative to account for the individual differences that yield changes in neural activity and not rely on the expected changes in neural excitability based on proximity to the anode or the cathode. Only then can we make claims about the causal role of PPC (and other regions) in position perception.

Chapter 6: **General Discussion**

We first summarize our results briefly and address the questions outlined in the *General Introduction* section. We then review the methods used across our experiments: behavior, tDCS and fMRI, and highlight their usefulness, their limitations and outstanding technical issues. We discuss some of the potential neural mechanisms underlying the results of our experiments and lastly, we discuss the significance of this work for disorders such as spatial neglect.

In Aim 1, we quantified visuospatial integration in centroid localization behaviorally in healthy human subjects and examined the effects of two factors, target component eccentricity and non-predictive attentional cues, on this process. Our results showed that:

- Both factors alter the local processing of the RDP as evidenced by differential weighting of the individual dots based on the distance relative to the fovea and to the locus of attention.
- Target component eccentricity generates two distinct weighting patterns: higher or lower weights closer to the fovea.
- These results suggest that position perception may be explained by a labeled line model.

In Aim 2, we examined the causal role of PPC in position perception and applied tDCS over PPC. We examined the behavioral changes in a 1-D centroid task. Our results show that:

- Placing the anode over left PPC and the cathode over right PPC induces a rightward shift in perceived centroid location relative to the reverse montage.
- Although we saw changes in behavior, there was no evidence that tDCS systematically altered an underlying weighting pattern (data not shown). This finding suggests that PPC governs the post-integration computations of perceived position, i.e. a late bias.
- Our results provide support for the ICT of attentional allocation and suggest that the tDCS-induced changes in centroid perception may be mediated through attention networks.

Aim 3 examined the spatial extent of tDCS modulation of the BOLD signal and whether the BOLD signal predicted the perceived centroid position.

- We show that tDCS did not induce widespread changes in the BOLD signal. Although we saw changes in the BOLD signal in PPC and OC they were inconsistent across subjects and functional runs.
- tDCS-induced changes in the BOLD signal predict response error differences between tDCS conditions (rPPCa, rPPCc and sham) in a manner consistent with the ICT.

Methodological Approach

Behavioral Studies

Each of the methods used provides insight into position perception however each has advantages and disadvantages. We are interested in studying visual localization behavior because errors or biases in this behavior provide

insight into the neural mechanisms governing position perception. Behavioral studies are an effective and noninvasive way to probe localization and assess these limitations. Results from behavioral studies can generate testable hypotheses for future stimulation, electrophysiological or fMRI experiments. For example, in Aim 1 the systematic shifts in localization due to the attentional cues suggest that brain areas implicated in visual spatial attention may influence position perception processing. Therefore, we hypothesized that PPC may causally influence position perception, which we tested and confirmed in Aim 2 and 3. Since a computational model that allows for changes in the local processing of the centroid best described these cue-induced biases, we hypothesized that PPC may send feedback to early visual cortical areas that altered weighting. However, a weighted integration model did not well describe the mislocalizations induced from tDCS over PPC. Therefore, we did not include similar computational modeling in Aim 2. The lack of evidence for PPC modulations of local processing, suggests that PPC may control the global processing in position perception. This is further supported by the tDCS-induced changes in the BOLD signal within PPC (and not in OC) predicting the localization error relative to the actual centroid across tDCS conditions. However, reducing the spatial extent of the RDP from two to one dimension may have reduced the modulations in local processing and masked some of the changes in weighting.

Although our results do not implicate PPC in the modulation of local processing, this does not eliminate the involvement of another brain area in this

process. Behavioral studies cannot distinguish which brain areas or neural mechanisms underlie a behavior. Computational modeling combined with electrophysiology, examining the neural changes in firing rate across a population of neurons, or fMRI, examining BOLD signal time courses across a collection of voxels, may be used to decode position perception. Results from studies utilizing these complimentary methods may link early visual cortical areas or other regions to position perception.

Behavioral studies also allow for the repetition of many trials and testing in human subjects. Therefore, it is possible to measure small but consistent behavioral changes with these types of studies. For example, most of our effect sizes were less than half a degree of visual angle, see Figure 3-2, Figure 4-2, Figure 4-6, and Figure 5-6 to Figure 5-9. However, there is a minimum number of trials required to determine whether a significant behavioral effect exists. When we assessed the changes in localization over time (Figure 4-3 and Figure 4-5), we used a bin size of 250 s to have a sufficient number of trials (no less than 30). Our results showed a significant behavioral effect at 250 s, however, this analysis does not show at what time the tDCS-induced mislocalizations first manifested during tDCS (Figure 4-5). In order to improve the temporal resolution, one could change the mode of response from a cursor movement to a 2AFC similar to Experiment 2, which may reduce the intertrial interval. Additional data sessions could also be collected and the analysis adjusted to bin trials across sessions.

tDCS

One way to determine whether a brain area has a causal role in a particular behavior is to alter the neuronal activity in that area and then determine the changes in that behavior. To assess the role of PPC in position perception, we utilized tDCS to modulate the neural activity in this region. Although tDCS has been utilized for hundreds of years (for a review see Wagner, Valero-Cabre, & Pascual-Leone, 2007), it has had a resurgence in research studies. Over the past almost 15 years tDCS has been applied over numerous brain areas and has been shown to mitigate the behavioral deficits from a variety of clinical disorders including stroke, chronic depression, fibromyalgia and traumatic spinal cord injury to name a few (for a review see Stagg & Nitsche, 2011). Its ability to alleviate the symptoms of a variety of disorders (Rogalewski et al., 2004) at first may make tDCS an appealing treatment method given its relative low cost. However, since we have a limited understanding of its underlying neural mechanisms and long term effects we should also approach this method with caution.

Although some studies report that the current density is greatest in brain areas under the electrode (Miranda, Lomarev, & Hallett, 2006; Wagner, Fregni, et al., 2007), others show that tDCS may influence regions between the electrodes (Antal, Bikson, et al., 2012). In other words, the exact spatial extent of the current, how much of the current reaches the cortex and the local variations in current density remain unclear. To reduce the spatial extent of current and therefore, improve the focality of tDCS neuronal modulations, one may first assume it is necessary to use smaller electrodes. However, smaller electrodes

increase the shunting of current, i.e. the amount of current that will not reach the cortex (Wagner, Fregni, et al., 2007). For the current to reach the brain region of interest, it must pass through various layers including the skin, skull, meninges and CSF, each with different levels of resistivity. Therefore, a portion of the current will not pass through each layer. One study used computation modeling and suggested that only 10% of the current applied at the scalp reaches the cortex (Miranda et al., 2006). However in an earlier study, Dymond and colleagues (1975) measured intracortical current between pairs of small electrodes and found that 45% of the applied current passed into the brain. This is also in line with predictions from an electrolytic tank model (Rush & Driscoll, 1968). Although we are unsure the exact percentage of current that penetrates to the brain, we minimized shunting by using larger (7.6 cm diameter) electrodes (Wagner, Fregni, et al., 2007).

It remains possible in our study that tDCS modulated more than just PPC, for instance motor cortex. However, we found no changes in motor control that could fully explain our behavioral results in Aim 2. Our fMRI results from Experiment 5B also suggest more localized changes in the BOLD signal dependent on the localization task. Future experiments using other electrode montages or another noninvasive stimulation method have the potential to improve the focality of the stimulation in PPC and further confirm the results from our experiments. Computational models have suggested that utilizing more than two electrodes in specific configurations improves the focality of tDCS stimulation (A. Datta et al., 2009). In addition, TMS is known to have a better spatial

resolution compared to transcranial electrical stimulation methods, including tDCS. Before we can make specific claims about improvements in focality from these montages and stimulation methods we need to not only quantify the neural effects computationally, but also test these methods using electrophysiological and imaging techniques. We discuss TMS and another electrical stimulation method further at the end of this section.

Once the residual current (after shunting) reaches the brain it is thought to modulate levels of excitability in neurons within the induced electrical field. It is these changes in excitability that are thought to drive the behavioral changes, such as in visual localization. In vitro methods have implicated different neural mechanisms that yield changes in neural excitability during stimulation, mediated through Na+ channels, and after stimulation, mediated through NMDA receptors, (for a review see Stagg & Nitsche, 2011). However, it remains unclear how these modulations impact an intact neuronal network especially with other tDCS effects on early gene expression (Islam, Aftabuddin, Moriwaki, & Hori, 1997), levels of cAMP (Hattori, Moriwaki, & Hori, 1990), BDNF (Fritsch et al., 2010) and concentrations of neurotransmitters such as GABA and glutamate (Stagg, Best, et al., 2009). Interestingly, our data showed two distinct periods, during and after tDCS, of centroid mislocalization dependent on the polarity of tDCS, see Figure 4-5. Therefore, it remains possible that different underlying neural mechanisms contributed to alterations in the neural networks that process position to yield these changes in behavior dependent on the timing of tDCS. In addition, there is uncertainty about the length of the delay between tDCS onset and the first

detectable change in behavior. Many prior studies examined behavioral changes after 10 or more minutes of tDCS (for a review see Ukueberuwa & Wassermann, 2010). However, changes in Na+ channels during tDCS should occur on the order of milliseconds. Experiment 4 showed effects of tDCS on localization after 2.5 min after onset, but does not allow for a smaller temporal resolution due to the limitations of the behavioral study. Experiments utilizing techniques such as microdialysis are needed to link changes in the concentration of neurotransmitters, for example, to changes in behavior as a function of tDCS timing.

Although generalized changes in neural excitability dependent on the proximity to the anode or cathode have been suggested in the literature, tDCS does not yield homogenous effects on the underlying neurons since the brain is an anisotropic conductor with complex geometry. This complexity has been revealed through computational models that predict the current density for specific tDCS montages and individuals (A. Datta et al., 2009; Wagner, Fregni, et al., 2007). The models reveal inhomogeneities in current density, and therefore in the electrical field, specific to individual brain folding dependent on the electrode placement, size and current amplitude. It is these idiosyncratic variations in current density that may contribute to the large variability across subjects when considering the effects of tDCS on position perception relative to sham (Figure 4-4 and Figure 4-7). However, the consistent changes in mislocalization dependent on the tDCS polarity, i.e. the anode over right PPC combined with the cathode over left PPC and vice versa, argue that some of these idiosyncracies

may be cancelled out when comparing conditions with different polarities. We further confirmed this in Aim 3 when we compared changes in the BOLD signal to localization error across conditions. Future electrophysiological experiments need to be conducted to validate the proposed complexities in current density variation and current spread. Once we have validated these models, then we can better compare the individualized variations in current density to individual behavioral differences. Although there are still many questions surrounding the mechanisms of tDCS, it does have significant and consistent temporary effects on behavior. Experiments 3 and 4 in Aim 2 and Experiment 5A in Aim 3 show polarity-dependent tDCS-induced changes in centroid localization that persist for approximately 15 min.

Transcranial alternating current stimulation (tACS) and TMS are other noninvasive transcranial stimulation methods that we could have used instead of tDCS to modulate PPC activity. Transcranial alternating current stimulation induces oscillating electrical fields, which are thought to synchronize or enhance ongoing neuronal activity (for a review see Zaghi et al., 2010). One of the known disadvantages of tACS is that it induces phosphenes (Kar & Krekelberg, 2012); flickering luminance in peripheral regions of the visual field that may interfere with visual tasks. Instead of electrical stimulation, TMS uses directed magnetic fields to target a specific brain region and induce above threshold neuronal changes. TMS also has a better spatial resolution than tDCS and tACS, but the equipment can be bulky and expensive, and therefore, not conducive for long term rehabilitative solutions for clinical populations. In addition, tDCS has longer

lasting modulations relative to TMS with no known serious side effects (for a review see Wagner, Valero-Cabre, et al., 2007). Many questions remain concerning the neural mechanisms that mediate the effects of all of these noninvasive stimulation methods. We chose tDCS over other methods because certain durations of tDCS have been shown to yield long-lasting behavioral aftereffects and to avoid confounds introduced by the presence of phosphenes.

fMRI

In order to learn more about the spatial extent of tDCS modulations, as well as assess the involvement of different cortical areas in position perception in humans, we used fMRI in our last experiment. fMRI has been utilized in many research studies since its invention in the early 1990s. fMRI allows us to measure the blood-oxygen-level dependent (BOLD) signal which is proportional to the ratio between oxygenated and deoxygenated hemoglobin in a volume of cortex (voxel). This ratio depends on the cerebral metabolic rate of oxygen consumption ($CMRO_2$) and the regional cerebral blood flow (rCBF). Although, an increase in the activity of neurons increases $CMRO_2$ and decreases the BOLD signal, the brain overcompensates the amount of oxygen needed and increases rCBF yielding an excess amount of oxygen in the blood supply. The excess oxygenated hemoglobin generates what we term as the hemodynamic response. This allows us to use the BOLD signal changes as an indirect measure of neural activity in humans. The BOLD signal has been better correlated to changes in the local field potential (LFP) rather than the action potentials in single cells (Logothetis & Wandell, 2004) suggesting that the BOLD signal accounts for

subthreshold membrane potentials in addition to action potentials. Although fMRI tells us little about changes at the single cell level it allows us to analyze changes in the BOLD signal across multiple brain regions at a time. This has revealed long range networks such as the resting state network (Biswal et al., 1997) and the attention networks (Corbetta & Shulman, 2002). We used this method to test for widespread influences of tDCS and to determine if the changes in activation levels of different cortical regions predict localization behavior.

Concurrent tDCS and fMRI

The combination of these techniques requires specific considerations to maintain proper safety for the subjects and prevent artifacts in the data. The addition of electrical circuits within the magnetic field may generate radiofrequency interference if the wires are not shielded properly. However, when properly shielded, the stimulation equipment/setup produces only a minor reduction in the signal to noise ratio with no distortion in the structural or functional images (Antal et al., 2011). The application of current may generate artifacts in the functional images, however, these artifacts have been shown to be near the scalp or restricted to the CSF (Antal, Bikson, et al., 2012; Antal et al., 2011; Holland et al., 2011). In our data analysis, we did see artifacts near the skull, however we removed voxels outside of the brain and limited analysis to regions within gray matter.

Given the recent development of techniques to safely and effectively combine transcranial electrical stimulation and MRI, there are only a small number of studies that have implemented tDCS with fMRI. Therefore, many

questions remain concerning how tDCS interacts with the BOLD signal. It is thought that tDCS-induced changes in the BOLD signal arise from changes in the excitability of neurons, which in turn alter the levels of oxygen in the blood (for a review see Turi et al., 2012). However, as mentioned in Chapter 5, there are other non-neural mechanisms that may mediate effects of tDCS on the BOLD signal such as direct changes to the blood vessels (Freeman, Durand, Kiper, & Carandini, 2002) or influences of the tDCS-induced electromagnetic fields on factors influencing the MR signal. Before discussing tDCS and fMRI studies, we first describe the effects of tDCS on rCBF since changes in rCBF are proportional to changes in the BOLD signal. We then briefly review the studies combining tDCS and fMRI and highlight specific factors applicable to Experiment 5.

Although most studies show an increase in rCBF in regions under the anode, these same studies have shown variable results in rCBF in regions under the cathode: increases (Zheng et al., 2011), decreases (Paquette et al., 2011; Wachter et al., 2011), and no change (Lang et al., 2005). Although it is thought that regions under the cathode reduce in excitability, which one may think should reduce rCBF, the inhomogeneities in the electrical field from tDCS and varying orientations of the neurons within the electrical field still cause a percentage of the neurons under the cathode to increase in excitability. The results from Zheng and colleagues (2011) also showed other widespread changes in rCBF in regions known to be anatomically or functionally connected to the stimulated region, whereas another study revealed widespread nonspecific cortical and subcortical increases and decreases in rCBF that lasted for at least 50 min post

stimulation (Lang et al., 2005). It does not necessarily follow that the variability shown in tDCS effects on rCBF will be comparable to the variability seen in the literature for the effects of tDCS on the BOLD signal since the BOLD signal depends on more than just rCBF.

Similar to behavioral studies with tDCS many of the early experiments with concurrent tDCS and fMRI studied motor tasks (Antal et al., 2011; Kwon & Jang, 2011; Kwon et al., 2008; Stagg, O'Shea, et al., 2009) and, therefore, applied tDCS over primary motor cortex. More recent studies have applied tDCS over other regions including hMT+ (Antal, Kovacs, et al., 2012), dorsolateral prefrontal cortex (Palm et al., 2011) and inferior frontal cortex (IFC) (Holland et al., 2011; Meinzer et al., 2012; Meinzer et al., 2013). However, to our knowledge, our fMRI study (Experiment 5B) is the only study to apply tDCS over PPC concurrent with fMRI. Unlike the consistent increase in rCBF under the tDCS anode, which predicts a consistent increase in the BOLD signal under the anode, some of the fMRI studies failed to show BOLD changes in voxels under the anode (Antal et al., 2011; Baudewig, Nitsche, Paulus, & Frahm, 2001) or even showed decreases (Holland et al., 2011; Meinzer et al., 2012). Similar to the variability in effects of the cathode on rCBF, studies showed varying changes in the BOLD signal under the cathode (Antal, Kovacs, et al., 2012; Antal et al., 2011; Stagg, O'Shea, et al., 2009). Several of the rCBF studies that showed increases in rCBF under the anode (Lang et al., 2005; Wachter et al., 2011; Zheng et al., 2011) applied tDCS for seven or more minutes. In addition, a study that applied tDCS for 10 minutes over M1 (Stagg, O'Shea, et al., 2009) showed an increase in the

BOLD signal in M1 regardless of tDCS polarity. However, tDCS duration alone is not enough to predict changes in the BOLD signal since studies using 1 – 2 min of stimulation showed increases in the BOLD signal in M1 (Kwon & Jang, 2011; Kwon et al., 2008), whereas another study with a similar electrode montage showed no changes in the BOLD signal in M1 after 5 min of tDCS (Baudewig et al., 2001). Interestingly, the application of tDCS for 20 min during rest periods between motor tasks decreased BOLD signal in M1 after repetition across 4 consecutive days. This suggests that the timing of stimulation relative to task performance and/or the repetition of tDCS over time may contribute to tDCS effects on the BOLD signal. Our results from Experiment 5B also suggest that individual subject differences may yield inconsistent changes in the BOLD signal as a result of tDCS. In summary, the literature shows a large amount of variability in the tDCS-induced changes in rCBF and the BOLD signal. Therefore, many questions remain concerning how the different stimulation and experimental parameters interact to alter the induction and duration of the tDCS-induced behavioral and BOLD effects.

In addition to the more local changes in the BOLD signal in regions under the electrodes, studies have also shown long-range changes in the BOLD signal in regions far from the electrodes. The ubiquitous tDCS-induced changes, however, shown by Lang and colleagues have not been replicated in our study or in other fMRI studies even those that have used similar electrode placement (Antal et al., 2011; Baudewig et al., 2001; Meinzer et al., 2012; Stagg, O'Shea, et al., 2009). Instead, fMRI studies have shown BOLD signal changes in regions

functionally or anatomically connected to the regions under the electrode (Pena-Gomez et al., 2012).

Although different experiments and different subjects show inconsistent or even counterintuitive effects of tDCS on the BOLD signal, our study (Experiment 5) and others show that these differences predict changes in behavior. A few recent studies have shown BOLD decreases in the IFC, with the anode over this area, in more cognitive tasks; picture naming or semantic word generation (Holland et al., 2011; Meinzer et al., 2012). A simple explanation of the anode increasing excitability does not explain these results. The researchers suggested that tDCS may improve efficiency; the reduction in the amount of energy (oxygen and glucose) required to complete the task. Haier and colleagues (1988) introduced the neural efficiency hypothesis to explain the reduction in cortical metabolic rates ($CMRO_2$) in individuals with increased cognitive ability. In support of tDCS improving neural efficiency and thereby decreasing the BOLD signal, Meinzer and colleagues (2013) showed that tDCS reduced the age-related increases in the BOLD signal, suggestive of hyperactivity, in an elderly population to improve performance on a word task. Therefore the local effects of tDCS on the BOLD signal in regions under the electrodes may be governed by two competing mechanisms; (1) tDCS increases in rCBF yielding increases in the BOLD signal and (2) tDCS reductions in $CMRO_2$ (increases in neural efficiency) yielding decreases in the BOLD signal. The resultant change in the BOLD signal as a result of tDCS application depends on the relative contribution of each of these mechanisms (for a review see Kar & Wright, 2014).

The literature does not support a simple statement such as anodal stimulation yields increases in neural excitability and concomitant increases in the BOLD signal and vice versa for cathodal stimulation. Even the terms anodal or cathodal stimulation are misleading since under both electrodes there are cells that will have excitability increased and decreased. Current research techniques do not provide adequate ways to determine the predicted change in a brain area from a specific tDCS montage because they are unable to account fully for the idiosyncratic differences in brain folding across subjects and tDCS-mediated effects through neural and non-neural mechanisms. Computational modeling has the potential to drive these predictions once we test their validity, but further research is needed to better understand the neural and non-neural mechanisms underlying tDCS and its effects on the BOLD signal.

Neural Mechanisms

In the context of position perception, the experiments in this thesis extend our understanding of visuospatial localization behavior, implicate PPC as a critical region for localization and suggest that the PPC may alter perceived position in a manner consistent with the ICT. Although questions still remain about the underlying neural mechanisms of position perception, we discuss this research in the context of various known mechanisms and make predictions about which mechanisms are most likely to govern the results seen from our experiments.

Neural Differences due to Eccentricity

Experiment 1 suggested that retinal eccentricity, in part, drives the influence of a target component on the localization of the target as a whole with two distinct weighting patterns. From a neural perspective, what could yield these differences in localization processing between foveal and peripheral regions? There are differences in receptive field size, cortical magnification, latency differences, and local circuitry (Roberts et al., 2007) between populations of neurons that respond to portions of the visual field closer to the fovea and those that respond to more peripheral regions of the visual field. We first consider why some subjects may show a pattern of higher weights at more foveal target components. One hypothesis is that signals from cells responding to these features may be more reliable. In the context of target (signal) detection, the cells responding to foveal components will be less influenced by external noise (features unrelated to the target) because they have smaller receptive fields. It may be advantageous to weight these responses higher when integrating across a population of cells. The reverse weighting pattern may arise because peripheral cells are tuned more to transient stimuli (Croner & Kaplan, 1995), which we used in our experiments, and optimized to average target components (Rosenholtz, 2011). Carrasco and colleagues (2003) have shown that the speed of visual processing is greater in more peripheral regions, which is consistent with peripheral regions having a higher sensitivity to the temporal properties of a stimulus. Therefore, another hypothesis is that it may be better to weight the responses from cells optimized for a specific task higher. Our results from

Experiment 1 suggest that some subjects may optimize the peripheral components for the brief stimulus, whereas other subjects may optimize components closer to the fovea that fall within regions of higher acuity. We also found similar patterns of responses in Experiments 3 and 4 (data not shown). We chose a brief stimulus to increase the likelihood of mislocalization to probe the limitations of visual localization. However, future experiments could examine stimuli at different durations to determine if different weighting patterns emerge. This would suggest that localization may not be a static process, but instead governed by a dynamic network that may be optimized for different tasks.

Neural Changes due to Attentional Cueing

How might the changes in neural networks due to attentional manipulations result in a change in perceived position? Increases in the weighting of target components around the attentional cue could result from increases in neuronal firing in visual areas (Reynolds, Pasternak, & Desimone, 2000), sharpening of neuronal tuning (Martinez-Trujillo & Treue, 2004; Spitzer, Desimone, & Moran, 1988), improvements in gamma synchrony across cells responsive to attended regions (Fries, Reynolds, Rorie, & Desimone, 2001) or increases in the degree of functional integration of attended stimuli (Haynes, Tregellas, & Rees, 2005). All of these factors could induce attentional biases that shift localization towards the spatial position designated by the cue and yield increases in the weights around the attentional cue (Figure 3-7). For example, assume the brain encodes position perception as an average of the response across a population of labeled line cells (as in Figure 1-1). An attended cell with a

higher firing rate (and potentially higher weight during integration) could skew the population response towards the attended location. We refer to these effects as attentional attraction, i.e. the shift of perceived position in the same direction as attention. In support of this, shifts in localization in the direction of attention have been shown behaviorally (Tsal & Bareket, 1999). Although our results support an attractional effect of attention, other studies have shown attentional repulsion effects (Suzuki & Cavanagh, 1997); the shift of perceived position in the direction opposite to attention that could correlate to a reduction in the weights around the attentional cue. Repulsive effects of attention have been linked to receptive field shifts towards the site of attention in V4 (Connor, Gallant, Preddie, & Van Essen, 1996) and MT (Womelsdorf et al., 2006; Womelsdorf et al., 2008) even when the receptive field is far from the attended locus. In the context of the labeled line model, the receptive field shifts would not alter the “label” of a neuron and this results in shifts in the perceived position of a stimulus in the direction opposite to attention. For example, in Figure 1-1, if we consider one of the black dots as a cell, then the brain will still maintain the link between that cell and its respective grid location (the grid label remains the same) under conditions without attention, even if it’s response is actually to adjacent grid location from a receptive field shift due to attention. Experiments 1-4 show an attractive bias in localization as a result of attentional cues. Experiment 1 suggests it may be due to a biased integration of the stimulus components with increased weight in components around the position of the cue, albeit with variability in spatial extent across subjects, see Figure 3-7. Therefore, at least in the context of our centroid task,

we do not find effects of attentional repulsion. However, our behavioral data are too coarse to distinguish among the relative contributions (attraction versus repulsion) of attentional modulation of neuronal activity of early visual areas (for a review see Kastner & Ungerleider, 2000; Reynolds & Chelazzi, 2004), attentional modulation of receptive field location (Womelsdorf et al., 2006; Womelsdorf et al., 2008), or the eccentricity-dependent attentional modulation of spatial integration (Roberts et al., 2007). Future studies using functional imaging or electrophysiological recordings are required to determine how visual cortex integrates spatial information and generates a percept of position.

PPC may be the site of integration or encode the final position percept. Therefore, tDCS over PPC may alter this processing or it may amplify biases inherited from early visual cortical areas. Mislocalizations of the basic features of an object could influence object localization as a whole and a recent study has suggested that information about the perceived location of an object may be available as early as V1 (Fischer, Spotswood, & Whitney, 2011). Given PPC's role in attention, we hypothesized that tDCS-induced modulations in PPC may instead generate feedback to early visual cortical areas. Influences of attention have been shown throughout various visual cortical areas resulting in attention weight maps (R. Datta & DeYoe, 2009). Increases in the BOLD signal due to attention have been shown in tasks requiring motion discrimination (Gandhi, Heeger, & Boynton, 1999), comparison of multiple stimuli (Haynes et al., 2005) or detection of orientation and color conjunctions (Brefczynski & DeYoe, 1999) as early as primary visual cortex, V1. Our results from Aim 2 and Aim 3 do not

support that PPC modulates position perception by alterations in local processing or feedback to early visual cortical areas. Instead our results suggest that PPC may influence the global processing of the centroid estimation based on the bilateral activation levels across left and right PPC in a manner consistent with the ICT (see *Spatial Attention* section).

Position Encoding

We present our results in the context of a conceptual model based on the principles of the labeled line theory (Figure 1-1). We acknowledge that this conceptual model ignores additional complexities from lateral connectivity within neuronal populations (Gilbert, 1992) and integration of information from cells with different feature preferences, i.e. orientation, contrast, and spatial frequency, both within and across different cortical areas. Therefore, the integration across populations of cells may not be a simple linear combination of component driven active neural populations with biases introduced by local differences in neural circuitry. However, this model provides a framework for us to test behavioral and neural predictions. From a behavioral standpoint, much of the variance in Experiment 1 is well explained by a labeled line model. Although Experiments 3-5 do not provide evidence for a labeled line model per se, they suggest that PPC may introduce a bias in perceived position at later processing stages.

Future experiments to test our predictions of an early bias in localization mediated by changes in the neural signals in early visual cortical areas could examine patterns in neural firing or BOLD signals that correlate to perceived position. Previous work has shown that these regions contain information about

perceived position (Fischer et al., 2011), but it has not been shown whether trial by trial fluctuations in these signals generate errors in perceived position, which can be tested with or without attentional manipulations. This is an initial step to confirming a labeled line model in perceived position. If found, by using TMS or other stimulation techniques, it may be possible to target regions within and outside of occipital cortex and examine neural changes in early visual cortical areas. This may quantify if and how a particular region alters the “weighting” of activity in early visual areas and whether these modulations correlate to changes in perceived position.

Spatial Attention

Our results (Experiment 3-5) show that tDCS over PPC induced changes in perceived centroid position consistent with predictions of the ICT as discussed in Chapters 4 and 5. However, other global theories of attention also make predictions about the outcome of our experiments and the influence of attention on localization. The hemispatial theory, for instance, proposes that the right hemisphere directs attention to both visual fields, potentially with a bias towards the left visual field (Duncan et al., 1999), whereas the left hemisphere directs attention solely to the right visual field (Heilman & Van Den Abell, 1980; Mesulam, 1981). If the right hemisphere can indeed direct attention to both visual fields without any interference or contribution from the left hemisphere, then we would expect mislocalization in the rPPCc condition (which is thought to decrease excitability of the right hemisphere) but no mislocalization in the rPPCa condition (which is thought to increase excitability in the right hemisphere). Our

data from Experiments 3 and 4 however, are inconsistent with this as rPPCa stimulation induced perceived centroid shifts in the majority of subjects. In addition, the hemispatial theory suggests that activation solely in the left PPC is enough to determine whether attention, and thereby perceived position, is directed towards the left or right visual field. This suggests that changes within the left PPC may better correlate to differences in behavior rather than a comparison of left and right PPC, however Aim 3 disproves this hypothesis. Therefore, we conclude that the balance in activation between hemispheres plays a critical role in the allocation of attention.

The ICT postulates that the connections between left and right PPC are mutually inhibitory, however, another theory posits that attention operates through facilitatory interactions between homologous regions in the two hemispheres (Siman-Tov et al., 2007) and that both hemispheres respond to stimuli in the left and right visual field. In our experimental design, tDCS always excited one hemisphere while it suppressed the other (assuming traditional effects of excitability changes under the anode and cathode, respectively). If facilitation were a purely linear additive process, our manipulation should have had no effect. The effects in a nonlinearly coupled system, however, are much harder to predict and depend critically on the details of the (facilitatory and/or inhibitory) connections and their dynamics.

Conclusions

Visuospatial localization is a fundamental aspect of visual processing that is imperative for us to complete many of our daily tasks. Although we know many

properties of the neurons underlying visual processing, it remains unclear how the distributed processing of object components resolves into a single percept of position. This thesis addressed only a few of the many outstanding questions in this field. Although we provide evidence for the influence of different factors and different cortical areas on position perception, additional studies are needed to understand how attention alters spatial processing, what brain area(s) completes the integration of target components and when and where errors are introduced into the computations of perceived position.

Significance

Understanding the mechanisms of spatial perception is necessary not just to understand visuospatial processing in healthy humans, but to also target rehabilitative methods to restore perception and increase the independence of persons with visuospatial neglect and other visuospatial disorders. We discuss our research findings in the context of spatial neglect, however, the application of our results can extend to other visuospatial disorders.

Damage to particular cortical and subcortical regions will induce local dysfunction of neurons at the site of the lesion (local injury hypothesis), as well as alterations in the functioning of separate but connected regions within a larger network (distributed injury hypothesis). Corbetta and colleagues (2005) showed abnormal activation in both the dorsal and ventral frontoparietal attention networks following lesions to ventral frontal cortex. In addition to alterations in function within the damaged hemisphere, damage to these regions may also disinhibit cortical regions in the contralateral hemisphere as proposed by the ICT

(Kinsbourne, 1977). Therefore, decreased levels of activity in the damaged hemisphere not only reduce spatial processing in the contralesional visual field but also reduce inhibition in the unaffected hemisphere. The unaffected hemisphere may then become overactive and exacerbate the condition (Oliveri et al., 2000). Transcranial direct current stimulation has been shown to improve line bisection performance in spatial neglect patients (Sparing et al., 2009). Therefore, tDCS over PPC or other frontal areas has the potential to be an effective and accessible therapeutic tool for spatial neglect patients. Our results from Experiment 5 suggest that tDCS can alter neural activity and influence perceived position, however, the traditional tDCS montage for spatial neglect patients; anode (cathode) over the lesioned (nonlesioned) hemisphere, may not be the best to mitigate localization deficits. Rehabilitation methods need to account for individualized effects of tDCS. Computational modeling may be useful to predict current density in conjunction with fMRI to confirm expected changes in critical cortical areas in individual patients.

Since the damage in spatial neglect best corresponds to higher cognitive centers mediating attention or sensorimotor integration, this suggests that some amount of sensory input is still processed, but potentially ignored. Some studies have suggested that this sensory input may still influence behavior even without perceptual awareness of the stimuli (Berti, 2002). Given this, spatial neglect may be induced from errors in integration or global processing as opposed to changes in the weighting of visual input. Although we did not test spatial neglect subjects, Aims 2 and 3 show that tDCS over PPC alters visual localization in a manner

consistent with the ICT. This shows PPC plays a critical role in position perception and raises the possibility that targeting this region may yield rehabilitative solutions for neglect.

Chapter 7: **References**

Adam, J. J., Davelaar, E. J., van der Gouw, A., & Willems, P. (2008). Evidence for attentional processing in spatial localization. *Psychological Research, 72*(4), 433-442.

Adam, J. J., Ketelaars, M., Kingma, H., & Hoek, T. (1993). On the time course and accuracy of spatial localization: basic data and a two-process model. *Acta Psychologica, 84*(2), 135-159.

Adam, J. J., Paas, F. G., Ekering, J., & van Loon, E. M. (1995). Spatial localization: tests of a two-process model. *Experimental Brain Research, 102*(3), 531-539.

Andersen, R. A., Essick, G. K., & Siegel, R. M. (1985). Encoding of spatial location by posterior parietal neurons. *Science, 230*(4724), 456-458.

Antal, A., Bikson, M., Datta, A., Lafon, B., Dechent, P., Parra, L. C., et al. (2012). Imaging artifacts induced by electrical stimulation during conventional fMRI of the brain. *NeuroImage, 85*(Pt 3), 1040-1047.

Antal, A., Kovacs, G., Chaieb, L., Cziraki, C., Paulus, W., & Greenlee, M. W. (2012). Cathodal stimulation of human MT+ leads to elevated fMRI signal: a tDCS-fMRI study. *Restorative Neurology and Neuroscience, 30*(3), 255-263.

Antal, A., Nitsche, M. A., Kincses, T. Z., Kruse, W., Hoffmann, K. P., & Paulus, W. (2004). Facilitation of visuo-motor learning by transcranial direct current stimulation of the motor and extrastriate visual areas in humans. *European Journal of Neuroscience, 19*(10), 2888-2892.

Antal, A., Nitsche, M. A., & Paulus, W. (2001). External modulation of visual perception in humans. *Neuroreport, 12*(16), 3553-3555.

Antal, A., Polania, R., Schmidt-Samoa, C., Dechent, P., & Paulus, W. (2011). Transcranial direct current stimulation over the primary motor cortex during fMRI. *NeuroImage, 55*(2), 590-596.

Anton-Erxleben, K., Henrich, C., & Treue, S. (2007). Attention changes perceived size of moving visual patterns. *Journal of Vision, 7*(11), 51-59.

Baudewig, J., Nitsche, M. A., Paulus, W., & Frahm, J. (2001). Regional modulation of BOLD MRI responses to human sensorimotor activation by transcranial direct current stimulation. *Magnetic resonance in medicine: official journal of the Society of Magnetic Resonance in Medicine / Society of Magnetic Resonance in Medicine, 45*(2), 196-201.

Benucci, A., Saleem, A. B., & Carandini, M. (2013). Adaptation maintains population homeostasis in primary visual cortex. *Nature Neuroscience, 16*(6), 724-729.

Berti, A. (2002). Unconscious processing in neglect. In D. M. H. O. Karnath, and G. Vallar (Ed.), *The Cognitive and Neural Bases of Spatial Neglect* (pp. 313-326). Oxford: Oxford University Press.

Bisley, J. W., & Goldberg, M. E. (2003). Neuronal activity in the lateral intraparietal area and spatial attention. *Science, 299*(5603), 81-86.

Biswal, B. B., Van Kylen, J., & Hyde, J. S. (1997). Simultaneous assessment of flow and BOLD signals in resting-state functional connectivity maps. *NMR in Biomedicine, 10*(4-5), 165-170.

Bocianski, D., Müsseler, J., & Erlhagen, W. (2010). Effects of attention on a relative mislocalization with successively presented stimuli. *Vision Research, 50*(18), 1793-1802.

Borra, E., Belmalih, A., Calzavara, R., Gerbella, M., Murata, A., Rozzi, S., et al. (2008). Cortical connections of the macaque anterior intraparietal (AIP) area. *Cerebral Cortex, 18*(5), 1094-1111.

Bowers, D., & Heilman, K. M. (1980). Pseudoneglect: effects of hemispace on a tactile line bisection task. *Neuropsychologia, 18*(4-5), 491-498.

Brefczynski, J. A., & DeYoe, E. A. (1999). A physiological correlate of the 'spotlight' of visual attention. *Nature Neuroscience, 2*(4), 370-374.

Bremmer, F., Distler, C., & Hoffmann, K. P. (1997). Eye position effects in monkey cortex. II. Pursuit- and fixation-related activity in posterior parietal areas LIP and 7A. *Journal of Neurophysiology, 77*(2), 962-977.

Bridgeman, B., Peery, S., & Anand, S. (1997). Interaction of cognitive and sensorimotor maps of visual space. *Perception and Psychophysics, 59*(3), 456-469.

Brighina, F., Bisiach, E., Piazza, A., Oliveri, M., La Bua, V., Daniele, O., et al. (2002). Perceptual and response bias in visuospatial neglect due to frontal and parietal repetitive transcranial magnetic stimulation in normal subjects. *Neuroreport, 13*(18), 2571-2575.

Brocke, J., Schmidt, S., Irlbacher, K., Cichy, R. M., & Brandt, S. A. (2008). Transcranial cortex stimulation and fMRI: electrophysiological correlates of dual-pulse BOLD signal modulation. *NeuroImage, 40*(2), 631-643.

Burnham, K. P., & Anderson, D. R. (2002). *Model selection and multi-model inference: A practical Information-theoretic approach* (2nd ed.). New York: Springer-Verlag.

Carpenter, R. H. S. (1988). *Movements of the eyes* (2nd ed.). London: Pion.

Carrasco, M., McElree, B., Denisova, K., & Giordano, A. M. (2003). Speed of visual processing increases with eccentricity. *Nature Neuroscience, 6*(7), 699-670.

Chan, C. Y., Hounsgaard, J., & Nicholson, C. (1988). Effects of electric fields on transmembrane potential and excitability of turtle cerebellar Purkinje cells in vitro. *The Journal of Physiology, 402*, 751-771.

Cheal, M., & Lyon, D. R. (1991). Central and peripheral precuing of forced-choice discrimination. *Quarterly Journal of Experimental Psychology. A, Human Experimental Psychology, 43*(4), 859-880.

Cohen, E. H., Schnitzer, B. S., Gersch, T. M., Singh, M., & Kowler, E. (2007). The relationship between spatial pooling and attention in saccadic and perceptual tasks. *Vision Research, 47*(14), 1907-1923.

Cohen, J. D., Romero, R. D., Servan-Schreiber, D., & Farah, M. J. (1994). Mechanisms of spatial attention: the relation of macrostructure to microstructure in parietal neglect. *Journal of Cognitive Neuroscience, 6*(4), 377-387.

Colby, C. L., Duhamel, J. R., & Goldberg, M. E. (1996). Visual, presaccadic, and cognitive activation of single neurons in monkey lateral intraparietal area. *Journal of Neurophysiology, 76*(5), 2841-2852.

Connor, C. E., Gallant, J. L., Preddie, D. C., & Van Essen, D. C. (1996). Responses in area V4 depend on the spatial relationship between stimulus and attention. *Journal of Neurophysiology, 75*(3), 1306-1308.

Cook, E. P., & Maunsell, J. H. (2002). Attentional modulation of behavioral performance and neuronal responses in middle temporal and ventral intraparietal areas of macaque monkey. *Journal of Neuroscience, 22*(5), 1994-2004.

Corbetta, M., Kincade, M. J., Lewis, C., Snyder, A. Z., & Sapir, A. (2005). Neural basis and recovery of spatial attention deficits in spatial neglect. *Nature Neuroscience, 8*(11), 1603-1610.

Corbetta, M., & Shulman, G. L. (2002). Control of goal-directed and stimulus-driven attention in the brain. *Nature Reviews: Neuroscience, 3*(3), 215-229.

Croner, L. J., & Kaplan, E. (1995). Receptive fields of P and M ganglion cells across the primate retina. *Vision Research, 35*, 7-24.

Dambeck, N., Sparing, R., Meister, I. G., Wienemann, M., Weidemann, J., Topper, R., et al. (2006). Interhemispheric imbalance during visuospatial attention investigated by unilateral and bilateral TMS over human parietal cortices. *Brain Research, 1072*(1), 194-199.

Datta, A., Baker, J. M., Bikson, M., & Fridriksson, J. (2011). Individualized model predicts brain current flow during transcranial direct-current stimulation treatment in responsive stroke patient. *Brain Stimulation, 4*(3), 169-174.

Datta, A., Bansal, V., Diaz, J., Patel, J., Reato, D., & Bikson, M. (2009). Gyri-precise head model of transcranial direct current stimulation: improved

spatial focality using a ring electrode versus conventional rectangular pad. *Brain Stimulation, 2*(4), 201-207.

Datta, A., Zhou, X., Su, Y., Parra, L. C., & Bikson, M. (2013). Validation of finite element model of transcranial electrical stimulation using scalp potentials: implications for clinical dose. *Journal of Neural Engineering, 10*(3), 036018.

Datta, R., & DeYoe, E. A. (2009). I know where you are secretly attending! The topography of human visual attention revealed with fMRI. *Vision Research, 49*(10), 1037-1044.

De Valois, R. L., & De Valois, K. K. (1991). Vernier acuity with stationary moving Gabors. *Vision Research, 31*(9), 1619-1626.

Drew, S. A., Chubb, C. F., & Sperling, G. (2010). Precise attention filters for Weber contrast derived from centroid estimations. *Journal of Vision, 10*(10), 20.

Duncan, J., Bundesen, C., Olson, A., Humphreys, G., Chavda, S., & Shibuya, H. (1999). Systematic analysis of deficits in visual attention. *Journal of Experimental Psychology: General, 128*(4), 450-478.

Durand, J. B., Trotter, Y., & Celebrini, S. (2010). Privileged processing of the straight-ahead direction in primate area V1. *Neuron, 66*(1), 126-137.

Durand, S., Fromy, B., Bouye, P., Saumet, J. L., & Abraham, P. (2002). Vasodilatation in response to repeated anodal current application in the human skin relies on aspirin-sensitive mechanisms. *The Journal of Physiology, 540*(Pt 1), 261-269.

Dymond, A. M., Coger, R. W., & Serafetinides, E. A. (1975). Intracerebral current levels in man during electrosleep therapy. *Biological Psychiatry, 10*(1), 101-104.

Elbert, T., Lutzenberger, W., Rockstroh, B., & Birbaumer, N. (1981). The influence of low-level transcortical DC-currents on response speed in humans. *International Journal of Neuroscience, 14*(1-2), 101-114.

Felleman, D. J., & Van Essen, D. C. (1991). Distributed hierarchical processing in the primate cerebral cortex. *Cerebral Cortex, 1*(1), 1-47.

Fierro, B., Brighina, F., Oliveri, M., Piazza, A., La Bua, V., Buffa, D., et al. (2000). Contralateral neglect induced by right posterior parietal rTMS in healthy subjects. *Neuroreport, 11*(7), 1519-1521.

Findlay, J. M. (1982). Global visual processing for saccadic eye movements. *Vision Research, 22*(8), 1033-1045.

Findlay, J. M., Brogan, D., & Wenban-Smith, M. G. (1993). The spatial signal for saccadic eye movements emphasizes visual boundaries. *Perception & Psychophysics, 53*(6), 633-641.

Fink, G. R., Marshall, J. C., Shah, N. J., Weiss, P. H., Halligan, P. W., Grosse-Ruyken, M., et al. (2000). Line bisection judgments implicate right parietal cortex and cerebellum as assessed by fMRI. *Neurology, 54*(6), 1324-1331.

Fischer, J., Spotswood, N., & Whitney, D. (2011). The emergence of perceived position in the visual system. *Journal of Cognitive Neuroscience, 23*(1), 119-136.

Fortenbaugh, F. C., & Robertson, L. C. (2011). When here becomes there: Attentional distribution modulates foveal bias in peripheral localization. *Attention, Perception & Psychophysics, 73*(3), 809-828.

Freeman, T. C., Durand, S., Kiper, D. C., & Carandini, M. (2002). Suppression without inhibition in visual cortex. *Neuron, 35*(4), 759-771.

Fries, P., Reynolds, J. H., Rorie, A. E., & Desimone, R. (2001). Modulation of oscillatory neuronal synchronization by selective visual attention. *Science, 291*(5508), 1560-1563.

Fritsch, B., Reis, J., Martinowich, K., Schambra, H. M., Ji, Y., Cohen, L. G., et al. (2010). Direct current stimulation promotes BDNF-dependent synaptic plasticity: potential implications for motor learning. *Neuron, 66*(2), 198-204.

Gandhi, S. P., Heeger, D. J., & Boynton, G. M. (1999). Spatial attention affects brain activity in human primary visual cortex. *Proceedings of the National Academy of Sciences USA, 96*(6), 3314-3319.

Gandiga, P. C., Hummel, F. C., & Cohen, L. G. (2006). Transcranial DC stimulation (tDCS): a tool for double-blind sham-controlled clinical studies in brain stimulation. *Clinical Neurophysiology, 117*(4), 845-850.

Giglia, G., Mattaliano, P., Puma, A., Rizzo, S., Fierro, B., & Brighina, F. (2011). Neglect-like effects induced by tDCS modulation of posterior parietal cortices in healthy subjects. *Brain Stimulation, 4*(4), 294-299.

Gilbert, C. D. (1992). Horizontal integration and cortical dynamics. *Neuron, 9*(1), 1-13.

Gnadt, J. W., & Andersen, R. A. (1988). Memory related motor planning activity in posterior parietal cortex of macaque. *Experimental Brain Research, 70*(1), 216-220.

Goldberg, M. E., Bisley, J. W., Powell, K. D., & Gottlieb, J. (2006). Saccades, salience and attention: the role of the lateral intraparietal area in visual behavior. *Progress in Brain Research, 155*(Pt B), 157-175.

Goldberg, M. E., & Wurtz, R. H. (1972). Activity of superior colliculus in behaving monkey. II. Effect of attention on neuronal responses. *Journal of Neurophysiology, 35*(4), 560-574.

Goodale, M. A., & Milner, A. D. (2010). Two visual streams: Interconnections do not imply duplication of function. *Cognitive Neuroscience, 1*(1), 65-68.

Haier, R. J., Siegel, B. V., Nuechterlein, K. H., Hazlett, E., Wu, J. C., Paek, J., et al. (1988). Cortical glucose metabolic-rate correlates of abstract reasoning and attention studied with positron emission tomography. *Intelligence, 12*(2), 199-217.

Hartmann, T. S., Bremmer, F., Albright, T. D., & Krekelberg, B. (2011). Receptive field positions in area MT during slow eye movements. *Journal of Neuroscience, 31*(29), 10437-10444.

Hattori, Y., Moriwaki, A., & Hori, Y. (1990). Biphasic effects of polarizing current on adenosine-sensitive generation of cyclic AMP in rat cerebral cortex. *Neuroscience Letters, 116*(3), 320-324.

Haynes, J. D., Tregellas, J., & Rees, G. (2005). Attentional integration between anatomically distinct stimulus representations in early visual cortex. *Proceedings of the National Academy of Sciences USA, 102*(41), 14925-14930.

He, P., & Kowler, E. (1991). Saccadic localization of eccentric forms. *Journal of the Optical Society of America A: Optics and Image Science, 8*(2), 440-449.

Heeger, D. J. (1992). Normalization of cell responses in cat striate cortex. *Visual Neuroscience, 9*(2), 181-197.

Heilman, K. M., & Van Den Abell, T. (1980). Right hemisphere dominance for attention: the mechanism underlying hemispheric asymmetries of inattention (neglect). *Neurology, 30*(3), 327-330.

Herwig, U., Satrapi, P., & Schonfeldt-Lecuona, C. (2003). Using the international 10-20 EEG system for positioning of transcranial magnetic stimulation. *Brain Topography, 16*(2), 95-99.

Hilgetag, C. C., Theoret, H., & Pascual-Leone, A. (2001). Enhanced visual spatial attention ipsilateral to rTMS-induced 'virtual lesions' of human parietal cortex. *Nature Neuroscience, 4*(9), 953-957.

Holland, R., Leff, A. P., Josephs, O., Galea, J. M., Desikan, M., Price, C. J., et al. (2011). Speech facilitation by left inferior frontal cortex stimulation. *Current Biology, 21*(16), 1403-1407.

Honda, H. (1989). Perceptual localization of visual stimuli flashed during saccades. *Perception & Psychophysics, 45*(2), 162-174.

Honda, H. (1991). The time courses of visual mislocalization and of extraretinal eye position signals at the time of vertical saccades. *Vision Research, 31*(11), 1915-1921.

Ibbotson, M., & Krekelberg, B. (2011). Visual perception and saccadic eye movements. *Current Opinion in Neurobiology, 21*(4), 553-558.

Islam, N., Aftabuddin, M., Moriwaki, A., & Hori, Y. (1997). Effects of anodal polarization on protein kinase Cγ (PKCγ) in the rat brain. *Indian Journal of Physiology and Pharmacology, 41*(3), 204-210.

Iyer, M. B., Mattu, U., Grafman, J., Lomarev, M., Sato, S., & Wassermann, E. M. (2005). Safety and cognitive effect of frontal DC brain polarization in healthy individuals. *Neurology, 64*(5), 872-875.

Iyer, M. B., Schleper, N., & Wassermann, E. M. (2003). Priming stimulation enhances the depressant effect of low-frequency repetitive transcranial magnetic stimulation. *Journal of Neuroscience, 23*(34), 10867-10872.

Jaeger, D. E. T., Lutzenberger, W., & Birbaumer, N. (1987). The effects of externally applied transcephalic weak direct currents on lateralization in choice reaction tasks. *Journal of Psychophysiology, 1*(1987), 127-133.

Jewell, G., & McCourt, M. E. (2000). Pseudoneglect: a review and meta-analysis of performance factors in line bisection tasks. *Neuropsychologia, 38*(1), 93-110.

Johnson, C. A., Keltner, J. L., & Balestrery, F. (1978). Effects of target size and eccentricity on visual detection and resolution. *Vision Research, 18*(9), 1217-1222.

Kaiser, M., & Lappe, M. (2004). Perisaccadic mislocalization orthogonal to saccade direction. *Neuron, 41*(2), 293-300.

Kar, K., & Krekelberg, B. (2012). Transcranial electrical stimulation over visual cortex evokes phosphenes with a retinal origin. *Journal of Neurophysiology, 108*(8), 2173-2178.

Kar, K., & Krekelberg, B. (2013, November). *Transcranial electrical stimulation mitigates motion adaption in V1, MT, and MST neurons of awake, behaving macaques.* Paper presented at the Annual meeting of the Society for Neuroscience, San Diego, CA.

Kar, K., & Krekelberg, B. (2014). Transcranial Alternating Current Stimulation Attenuates Visual Motion Adaptation. *Journal of Neuroscience, 34*(21), 7334-7340.

Kar, K., & Wright, J. (2014). Probing the mechanisms underlying the mitigation of cognitive aging with anodal transcranial direct current stimulation. *Journal of Neurophysiology, 111*(7), 1397-1399.

Karnath, H. O., Milner, A. D., & Vallar, G. (2002). *The cognitive and neural bases of spatial neglect*. Oxford, UK: Oxford University Press.

Kastner, S., & Ungerleider, L. G. (2000). Mechanisms of visual attention in the human cortex. *Annual Review of Neuroscience, 23*, 315-341.

Kaufman, L., & Richards, W. (1969). Spontaneous fixation tendencies for visual forms. *Perception and Psychophysics, 5*(2), 85-88.

Keizer, A. W., Colzato, L. S., & Hommel, B. (2008). Integrating faces, houses, motion, and action: spontaneous binding across ventral and dorsal processing streams. *Acta psychologica, 127*(1), 177-185.

Kerzel, D. (2003). Attention maintains mental extrapolation of target position: irrelevant distractors eliminate forward displacement after implied motion. *Cognition, 88*(1), 109-131.

Kinsbourne, M. (1977). Hemi-neglect and hemisphere rivalry. *Advances in Neurology, 18*, 41-49.

Ko, M. H., Han, S. H., Park, S. H., Seo, J. H., & Kim, Y. H. (2008). Improvement of visual scanning after DC brain polarization of parietal cortex in stroke patients with spatial neglect. *Neuroscience Letters, 448*(2), 171-174.

Korsakov, I. A., & Matveeva, L. V. (1982). Psychophysical characteristics of perception and of brain electrical activity during occipital micropolarization. *Human Physiology, 8*(4), 259-266.

Kosovicheva, A. A., Fortenbaugh, F. C., & Robertson, L. C. (2010). Where does attention go when it moves? Spatial properties and locus of the attentional repulsion effect. *Journal of Vision, 10*(12), 1-13.

Kowler, E., & Blaser, E. (1995). The accuracy and precision of saccades to small and large targets. *Vision Research, 35*(12), 1741-1754.

Kravitz, D. J., Saleem, K. S., Baker, C. I., & Mishkin, M. (2011). A new neural framework for visuospatial processing. *Nature Reviews. Neuroscience, 12*(4), 217-230.

Krekelberg, B., & Lappe, M. (1999). Temporal recruitment along the trajectory of moving objects and the perception of position. *Vision Research, 39*(16), 2669-2679.

Krekelberg, B., & Lappe, M. (2001). Neuronal latencies and the position of moving objects. *Trends in Neurosciences, 24*(6), 335-339.

Kwon, Y. H., & Jang, S. H. (2011). The enhanced cortical activation induced by transcranial direct current stimulation during hand movements. *Neuroscience Letters, 492*(2), 105-108.

Kwon, Y. H., Ko, M. H., Ahn, S. H., Kim, Y. H., Song, J. C., Lee, C. H., et al. (2008). Primary motor cortex activation by transcranial direct current stimulation in the human brain. *Neuroscience Letters, 435*(1), 56-59.

Landy, M. S. (1993). *Combining multiple cues for texture edge localization.* Paper presented at the Human Vision, Visual Processing, and Digital Display IV, SPIE Proceedings, San Jose, CA.

Landy, M. S., & Kojima, H. (2001). Ideal cue combination for localizing texture-defined edges. *Journal of the Optical Society of America A, 18*(9), 2307-2320.

Lang, N., Siebner, H. R., Ward, N. S., Lee, L., Nitsche, M. A., Paulus, W., et al. (2005). How does transcranial DC stimulation of the primary motor cortex alter regional neuronal activity in the human brain? *European Journal of Neuroscience, 22*(2), 495-504.

Lappe, M., & Krekelberg, B. (1998). The Position of Moving Objects. *Perception, 27*(12), 1437-1449.

Liebetanz, D., Nitsche, M. A., Tergau, F., & Paulus, W. (2002). Pharmacological approach to the mechanisms of transcranial DC-stimulation-induced after-effects of human motor cortex excitability. *Brain, 125*(10), 2238-2247.

Logothetis, N. K., & Wandell, B. A. (2004). Interpreting the BOLD Signal. *Annual Review of Physiology, 66*(1), 735-769.

Lopez, L., Chan, C. Y., Okada, Y. C., & Nicholson, C. (1991). Multimodal characterization of population responses evoked by applied electric field in vitro: extracellular potential, magnetic evoked field, transmembrane potential, and current-source density analysis. *Journal of Neuroscience, 11*(7), 1998-2010.

Mahon, B. Z., Milleville, S. C., Negri, G. A., Rumiati, R. I., Caramazza, A., & Martin, A. (2007). Action-related properties shape object representations in the ventral stream. *Neuron, 55*(3), 507-520.

Martinez-Trujillo, J. C., & Treue, S. (2004). Feature-based attention increases the selectivity of population responses in primate visual cortex. *Current Biology, 14*(9), 744-751.

Mateeff, S., & Gourevich, A. (1983). Peripheral vision and perceived visual direction. *Biological Cybernetics, 49*(2), 111-118.

Mathys, C., Loui, P., Zheng, X., & Schlaug, G. (2010). Non-invasive brain stimulation applied to Heschl's gyrus modulates pitch discrimination. *Frontiers in Psychology, 1*, 193.

Matin, L., & Pearce, D. G. (1965). Visual perception of direction for stimuli flashed during voluntary saccadic eye movements. *Science, 148*(3676), 1485-1488.

Matsunaga, K., Nitsche, M. A., Tsuji, S., & Rothwell, J. C. (2004). Effect of transcranial DC sensorimotor cortex stimulation on somatosensory evoked potentials in humans. *Clinical Neurophysiology, 115*(2), 456-460.

McCloskey, M., & Rapp, B. (2000). Attention-referenced visual representations: evidence from impaired visual localization. *Journal of Experimental Psychology. Human Perception and Performance, 26*(3), 917-933.

McGowan, J. W., Kowler, E., Sharma, A., & Chubb, C. (1998). Saccadic localization of random dot targets. *Vision Research, 38*(6), 895-909.

Meinzer, M., Antonenko, D., Lindenberg, R., Hetzer, S., Ulm, L., Avirame, K., et al. (2012). Electrical brain stimulation improves cognitive performance by modulating functional connectivity and task-specific activation. *Journal of Neuroscience, 32*(5), 1859-1866.

Meinzer, M., Lindenberg, R., Antonenko, D., Flaisch, T., & Floel, A. (2013). Anodal transcranial direct current stimulation temporarily reverses age-associated cognitive decline and functional brain activity changes. *Journal of Neuroscience, 33*(30), 12470-12478.

Melcher, D., & Kowler, E. (1999). Shapes, surfaces and saccades. *Vision Research, 39*(17), 2929-2946.

Merriam, E. P., Gardner, J. L., Movshon, J. A., & Heeger, D. J. (2013). Modulation of visual responses by gaze direction in human visual cortex. *Journal of Neuroscience, 33*(24), 9879-9889.

Mesulam, M. M. (1981). A cortical network for directed attention and unilateral neglect. *Annals of Neurology, 10*(4), 309-325.

Michel, M. M., Chen, Y., Geisler, W. S., & Seidemann, E. (2013). An illusion predicted by V1 population activity implicates cortical topography in shape perception. *Nature Neuroscience, 16*(10), 1477-1483.

Mielke, D., Wrede, A., Schulz-Schaeffer, W., Taghizadeh-Waghefi, A., Nitsche, M. A., Rohde, V., et al. (2013). Cathodal transcranial direct current stimulation induces regional, long-lasting reductions of cortical blood flow in rats. *Neurological Research, 35*(10), 1029-1037.

Miranda, P. C., Lomarev, M., & Hallett, M. (2006). Modeling the current distribution during transcranial direct current stimulation. *Clinical Neurophysiology, 117*(7), 1623-1629.

Moos, K., Vossel, S., Weidner, R., Sparing, R., & Fink, G. R. (2012). Modulation of top-down control of visual attention by cathodal tDCS over right IPS. *Journal of Neuroscience, 32*(46), 16360-16368.

Morris, A. P., Bremmer, F., & Krekelberg, B. (2013). Eye position signals in the dorsal visual system are accurate and precise on short time-scales. *Journal of Neuroscience, 33*(30), 12395-12406.

Morris, A. P., Chambers, C. D., & Mattingley, J. B. (2007). Parietal stimulation destabilizes spatial updating across saccadic eye movements. *Proceedings of the National Academy of Sciences of the United States of America, 104*(21), 9069-9074.

Morris, A. P., Kubischik, M., Hoffmann, K. P., Krekelberg, B., & Bremmer, F. (2012). Dynamics of eye-position signals in the dorsal visual system. *Current Biology, 22*(3), 173-179.

Morris, A. P., Liu, C. C., Cropper, S. J., Forte, J. D., Krekelberg, B., & Mattingley, J. B. (2010). Summation of visual motion across eye movements reflects a nonspatial decision mechanism. *Journal of Neuroscience, 30*(29), 9821-9830.

Muller, H. J., & Rabbitt, P. M. (1989). Reflexive and voluntary orienting of visual attention: time course of activation and resistance to interruption. *Journal of Experimental Psychology: Human Perception and Performance, 15*(2), 315-330.

Müsseler, J., van der Heijden, A. H. C., Mahmud, S. H., Deubel, H., & Ertsey, S. (1999). Relative mislocalization of briefly presented stimuli in the retinal periphery. *Perception and Psychophysics, 61*(8), 1646-1661.

Najemnik, J., & Geisler, W. S. (2005). Optimal eye movement strategies in visual search. *Nature, 434*(7031), 387-391.

Newby, E. A., & Rock, I. (2001). Location and attention. *The Quarterly Journal of Experimental Psychology. A, Human Experimental Psychology, 54*(1), 155-168.

Nitsche, M. A., Cohen, L. G., Wassermann, E. M., Priori, A., Lang, N., Antal, A., et al. (2008). Transcranial direct current stimulation: State of the art 2008. *Brain Stimulation, 1*(3), 206-223.

Nitsche, M. A., Fricke, K., Henschke, U., Schlitterlau, A., Liebetanz, D., Lang, N., et al. (2003). Pharmacological modulation of cortical excitability shifts

induced by transcranial direct current stimulation in humans. *Journal of Physiology, 553*(Pt 1), 293-301.

Nitsche, M. A., Liebetanz, D., Lang, N., Antal, A., Tergau, F., & Paulus, W. (2003). Safety criteria for transcranial direct current stimulation (tDCS) in humans. *Clinical Neurophysiology, 114*(11), 2220-2222.

Nitsche, M. A., & Paulus, W. (2000). Excitability changes induced in the human motor cortex by weak transcranial direct current stimulation. *Journal of Physiology, 527*, 633-639.

Nitsche, M. A., & Paulus, W. (2001). Sustained excitability elevations induced by transcranial DC motor cortex stimulation in humans. *Neurology, 57*(10), 1899-1901.

Nitsche, M. A., Schauenburg, A., Lang, N., Liebetanz, D., Exner, C., Paulus, W., et al. (2003). Facilitation of implicit motor learning by weak transcranial direct current stimulation of the primary motor cortex in the human. *J Cogn Neurosci, 15*(4), 619-626.

Nitsche, M. A., Seeber, A., Frommann, K., Klein, C. C., Rochford, C., Nitsche, M. S., et al. (2005). Modulating parameters of excitability during and after transcranial direct current stimulation of the human motor cortex. *Journal of Physiology, 568*(1), 291-303.

Norrsell, U., Finger, S., & Lajonchere, C. (1999). Cutaneous sensory spots and the "law of specific nerve energies": history and development of ideas. *Brain Research Bulletin, 48*(5), 457-465.

O'Regan, J. K. (1984). Retinal versus extraretinal influences in flash localization during saccadic eye movements in the presence of a visible background. *Perception & Psychophysics, 36*(1), 1-14.

Oliveri, M., Rossini, P. M., Filippi, M. M., Traversa, R., Cicinelli, P., Palmieri, M. G., et al. (2000). Time-dependent activation of parieto-frontal networks for directing attention to tactile space. A study with paired transcranial magnetic stimulation pulses in right-brain-damaged patients with extinction. *Brain, 123 (Pt 9)*, 1939-1947.

Palm, U., Schiller, C., Fintescu, Z., Obermeier, M., Keeser, D., Reisinger, E., et al. (2011). Transcranial direct current stimulation in treatment resistant depression: a randomized double-blind, placebo-controlled study. *Brain Stimulation, 5*(3), 242-251.

Paquette, C., Sidel, M., Radinska, B. A., Soucy, J. P., & Thiel, A. (2011). Bilateral transcranial direct current stimulation modulates activation-induced regional blood flow changes during voluntary movement. *Journal of Cerebral Blood Flow and Metabolism, 31*(10), 2086-2095.

Pena-Gomez, C., Sala-Lonch, R., Junque, C., Clemente, I. C., Vidal, D., Bargallo, N., et al. (2012). Modulation of large-scale brain networks by transcranial direct current stimulation evidenced by resting-state functional MRI. *Brain Stimulation, 5*(3), 252-263.

Ploner, C. J., Ostendorf, F., & Dick, S. (2004). Target size modulates saccadic eye movements in humans. *Behavioral Neuroscience, 118*(1), 237-242.

Posner, M. I., & Petersen, S. E. (1990). The attention system of the human brain. *Annual Review of Neuroscience, 13*, 25-42.

Pourtois, G., Vandermeeren, Y., Olivier, E., & de Gelder, B. (2001). Event-related TMS over the right posterior parietal cortex induces ipsilateral visuo-spatial interference. *Neuroreport, 12*(11), 2369-2374.

Prinzmetal, W., Amiri, H., Allen, K., & Edwards, T. (1998). Phenomenology of attention: 1. Color, location, orientation, and spatial frequency. *Journal of Experimental Psychology: Human Perception and Performance, 24*(1), 261-282.

Radman, T., Ramos, R. L., Brumberg, J. C., & Bikson, M. (2009). Role of cortical cell type and morphology in subthreshold and suprathreshold uniform electric field stimulation in vitro. *Brain Stimulation, 2*(4), 215-228.

Rafal, R. D., Calabresi, P. A., Brennan, C. W., & Sciolto, T. K. (1989). Saccade preparation inhibits reorienting to recently attended locations. *Journal of Experimental Psychology. Human Perception and Performance., 15*(4), 673-685.

Ragert, P., Vandermeeren, Y., Camus, M., & Cohen, L. G. (2008). Improvement of spatial tactile acuity by transcranial direct current stimulation. *Clinical Neurophysiology, 119*(4), 805-811.

Rauk, M., & Luuk, A. (1980). Identification and detection of spatial position in one-dimensional patterns. In *Problems of Cognitive Psychology (Acta et Commentationes Universitatis Tartuensis)* (Vol. 522, pp. 143-163). Tartu: Tartu State University, Department of Psychology.

Remington, R. W. (1980). Attention and saccadic eye movements. *Journal of Experimental Psychology: Human Perception and Performance, 6*(4), 726-744.

Reuter-Lorenz, P. A., Kinsbourne, M., & Moscovitch, M. (1990). Hemispheric control of spatial attention. *Brain and Cognition, 12*(2), 240-266.

Reynolds, J. H., & Chelazzi, L. (2004). Attentional modulation of visual processing. *Annual Review of Neuroscience, 27*(1), 611-647.

Reynolds, J. H., & Heeger, D. J. (2009). The normalization model of attention. *Neuron, 61*(2), 168-185.

Reynolds, J. H., Pasternak, T., & Desimone, R. (2000). Attention increases sensitivity of V4 neurons. *Neuron, 26*(3), 703-714.

Richards, W., & Kaufman, L. (1969). "Center-of-gravity" tendencies for fixations and flow patterns. *Perception and Psychophysics, 5*(2), 81-84.

Roberts, M., Delicato, L. S., Herrero, J., Gieselmann, M. A., & Thiele, A. (2007). Attention alters spatial integration in macaque V1 in an eccentricity-dependent manner. *Nature Neuroscience, 10*(11), 1483-1491.

Roelofs, C. O. (1935). Die optische localisation. *Archiv für Augenheilkunde, 109*(1935), 395-415.

Rogalewski, A., Breitenstein, C., Nitsche, M. A., Paulus, W., & Knecht, S. (2004). Transcranial direct current stimulation disrupts tactile perception. *European Journal of Neuroscience, 20*(1), 313-316.

Rose, D., & Halpern, D. L. (1992). Stimulus mislocalization depends on spatial frequency. *Perception, 21*(3), 289-296.

Rosenholtz, R. (2011). *What your visual system sees where you are not looking.* Paper presented at the Proceedings of SPIE: Human Vision and Electronic Imaging, San Francisco, CA.

Ross, J., Morrone, M. C., Goldberg, M. E., & Burr, D. C. (2001). Changes in visual perception at the time of saccades. *Trends in Neurosciences, 24*(2), 113-121.

Rush, S., & Driscoll, D. A. (1968). Current distribution in the brain from surface electrodes. *Anesthesia and Analgesia, 47*(6), 717-723.

Sack, A. T., Hubl, D., Prvulovic, D., Formisano, E., Jandl, M., Zanella, F. E., et al. (2002). The experimental combination of rTMS and fMRI reveals the functional relevance of parietal cortex for visuospatial functions. *Brain Research. Cognitive Brain Research, 13*(1), 85-93.

Schenk, T., & Milner, A. D. (2006). Concurrent visuomotor behaviour improves form discrimination in a patient with visual form agnosia. *European Journal of Neuroscience, 24*(5), 1495-1503.

Shepherd, M., Findlay, J. M., & Hockey, R. J. (1986). The relationship between eye movements and spatial attention. *The Quarterly Journal of Experimental Psychology. A, Human Experimental Psychology, 38*(3), 475-491.

Silvanto, J., Muggleton, N., Lavie, N., & Walsh, V. (2009). The perceptual and functional consequences of parietal top-down modulation on the visual cortex. *Cerebral Cortex, 19*(2), 327-330.

Siman-Tov, T., Mendelsohn, A., Schonberg, T., Avidan, G., Podlipsky, I., Pessoa, L., et al. (2007). Bihemispheric leftward bias in a visuospatial attention-related network. *Journal of Neuroscience, 27*(42), 11271-11278.

Sparing, R., Thimm, M., Hesse, M. D., Kust, J., Karbe, H., & Fink, G. R. (2009). Bidirectional alterations of interhemispheric parietal balance by non-invasive cortical stimulation. *Brain, 132*(Pt 11), 3011-3020.

Spitzer, H., Desimone, R., & Moran, J. (1988). Increased attention enhances both behavioral and neuronal performance. *Science, 240*(4850), 338-340.

Stagg, C. J., Best, J. G., Stephenson, M. C., O'Shea, J., Wylezinska, M., Kincses, Z. T., et al. (2009). Polarity-sensitive modulation of cortical neurotransmitters by transcranial stimulation. *Journal of Neuroscience, 29*(16), 5202-5206.

Stagg, C. J., & Nitsche, M. A. (2011). Physiological basis of transcranial direct current stimulation. *The Neuroscientist, 17*(1), 37-53.

Stagg, C. J., O'Shea, J., Kincses, Z. T., Woolrich, M., Matthews, P. M., & Johansen-Berg, H. (2009). Modulation of movement-associated cortical activation by transcranial direct current stimulation. *European Journal of Neuroscience, 30*(7), 1412-1423.

Stone, D. B., & Tesche, C. D. (2009). Transcranial direct current stimulation modulates shifts in global/local attention. *Neuroreport, 20*(12), 1115-1119.

Stork, S., Musseler, J., & van der Heijden, A. H. (2010). Perceptual judgment and saccadic behavior in a spatial distortion with briefly presented stimuli. *Advances in Cognitive Psychology, 6*, 1-14.

Suzuki, S., & Cavanagh, P. (1997). Focused attention distorts visual space: an attentional repulsion effect. *Journal of Experimental Psychology: Human Perception and Performance, 23*(2), 443-463.

Szczepanski, S. M., & Kastner, S. (2013). Shifting attentional priorities: control of spatial attention through hemispheric competition. *Journal of Neuroscience, 33*(12), 5411-5421.

Szczepanski, S. M., Konen, C. S., & Kastner, S. (2010). Mechanisms of spatial attention control in frontal and parietal cortex. *Journal of Neuroscience, 30*(1), 148-160.

Tsal, Y., & Bareket, T. (1999). Effects of attention on localization of stimuli in the visual field. *Psychonomic Bulletin & Review, 6*(2), 292-296.

Tsal, Y., & Bareket, T. (2005). Localization judgments under various levels of attention. *Psychonomic Bulletin & Review, 12*(3), 559-566.

Turi, Z., Paulus, W., & Antal, A. (2012). Functional neuroimaging and transcranial electrical stimulation. *Clinical EEG and Neuroscience, 43*(3), 200-208.

Turrigiano, G. G., Leslie, K. R., Desai, N. S., Rutherford, L. C., & Nelson, S. B. (1998). Activity-dependent scaling of quantal amplitude in neocortical neurons. *Nature, 391*(6670), 892-896.

Ukueberuwa, D., & Wassermann, E. M. (2010). Direct current brain polarization: a simple, noninvasive technique for human neuromodulation. *Neuromodulation, 13*(3), 168-173.

Utz, K. S., Dimova, V., Oppenlander, K., & Kerkhoff, G. (2010). Electrified minds: transcranial direct current stimulation (tDCS) and galvanic vestibular stimulation (GVS) as methods of non-invasive brain stimulation in neuropsychology--a review of current data and future implications. *Neuropsychologia, 48*(10), 2789-2810.

van der Heijden, A. H., van der Geest, J. N., de Leeuw, F., Krikke, K., & Musseler, J. (1999). Sources of position-perception error for small isolated targets. *Psychological Research, 62*(1), 20-35.

Vernieri, F., Assenza, G., Maggio, P., Tibuzzi, F., Zappasodi, F., Altamura, C., et al. (2010). Cortical neuromodulation modifies cerebral vasomotor reactivity. *Stroke; A Journal of Cerebral Circulation, 41*(9), 2087-2090.

Vicario, C. M., Martino, D., & Koch, G. (2013). Temporal accuracy and variability in the left and right posterior parietal cortex. *Journal of Neuroscience, 245*, 121-128.

Vines, B. W., Nair, D. G., & Schlaug, G. (2006). Contralateral and ipsilateral motor effects after transcranial direct current stimulation. *Neuroreport, 17*(6), 671-674.

Vines, B. W., Schnider, N. M., & Schlaug, G. (2006). Testing for causality with transcranial direct current stimulation: pitch memory and the left supramarginal gyrus. *Neuroreport, 17*(10), 1047-1050.

Vishwanath, D., & Kowler, E. (2003). Localization of shapes: eye movements and perception compared. *Vision Research, 43*(15), 1637-1653.

Wachter, D., Wrede, A., Schulz-Schaeffer, W., Taghizadeh-Waghefi, A., Nitsche, M. A., Kutschenko, A., et al. (2011). Transcranial direct current stimulation induces polarity-specific changes of cortical blood perfusion in the rat. *Experimental Neurology, 227*(2), 322-327.

Wagner, T., Fregni, F., Fecteau, S., Grodzinsky, A., Zahn, M., & Pascual-Leone, A. (2007). Transcranial direct current stimulation: a computer-based human model study. *Neuroimage, 35*(3), 1113-1124.

Wagner, T., Valero-Cabre, A., & Pascual-Leone, A. (2007). Noninvasive human brain stimulation. *Annual Review of Biomedical Engineering, 9*, 527-565.

Watson, A. B., & Robson, J. G. (1981). Discrimination at threshold: labelled detectors in human vision. *Vision Research, 21*(7), 1115-1122.

Whitaker, D., & McGraw, P. V. (1998). The effect of suprathreshold contrast on stimulus centroid and its implications for the perceived location of objects. *Vision Research, 38*(22), 3591-3599.

Whitaker, D., McGraw, P. V., & Levi, D. M. (1997). The influence of adaptation on perceived visual location. *Vision Research, 37*(16), 2207-2216.

Whitney, D., & Cavanagh, P. (2000). Motion distorts visual space: shifting the perceived position of remote stationary objects. *Nature Neuroscience, 3*(9), 954-959.

Wichmann, F. A., & Hill, N. J. (2001a). The psychometric function: I. Fitting, sampling, and goodness of fit. *Perception & Psychophysics, 63*(8), 1293-1313.

Wichmann, F. A., & Hill, N. J. (2001b). The psychometric function: II. Bootstrap-based confidence intervals and sampling. *Perception & Psychophysics, 63*(8), 1314-1329.

Wilson, J. A., & Anstis, S. M. (1969). Visual delay as a function of luminance. *American Journal of Psychology, 82*(3), 350-358.

Womelsdorf, T., Anton-Erxleben, K., Pieper, F., & Treue, S. (2006). Dynamic shifts of visual receptive fields in cortical area MT by spatial attention. *Nature Neuroscience, 9*(9), 1156-1160.

Womelsdorf, T., Anton-Erxleben, K., & Treue, S. (2008). Receptive field shift and shrinkage in macaque middle temporal area through attentional gain modulation. *Journal of Neuroscience, 28*(36), 8934-8944.

Wright, J. M., & Krekelberg, B. (2014). Transcranial direct current stimulation over posterior parietal cortex modulates visuospatial localization. *Journal of Vision, 14*(9).

Wright, J. M., Morris, A. P., & Krekelberg, B. (2011). Weighted integration of visual position information. *Journal of Vision, 11*(14).

Zaghi, S., Acar, M., Hultgren, B., Boggio, P. S., & Fregni, F. (2010). Noninvasive brain stimulation with low-intensity electrical currents: putative mechanisms of action for direct and alternating current stimulation. *Neuroscientist, 16*(3), 285-307.

Zanon, M., Busan, P., Monti, F., Pizzolato, G., & Battaglini, P. P. (2010). Cortical connections between dorsal and ventral visual streams in humans: Evidence by TMS/EEG co-registration. *Brain Topography, 22*(4), 307-317.

Zheng, X., Alsop, D. C., & Schlaug, G. (2011). Effects of transcranial direct current stimulation (tDCS) on human regional cerebral blood flow. *NeuroImage, 58*(1), 26-33.

Chapter 8: **Curriculum Vitae**

1979	Born November 5th in Manchester, CT
1997	Graduated from Watertown High School, Watertown, CT
2001	B.A. in Mathematics, Fairleigh Dickinson University, Madison, NJ
1999-2001	Technical Support Analyst, JAT Software, Bridgewater, NJ
2001-2003	Systems Analyst, Hewitt Associates, Bridgewater, NJ
2003-2004	High School Mathematics Instructor, Kenilworth Board of Education, Kenilworth, NJ
2004-2007	Lead Systems Analyst, Hewitt Associates, Bridgewater, NJ
2007-2009	HHMI Pre-doctoral fellowship for the Quantitative Neuroscience Program, NJIT, Rutgers University and UMDNJ, Newark, NJ
2011	Publication: Wright, J. M., Morris, A. P., & Krekelberg, B. (2011). Weighted integration of visual position information. *Journal of Vision, 11*(14).
2014	Publication: Kar, K., & Wright, J. (2014). Probing the mechanisms underlying the mitigation of cognitive aging with anodal transcranial direct current stimulation. *Journal of Neurophysiology, 111*(7), 1397-1399.
2014	Publication: Wright, J. M., & Krekelberg, B. (2014). Transcranial direct current stimulation over posterior parietal cortex modulates visuospatial localization. *Journal of Vision, 14*(9).
2014	Ph.D. in Behavioral and Neural Sciences, Rutgers University, Newark, NJ Advisor: Dr. Bart Krekelberg Dissertation: Neural Mechanisms of Position Perception